Inaugural dissertation

for

obtaining the doctoral degree

of the

Combined Faculty of Mathematics, Engineering and Natural Sciences

of the

Ruprecht - Karls - University

Heidelberg

presented by

Alice De Roia, M.Sc.

Born in: Pordenone, Italy

Oral examination: 7th September 2023

Non-viral nS/MAR DNA Vector-Based Genetic Modification of T Cells:

Revolutionizing Adoptive Cell Therapies

Referees: Prof. Dr. Michael Platten

Dr. Richard P. Harbottle

Summary

Adoptive cell therapies (ACT) employing Chimeric Antigen Receptors (CARs) or T cell receptors (TCRs), either personalized or off-the-shelf, have demonstrated promising results in cancer treatment. However, the current T cell engineering methods utilizing viral vectors face significant challenges due to their immunogenicity and potential for insertional mutagenesis. Furthermore, large-scale manufacturing of viral vectors is time-consuming and costly, posing obstacles for the application of CAR or TCR-transgenic T cells in personalized cancer immunotherapy with limited therapeutic windows.

This thesis uses an alternative non-viral genetic engineering approach of T cells with nano Scaffold/Matrix attachment region (nS/MAR) Vector technology, which holds potential for enhancing T cell-based therapies. These S/MAR DNA nanovectors, existing episomally and independent of antibiotic selection, offer numerous advantages over viral vectors. These benefits include cost-effectiveness, simplified manufacturing processes, reduced regulatory requirements, and the ability to modify T cells without the associated risk of mutagenesis while ensuring genetic transmission to daughter cells across unlimited cell divisions. Moreover, these vectors have no size limitations, facilitating the incorporation of larger transgenes, multiple expression cassettes, as well as desired gene regulatory and enhancer elements.

My work demonstrates the universal applicability of nS/MAR vectors for genetically modifying T cells in the field of ACT with broad applicability for CARs and TCRs transgenic receptors. nS/MAR vectors enable persistent reporter gene expression, such as GFP, in both cell lines and primary human T cells, without random integration or electroporation-induced cell toxicity. Furthermore, nS/MAR CAR-T cells exhibit comparable or superior anti-tumor efficacy to viral and other non-viral systems in several tumor models. Additionally, the versatility and efficacy of this technology in generating both off-the-shelf and patient-specific TCR-T cells were demonstrated *in vitro*. The platform also demonstrates potential in developing constructs with multiple expression cassettes, such as T cells redirected for antigen-unrestricted cytokine-initiated killing (TRUCKs), which enhance T cells with inducible cytokines, promising an improved therapeutic outcome in patients with brain tumor.

Furthermore, this thesis investigates the potential translation of the nS/MAR technology into clinical applications. The developed streamlined manufacturing process reduces regulatory requirements, time and costs, as well as enhances safety, making personalized T cell therapies more accessible to patients with limited treatment windows, such as those with brain tumors.

Overall, this platform represents an opportunity to improve patient outcomes and expand the application of non-viral CAR and TCR therapy in clinical practice.

Zusammenfassung

Adaptive Zelltherapien (AZT) verwenden chimäre Antigenrezeptoren (CARs) oder T-Zellrezeptoren (TZRs), wobei sowohl personalisierte Rezeptoren als auch bereits etablierte Rezeptoren vielversprechende Ergebnisse in der Krebstherapie erzielen konnten. Aktuell werden zur Modifizierung von T-Zellen virale Vektoren verwendet, die jedoch Probleme wie Immunogenität und das Risiko einer Insertionsmutagenese mit sich bringen. Zusätzlich fallen bei der zeitaufwendigen Virusproduktion im großen Maßstab hohe Kosten an, was die Applikation von CAR- oder TZR-transgenen T-Zellen in der personalisierten Immuntherapie mit bereits limitierten therapeutischen Fenster weiter einschränkt.

In dieser Doktorarbeit wird ein nicht-viraler Ansatz zur genetischen Modifizierung von T-Zellen mithilfe der nS/MAR Vektor Technologie verwendet, der das Potenzial besitzt, T-Zell-basierte Therapien leichter zu ermöglichen. Diese S/MAR DNA Nanovektoren, die Episomal persistieren und keine Antibiotikaselektion benötigen, besitzen eine Vielzahl an Vorteilen im Vergleich zu viralen Vektoren. Zu diesen Vorteilen zählt die Kosteneffizienz, ein im Vergleich zu viralen Produkten erleichterter Herstellungsprozess, geringere regulatorische Anforderungen, und die Möglichkeit, T-Zellen ohne das assoziierte Risiko einer Mutagenese zu modifizieren, während dennoch sichergestellt ist, dass das Gen unbegrenzt an Tochterzellen vererbt werden kann. Darüber hinaus haben diese Vektoren keine Limitation in Bezug auf die Größe der Plasmide, was die Integration von größeren Transgenen, mehreren Expressionskassetten, oder auch genregulatorischen- und Enhancer-Elementen ermöglicht.

Meine Arbeit demonstriert die universelle Anwendbarkeit der nS/MAR Vektoren für die genetische Modifizierung von T-Zellen im Bereich von AZT mit breiter Anwendbarkeit für CAR und TZR-transgenen T-Zellen. nS/MAR Vektoren ermöglichen die dauerhafte Expression von Reporter Genen wie GFP, sowohl in Zelllinien als auch in primären humanen T-Zellen, ohne dass diese sich willkürlich integrieren und ohne Induktion von zellulärer Toxizität als Folge der Elektroporation. Des Weiteren werden durch nS/MAR CAR T-Zellen vergleichbare oder überlegene anti-Tumor Effekte im Vergleich zu viralen oder nicht-viralen Systemen in verschiedenen Tumormodellen ausgelöst. Zusätzlich wurde die Vielseitigkeit und Effizienz dieser Technologie sowohl mit bereits etablierten als auch Patienten-spezifischen TZR T-Zellen *in vitro* demonstriert. The Plattform beweist auch ihr Potenzial dadurch, dass es möglich ist, Konstrukte mit mehreren Expressionskassetten zu verwenden, wie zum Beispiel TRUCKs. Diese fördern T-Zell-Antworten durch

induzierbare Zytokine, wodurch verbesserte therapeutische Erfolge in Patienten mit Hirntumoren erwartet werden können.

Des Weiteren wurde in dieser Doktorarbeit die mögliche Translation der nS/MAR Technologie in die klinische Praxis untersucht. Der entwickelte optimierte Herstellungsprozess verringert im Vergleich zu viralen Systemen regulatorische Anforderungen, Zeitaufwand und Kosten, und erhöht die Sicherheit der Technologie, wodurch personalisierte T-Zell-Therapien auch für Patienten mit limitiertem therapeutischem Fenster zugänglich wird, zu denen auch Patienten mit Hirntumoren zählen.

Insgesamt repräsentiert diese Plattform eine Möglichkeit, bessere Therapieerfolge in Patienten zu erreichen und nicht-viraler TZR-Therapie in die klinische Praxis zu überführen.

Disclosures

List of publications not related to this thesis

Bozza M., Green E.W., Espinet E., **De Roia A**., et al. *"Novel Non-integrating DNA Nano-S/MAR Vectors Restore Gene Function in Isogenic Patient-Derived Pancreatic Tumor Models,* Molecular Therapy - Methods & Clinical Development, vol. 17, pp. 957–968, Jun. 2020, doi: 10.1016/j.omtm.2020.04.017*"*.

List of publications related to this thesis

Bozza M., **De Roia A**., et al*. "A nonviral, nonintegrating DNA nanovector platform for the safe, rapid, and persistent manufacture of recombinant T cells".* Sci. Adv., vol. 7, no. 16, p. eabf1333, Apr. 2021, doi: 10.1126/sciadv.abf1333.

In submission/revision (possibly subjected to changes)

Not related to this thesis

Krämer C., Kilian M., Chih Y-C., Kourtesakis A., Boschert T., Sanghvi K., **De Roia A**., et al., *"NLGN4X TCR transgenic T cells to treat gliomas".* In revision, Neuro-Oncol.

Related to this thesis

Tan C.L, Lindner K., Boschert T., Meng Z., Rodriguez Ehrenfried A., **De Roia A**., et al., *"predicTCR – a machine learning classifier for rapid identification of tumor-reactive T cell receptors for personalised T cell therapy".* Submitted, Nat. Biotechnol.

Declaration of contributions

Animal experiments

Anti- CD19 CAR xenograft model	Alice De Roia/Patrick Schmidt/Matthias Bozza
Anti-CEA CAR xenograft model	Patrick Schmidt/Matthias Bozza
Anti- MART1 and anti-GB TCRs xenograft models	Alice De Roia/Yu-Chan Chin
T cells preparation: S/MAR CARs and TCRs Lentivirus CAR T cells γ-retrovirus TCRs T cells	 Alice De Roia Patrick Schmidt and Aileen Berger Yu-Chan Chin and Philipp Koopmann
Organ collection and dissection: CAR xenograft models TCR xenograft models	 Patrick Schmidt/Aileen Berger Alice De Roia/Yu-Chan Chin/Jessica Hunger/ Dennis Agardy/Amelie Dietsch.
Histology	Patrick Schmidt/Stephan Push

In vitro experiments

Anti- CD19 CAR	Alice De Roia/Matthias Bozza
Anti-CEA CAR	Aileen Berger/Patrick Schmidt/Matthias Bozza
Anti- MART1 TCR	Alice De Roia
Anti-GB TCR	Alice De Roia/Yu-Chan Chin
Anti-BT21 TCRs	Alice De Roia
Generation of GMP protocol for TCR T cells preparation	Alice De Roia/Matthias Bozza
TRUCKs experiments	Alice De Roia
Proliferation assays	Alice De Roia/Matthias Bozza
Immunophenotyping	Alice De Roia/Gayatri Kavishwar
Longitudinal transgene expression primary/Jurkat76 T cells	Alice De Roia/Matthias Bozza/Nicole Codeluppi
Spheroids	Alice De Roia

Others

Southern Blot analysis	Matthias Bozza
Rolling circle amplification	Alice De Roia

Table of Contents

List of Abbreviations

ACT Adoptive cell therapy

ADCC Antibody-dependent cytotoxicity

ALL acute lymphoblastic leukemia

AKT (or PKB) Protein kinase B

ANOVA Analysis of variance

APC Antigen-presenting cell

AP-1 Activator protein 1

HSC Hematopoietic stem cells

VEGF Vascular Endothelial Growth Factor

MAPK Mitogen-activated protein kinase

CAR Chimeric antigen receptor

CDC Complement-dependent cytotoxicity

cDNA Complementary DNA

CDR Complementarity-determining regions

CD137 (or 4-1BB) Tumor necrosis factor ligand superfamily member 9

CEA Carcino embryonic antigen

CLL chronic lymphoid leukaemia

CPPT central polypurine tract

CRISPR Clustered Regularly Interspaced Short Palindromic Repeats

CRS Cytokine release syndrome

CTLA-4 Cytotoxic T-lymphocyte-associated protein 4

CTS Central termination signal

CTV Cell trace violet

DAG Diacylglycerol

DAPI 4′,6-Diamidin-2-phenylindol

DC Dendritic cell

DLBCL Diffuse large B cell lymphoma

DMEM Dulbecco’s modified eagle medium

DMSO Dimethyl sulfoxide

DNA Deoxyribonucleic acid

ELISA Enzyme-linked immunosorbent assay

EMA European medicines agency

EP Electroporation

RT-qPCR Real-Time quantitative PCR

FACS Fluorescence-activated cell sorting

FasL First apoptosis signal ligand

FBS Fetal bovine serum

FcR Fc receptor

FDA Food and drug administration

Gamma-RV Gamma retrovirus

GBM Glioblastoma

GFP Green fluorescent protein

GP100 Glycoprotein 100

gRNA Guide RNA

HDR Homologous recombination end joining

HIV Human immunodeficiency virus

HLA Human major histocompatibility complex

HMGB1 high mobility group protein B1

HSC Hematopoietic stem cells

HSCT Hematopoietic stem cell transplantation

ICOS Inducible T cell costimulatory

IDO Indoleamine 2,3-dioxygenase

IFN Interferon

Ig Immunglobulin

IHC Immunohistochemistry

IL Interleukin

IL2RB Interleukin-2 receptor subunit beta

IP3 Inositol trisphosphate

IRES Internal ribosomal entry site

ITAM Immunoreceptor tyrosine-based activation motifs

LAG3 Lymphocyte-activation gene-3

LAT Linker of activated T cells

LDH Lactate dehydrogenase

LTR Long terminal repeats

LV lentivirus

MACS Magnetic-activated cell sorting

MAGE-A3 Melanoma-associated antigen 3

MCL Mantle cell lymphoma

MFI Median fluorescence intensity

MHC Major histocompatibility complex

MM Multiple myeloma

Mo-MLV Moloney murine leukaemia virus

NFAT Nuclear factor of activated T-cells

NHEJ Non-homologous end joining non-homologous end joining

NSG Immunodeficient non-obese diabetic scid gamma

NF-kB Nuclear factor kappa-light-chain-enhancer of activated B cells

NK cells Natural killer cells

NY-ESO1 New York-esophageal squamous cell carcinoma

ScFv single chain fragment variant

SNP Single nucleotide polymorphism

WT Wildtype

TLR Toll-like Receptors

PBMC Peripheral blood monocytic cells

PD1 Programmed death protein 1

PCK Protein kinase C

PCR Polymerase chain reaction

PLCγ1 Phospholipase C gamma 1

PB PiggyBac

PBS Phosphate-buffered saline

PD-L1 Programmed death-ligand 1

RCR/L Replication-competent retro

RPMI Roswell Park Memorial Institute

RT Room temperature

RV Retroviruses

SB Sleeping beauty

s.c. Subcutaneously

SD Standard Deviation

SIN Self-inactivating

S/MAR Scaffold/matrix attachment region

SLP-76 (or LCP2) Lymphocyte cytosolic protein 2

TAA tumor associated antigens

TALE transcription activator-like effectors

TALEN Transcription activator-like effector nucleases

TCR T cell receptor

TF Transcriptional Factor

TIL Tumor infiltrating lymphocyte

TIM3 T-cell immunoglobulin and mucin-domain containing-3

TIRs Terminal inverted repeats

TLR Toll-like receptors

TM transmembrane

TME tumor microenvironment

TN Naïve T cells

TNF Tumor necrosis factor

TNFR Tumour necrosis factor receptor

TRACR-RNA Trans-activating crRNA

TREG Regulatory T cell

TRUCKs T cells redirected for antigen-unrestricted cytokine-initiated killing

ZAP Zeta Chain Of T Cell Receptor Associated Protein Kinase 70

ZFN Zinc-finger nucleases

List of Tables

List of Figures

1. Introduction

1.1 The immune system and T cell-mediated immunity

During evolution, the immune system has developed as a defence mechanism in response to infectious pathogens and harmful substances [1][2]. The immune system is characterized by two fundamental defensive lines: the innate and the adaptive immune systems. The innate immune system is the evolutionary older defense line, it's the first response against pathogens. It consists of an antigen-independent, non-specific, and rapid immune response with no immunologic memory [1][3]. On the other hand, the adaptive immune system is a precise and specific antigen-dependent response, which exhibits a time delay between exposure to the antigen and the maximal response. It comprises B and T cells and, opposite to innate immunity, it possesses the unique characteristic of developing immunological memory. This memory enables a more rapid and intense immune reaction upon subsequent encounters with the same antigen [1][3]. Recently, it has become clear that T cells not only play a crucial role in recognizing and eliminating pathogens but also contribute significantly to tumor control. In fact, T cells can recognize mutated or overexpressed antigens associated with tumor cells [1].

In the upcoming sections, the basic T cell biology will be described, while in the section 1.4 the strategies that can be employed to enhance the effective T cell response against tumors will be discussed.

1.2 T cell receptor (TCR)

T cells are characterized by the presence of T cell receptors (TCRs) on their surface. TCRs are multi-subunit protein transmembrane complexes that primarily function in recognizing intracellular and extracellular processed antigens with high specificity. These antigens are presented by major histocompatibility complex (MHC) molecules[1][4]. The TCR is composed of two different heterodimers: αβ in most mature T cells, or γδ in a rare population [1][3]. The α and β chains have an extracellular domain, a transmembrane portion and cytoplasmatic tail. The extracellular domain consists of a constant region (C) and a variable region (V), which determines the antigen specificity. The two α and β chains

are linked and stabilized together by disulphide bonds and anchored to the cell membrane. The TCR chains are encoded by different genes located on separate chromosomes and are brought together through site-specific recombination during T cell development. These genes consist of the variable (V), the diversity (D, present in the β chain), and the joining (J) gene segments [1][4]. The recombination process results in rearranged V(D)J genes, which are found in the complementarity-determining regions (CDR) of the TCR chains. Among these regions, the CDR3 region plays a critical role in antigen specificity [1][5]. However, unlike antibodies, TCRs do not undergo somatic hypermutation. As a result, TCRs exhibit a relatively low affinity for the antigen [1].

1.2.1. Major histocompatibility complexes (MHC) class I and II

T cells are unable to recognize antigen in their naive form, they can only recognise antigens that have been processed and are presented by the major histocompatibility complexes (MHC). Depending on their structure and their function MHC can be divided into class I or class II (respectively MHC-I and MHC-II), which trigger two different T cell responses. MHC-I are involved in CD8-mediated responses, while MHC-II is involved in CD4-mediated responses. MHC-I is expressed in all nucleated cells and is responsible for presenting fragments of intracellular peptides, typically around 10 amino acids in length. These antigens can originate from self-peptides (such as tumor associated antigens, TAA) or foreign peptides (such as proteins from intracellular pathogens) [1].

MHC-I are comprised of an α chain (heavy chain), that spans the membrane, and a non-covalently associated β2-microglobulin extracellular chain (light chain). The α-chain consists of three extracellular domains, called α 1-3 domains, a transmembrane (TM) region and an intracellular tail. The α1-2 domains are involved in the antigen binding, while the α3 and the β2-microglobulin domains are responsible for the MHC stability [1].

On the other hand, MHC-II is expressed on the surface of immune cells, in particular of antigen presenting cells (APC) or also on tumor cells. It is responsible for presenting peptides (~15 amino acids) derived from extracellular foreign bodies, such as bacteria. MHC-II consists of two chains, α and β, both spanning the membrane. They comprise of a TM portion that binds them to the cell membrane and two globular domains. The α1 and β1 domains act as an antigen binding site [1][6].

1.2.2 MHC and TCR interaction and TCR signaling

The binding of an antigen to the TCR through the MHC complex follow a signaling cascade that results in T cell activation [7]. The first event in T cell activation, following TCR engagement, is the formation of the so-called immune synapse between T cells and APC. The TCR depends on the so-called TCR complex for the signaling pathways that occur during T cell activation [1][7]. This complex consists in the TCR itself and the CD3 molecules, δ, ε, γ, and ζ chains. In the ζ chain there is an immunoreceptor tyrosine-based activation motifs (ITAMs) that upon TCR engagement, initiate the signaling cascade (**Figure 1**) [1][7][8]. Two other important components of the TCR complex that play a role in the T cell activation are the CD4 and CD8 co-receptors, expressed respectively on helper and cytotoxic T cells [1][9]. Their main functions are stabilizing the interaction between the TCR and MHC and bringing closer to the TCR complex the lymphocyte-specific protein tyrosine kinase (Lck) [1][7][8][9]. When CD4 and CD8 bind to MHC-I and MHC-II respectively, Lck phosphorylates the ITAMs domains present on the CD3ζ chains, resulting in the recruitment of the cytosolic ζ-chain associated protein kinase of 70k (ZAP70) (**Figure 1**) [7][9]. Lck phosphorylates also ZAP70 which becomes active. Activated ZAP70 can subsequently phosphorylate and activate the linker of activated T cells (LAT) and the SH2 domain containing leukocyte protein of 76kDa (SLP-76), leading to the formation of a complex along with the phospholipase C gamma 1 (PLCγ1) (**Figure 1**). This results in the production of inositol trisphosphate (IP3) and diacylglycerol (DAG), that activate different pathways through three different transcriptional factors: the nuclear factor of activated T cells (NFAT), the nuclear factor kappa-light-chain-enhance (NF-kB) and the activator protein 1 (AP-1), which control multiple T cell responses, including proliferation, migration, cytokine production and effector functions [7][8]. The activation of NFAT-mediated signaling pathway is induced by IP3. IP3 induces Ca2+ release into the cytosol, leading to increased intracellular Ca2+ levels that stimulate the enzyme calmodulin which in turn stimulates the calcineurin (**Figure 1**). This results in the dephosphorylation and subsequent translocation of NFAT into the nucleus [7][8].

Another signaling pathway is initiated by DAG. DAG activates the protein kinase C (PKC) and the subsequent recruitment of the IκK complex. This will then lead to the phosphorylation and degradation of IκB inhibitors, resulting then in the nuclear translocation of the NF-kB [7][8]. A second pathway induced by DAG follows the

activation of Ras which activates in turn the mitogen-activated protein kinase MAPK cascade (**Figure 1**). This signaling results in the activation of the transcriptional factor AP-1 [7][8].

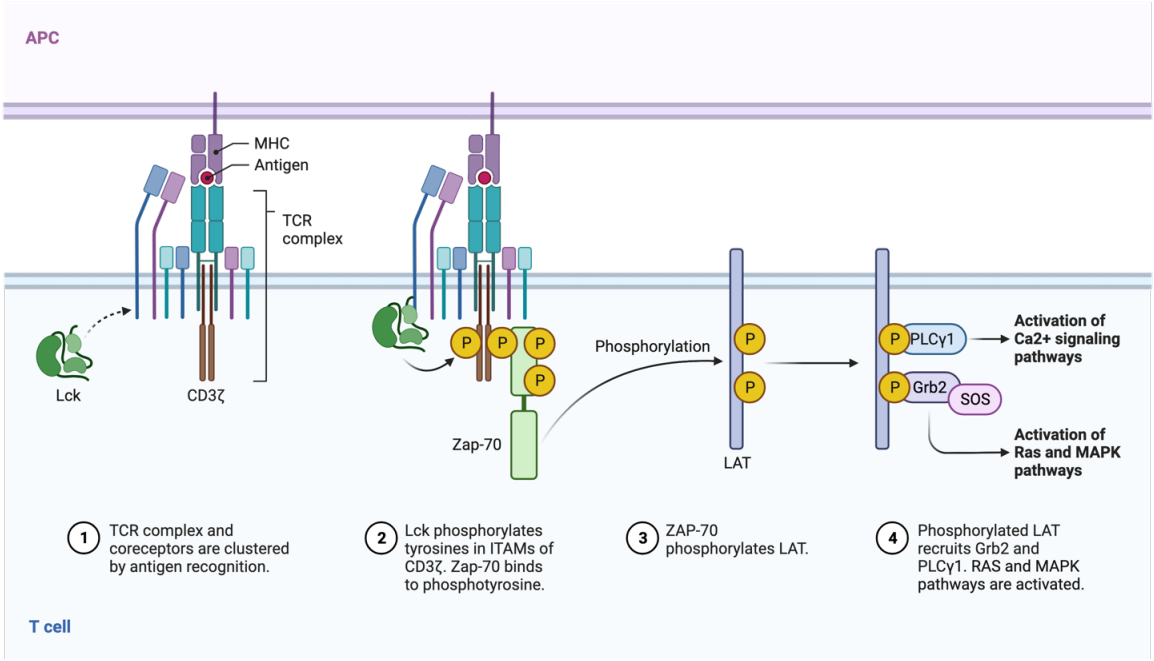

Figure 1 T cell receptor (TCR) signaling pathways. The TCR binds to the pMHC complex initiating a signaling cascade. CD4 are CD8 co-receptors recruit the Lck tyrosine kinase that phosphorylates the ITAMs domain contained in the CD3 subunit. ZAP70 is then in turn recruited and activated by phosphorylation mediated by Lck. ZAP70 will subsequently activate PLCγ1 that starts a signaling cascade that will activate the Ras and MAPK pathways. Created with BioRender.com

1.2.2.1 Co-stimulatory signals

TCR stimulation alone may leads to T cell anergy. Additional secondary co-stimulatory signals, provided by APCs, are needed for a full T cell activation and proliferation. One of the crucial pathways involves the CD80/CD86-CD28 interaction. CD80/CD86 and CD28 are expressed respectively by APCs and T cells. CD28 is constitutively expressed on the T cell surface and its intracellular domain is characterized by the presence of tyrosine and proline-rich highly conserved sequences. CD28 mediates the activation of the protein kinase B (PKB or Akt) pathway that results in the in the nuclear translocation of NF-kB and in the transcription of genes under the control of NFAT, such as IL2 [7][8][10]. Another important receptor of the CD28 family that plays a major role in different aspects of T cell activation and survival, is the inducible T cell costimulator (ICOS) [10][11]. ICOS is expressed only following T cell activation, and like CD28 also leads to Akt pathway

activation [10]. The other inducible receptors, OX40 and 4-1BB, are members of the tumour necrosis factor receptor (TNFR) family. 4-1BB is express in activated CD8+ and CD4+ T cells and is responsible of the amplification of the NF-kB signaling pathway. It is involved in enhanced cytokine secretion that lead to the augmentation of T cell effector function and their survival [8][10][11]. OX40 receptor, like 4-1BB, is expressed in activated T cells and plays a crucial role in the memory of the immune response mediated by the amplification of the NFAT and PI3K/PKB signaling pathways [10][11].

In summary, CD28 co-receptor seems to play a critical role in initial stages of T cells activation, while 4-1BB and OX40 are involved in the mediation of a prolonged and efficient response.

1.2.2.2 Co-inhibitory signals and checkpoints

In physiological conditions, T cells activation, expansion and effector functions need to be regulated in order to avoid autoimmune responses or healthy tissue damage. This negative regulator mechanism involves several proteins, the so-called co-inhibitory immune checkpoints [1][10].

One of the most important inhibitory feedback mechanisms is mediated by the Cytotoxic T-lymphocyte-associated protein 4 (CTLA-4). CTLA-4 is a member of the CD28 immunoglobulin subfamily, and its translocation into T cell surface is induced following TCR engagement [10]. CTLA-4 negatively regulates T cell activation by inhibiting CD28 signaling. In fact, CTLA-4 competes with CD28 for the binding with its ligands CD80 and CD86 but binds them with higher affinity leading to a co-inhibitory response. CTL-4 is crucial for the regulation of T cell homeostasis and self-tolerance [10][12]. Another important co-inhibitory receptor is the Programmed Death 1 (PD1). PD1 belongs to the B7/CD28 subfamily and is expressed on exhausted T cells that have been exposed to continuous antigen stimulation [13]. Exhausted T cells are the result of chronic infection or cancer, and its dysfunctional phenotype can negatively impact the control of cancer growth or infections. PD1 mediates the inhibition of cytokines production (IL2 and IFNγ), T cells proliferation and survival [13][14]. Lymphocyte activation 3 (LAG3) is a protein expressed in the surface of activated T cells approximately 3-4 days after stimulation. LAG3 belongs to the Ig superfamily and has a high structural homology with the CD4 receptor. Based on the structural homology both LAG3 and CD4 can bind to MHC-II, with a higher affinity for LAG3 [15]. It has been shown that LAG3 can interact with the

TCR/CD3 complex and can negatively regulate the Ca2+ release that follows TCR stimulation [16]. However, the mechanism by which LAG3 can modulate T cells homeostasis remains unclear. The T cell Immunoglobulin and Mucin domain-containing protein 3 (TIM3), is an inducible protein expressed on the surface of activated CD8+ T cells and CD4+ Th1 T cells. It belongs to the TIM immunoregulatory protein family and function as a negative regulator in T cell activation. Its expression has been correlated with T cells exhaustion in viral infection and cancer [17]. The high mobility group protein B1 (HMGB1) mediate an additional inhibitory effect of TIM3. The binding of HMGB1 to the DNA of dying cells and inhibit the transport of DNA into endosomes, resulting in the downregulation of the stimulation of the Toll-like receptors (TLR) and suppressing the activation of cell innate response mediated by dendritic cells [18]. Another inhibitory function is excreted by the ligand Galectin-9. This interaction has been shown to drive apoptosis in activated CD4+ and CD3+ T cells [19].

1.2.3 Cancer immunosurveillance

The immune system plays a critical role in the prevention of tumor formation by identifying and eliminating tumor cells. Tumor genomes contains a range of mutation that can derive from either onco-viral antigens, or neo-antigens derived from mutated or aberrantly expressed proteins. These mutations can evoke an immune response since an immune tolerance has not been developed yet. The interaction between tumor and immune cells is a dynamic process that paradoxically can control and promote cancer development at the same time [20]. This process is defined as immune editing and consists of three phases: elimination, equilibrium and escape [20]. During the elimination phase, the innate and adaptive immune systems are collaborating to trigger a response against the tumor [20]. However, sometime the initial immune response can fail in reaching complete tumor elimination. In fact, some tumor subclones can escape the elimination and enter the equilibrium phase [21]. The tumor genetic instability combined with the pressure induced by the interaction between the immune system and the tumor can shape the tumor's mutational evolution [20][21]. Consequently, selected subclones, with reduced immunogenicity will evade immune recognition [20][21]. Tumors have several mechanisms to escape immune recognition. One common mechanism is to downregulate antigen presentation by reducing either components of the antigen processing pathway or the MHC-I and MHC-II expression [22]. Another mechanism involves the inhibition of the

apoptosis signaling, resulting in clones that are apoptosis resistant [23]. Tumors can also reshape their tumor microenvironment by producing immunosuppressive cytokines and chemokines, expressing immune checkpoint molecules like the programmed death-ligand 1 PD-L1, and producing enzymes, such as indoleamine 2,3-dioxygenase (IDO), that negatively regulate T cell function [24][25][26].

Of an important note, the central tolerance also plays a critical role in the process of immunoediting. In fact, TAA are often "self-antigens" expressed on both tumor cells and healthy cells. This results in a less effective T cell responses due to the mechanism of central and peripheral T cell tolerance [27]. On the other hand, as a way to preventing over-reactivity of the immune system, the peripheral tolerance, can as well suppress the elimination of tumor cells [28].

The crosstalk between the immune system, the tumor microenvironment and the tumor is a complex mechanism that can lead to a non-effective response against tumor development facilitating therefore disease progression. On a fundamental remark, this process can occur naturally during tumor development, however, can also result because of therapy treatment.

1.3 Cancer immunotherapy

The concept of using the immune system as a tool to deploy tumor growth originated the first time in the 19th century. In the 20th century, Lewis Thomas and Sir Frank Macfarlane Burnet came with the idea of cancer immunosurveillance [29][30]. Over the past decade, the concept of using the immune system to treat cancer, the so-called cancer immunotherapy, has experienced significant growth and numerous groups are currently aiming at enhancing immune responses against tumors [31]. Cancer immunotherapy can be divided into three main categories:

- Vaccination. This approach relies on the activation of an endogenous immune response, via vaccination against tumor antigens [31].
- Antibody therapy. This approach can be further into: inhibitors of tumor antigens and signaling (Trastuzumab or Cetuximab); inhibitors of angiogenesis (Bevacizumab); antibodies that promote antibody-dependent cytotoxicity (ADCC) and the complement-dependent cytotoxicity (CDC) (Rituximab); antibodies-drug coniugates with cytotoxic agents, checkpoint blockade antibodies (aCTLA-4 and

aPD-1) and co-stimulatory agonists of the immune system (4-1BB and OX40) [31][32].

- Adoptive T cell therapy (ACT). This ecompass two main approaches: infusion of naturally occurring tumor-infiltrating lymphocytes (TILs) that have been *ex vivo* expanded; infusion of genetically modified T cells that have been generated *ex vivo* (TCR or CAR T cells) [31].

1.4 Adoptive T cell therapy (ACT)

In the past decade, the potency of immunotherapy, in particular immune checkpoint blockade in treating cancer has been a breakthrough in the treatment of cancer. Another approach to treat cancer that have shown promising results in several types of tumors is the ACT; it offers a potential additional treatment option for patient that do not respond to immune check point blockade, such as melanoma and non-small cell lung cancer patients. ACT refers to the infusion of effector cells, such as T cells or NK cells, to provide an anti-tumor function [31][33].

1.4.1 Tumor infiltrating lymphocytes (TIL) therapy

The first study with adoptive transfer of lymphocytes, and in particular with TILs, was conducted by Rosenberg and co-workers [34]. Early studies in pre-clinical models demonstrated that T cells eliminate cancer cells in *in vivo* models. Later in the ‘80s, based on previous knowledge on interleukin-2 (IL2) and its role in mediating T cell expansion, the first clinical trial was conducted using the TIL-based approach to treat melanoma [35]. Infiltrating T cells were isolated from resected tumor biopsies and grown *ex-vivo*, with the idea that removing exhausted TILs from the tumor immunosuppressive microenvironment and growing them with the support of IL2 would repristinate their effector abilites. The first study conducted using autologous TIL therapy for metastatic melanoma shown tumor regression, with 20% of complete responder, and 50% response rate of treated patients [35]. Since the success of this new approach, TIL therapy was then further investigated in several clinical trials with also other tumor entities, such as cervical cancer, breast cancer, renal cell cancer and non-small cell lung cancer [36][37][38][39]. While TIL therapy demonstrated promising clinical outcomes in melanoma, might be due by the high mutational rate of this tumors, its effectiveness in clinical trials was found to be limited in other tumor types, such as brain tumors [40][41]. This was observed despite the presence

of potential tumor-reactivity TIL cultures derived from patients with glioblastoma (GBM) [42][43][44].

Several factors restrict the broader application of TIL therapy. The availability and therefore the isolation of TILs can be limited for other tumor entities, in metastatic settings. Another limitation depends on the culturing conditions; the *ex vivo* process of TIL expansion is time and cost consuming and difficult to standardize [45]. Additionally, the extended *ex vivo* culture can also modify the T cell phenotype, potentially leading to promote the growth of suppressive T regulatory cells (T regs) after infusion into patient. Moreover, the high level of IL2 can induce toxicity in patients [40].

In conclusion, despite the success of TIL therapy in melanoma, alternative approaches have been investigated to generate tumor reactive T cells for other tumor entities, such as the use of genetically modified T cells.

1.4.2 Adoptive cell transfer

Genetic engineering of T cells has been used as an alternative strategy to confer T cells specificity against tumor antigens. T cells can be isolated from the blood and engineered to express a tumor-specific T cell receptor (TCR) with high avidity and optimal *in vivo* functionality, or a chimeric antigen receptor (CAR), which combines the antigen specificity of an antibody with the signaling capacity of the TCR receptor. This approach, known as adoptive T cell transfer, has emerged as an effective and durable therapy for cancer and infectious diseases.

1.4.2.1 TCR Therapy

T cells can be genetically modified to express a TCR able to recognise a TAA and confer therefore specificity against tumor. Once a TCR engages with a pMHC complex, the downstream TCR signaling is activated, resulting in the destruction of tumor cells. TCR technology has undergone several development steps since its first application in. The first generation comprises a subset of tumor antigen-specific TCRs isolated from patients, expanded *ex vivo* and subsequently infused back into the patient. A limitation of this approach is that some TCR clones are rare and with individual variability, which can result in a laborious and difficult to translate manufacture process. In a second generation, the sequences of the TCRs were cloned and transduced into patient T cells, making easier their

production and the use of this TCR T cells in the clinic. During the third phase of development, significant therapeutic improvements were achieved by enhancing the TCR affinity towards tumor cells. In the fourth generation of TCR T cells neoantigens are targeted, leading to a more specific, effective and safe therapy [46][47].

1.4.2.2 Overview on clinical applications

Numerous clinical trials have primarily focused on patients with metastatic melanoma with a poor survival prognosis. In 2006, Morgan and co-workers conducted a clinical trial using TCR T cells. They treated patients with metastatic melanoma by utilizing HLA-A2 restricted T cells expressing a low-affinity anti-MART1 TCR (clone DMF4) [48]. Later, in another clinical trial the use of high-affinity TCR (clone DMF5), which showed improved response rates even though some toxicities were observed [49]. Additionally, other targeted antigens, including the Glycoprotein 100 (gp100), the New York-esophageal squamous cell carcinoma (NY-ESO-1) and Melanoma-associated antigen 3 (MAGE-A3), have been explored in other clinical trials [50][49][51][52][53]. Treatment of patients with affinity-enhanced NY-ESO1 TCR resulted in a clinical response in 4 out of 6 synovial patients and 5 out of 11 melanoma patients with no toxicities observed [54].

TCR adoptive cell therapy has encountered several limitations that have contributed to its limited success and the restriction of its use on melanoma treatment. In fact, TCRs targeting TAAs while are universal, often demonstrate low avidity for their target due to central and peripheral tolerance mechanisms [55]. Patients treated with TCRs that exhibit higher avidity have shown improved responses. While it would be advantageous to target tumor-specific antigens (TSAs), which are mutated antigens expressed exclusively by a particular tumor, this approach would require a patient-specific therapy [54].

Moreover, the transfer of TCR-modified T cells in clinical trials has shown good tolerability, but there are limitations regarding their expansion, persistence, and patient safety. Improvements in these areas are needed to enhance safety and antitumor activity and achieve favourable clinical outcomes [56]. Another fundamental aspect to take into consideration is that, despite using the same TCR, there is inconsistency among clinical centers in the outcomes of TCR-engineered T cell trials. This is likely due to differences in manufacturing protocols, patient recruitment, and preconditioning regimens. Therefore, to ensure consistent and comparable patient data across centers, adjustments and standardization of the process and in the clinical protocols are required.

1.4.2.3 Chimeric antigen receptor (CAR) T cell therapy

The basic concept of CAR T cell therapy was introduced by Eshar and colleagues when they demonstrated that T cells could be modified in order to express a new synthetic receptor targeting a TAA, without affecting their functionality [57][58]. CARs consist of a combination of a single chain fragment variant (ScFv) of a monoclonal antibody and the intracellular signaling of a TCR [58]. Its structure allows the recognition of tumor cells independently from the MHC complex, conferring an advantage to common immune evasion strategies, such as MHC downregulation and the escape from the peptide processing [22]. In contrast to TCRs, one disadvantage is their limited capacity to recognize antigens that are exclusively expressed on the cell surface.

CAR T cells are currently classified into five different generations (**Figure 2**), each introducing advancements in the CAR construct to enhance its functionality. Initially, CARs consist only of a ScFv region connected with the CD3ζ signaling domain, where the ScFv is responsible for antigen recognition (**Figure 2**). However, it was shown that while CAR T cells where able to kill tumor cells, this was insufficient to induce a strong cytokine response and promote significant T cell expansion. In order to achieve a complete T cell function and avoid T cell anergy, CARs were then equipped with a co-stimulatory signal, such as CD28, 41BB or OX40 (**Figure 2**) [59][60][61][62]. Further advancements in CAR design were made in the third CAR generation, which includes the combination of two different costimulatory domains with an activation domain (**Figure 2**) [63][64][65]. This resulted in CAR T cells with better proliferation and survival, enhancing overall the functionality of the cells *in vitro* and *in vivo*. A recent development is the fourth generation of CARs, also known as T cells redirected for universal cytokine-mediated killing (TRUCKs) (**Figure 2**) [66][67]. This advancement equips T cells an inducible transgenic cytokine, such as IL12, which can stimulate other innate immune cells that help eliminating tumor cells. The latest advancement in CAR T cell therapy, known as the fifth generation, incorporates extra intracellular cytokine domain of a cytokine receptor, such as IL2Rb (**Figure 2**) [68].

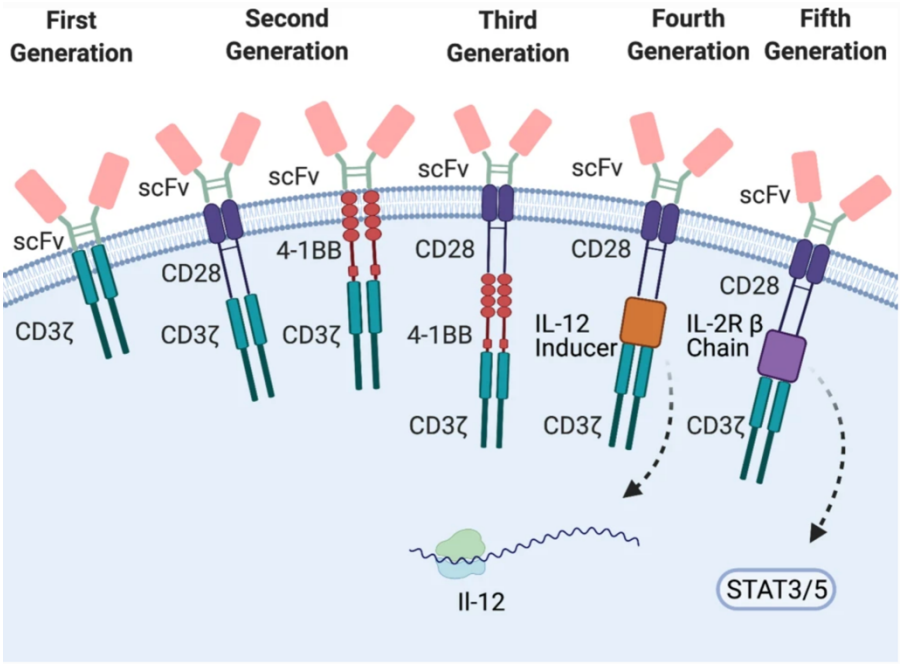

Figure 2 The five generation of Chimeric Antigen Receptors (CARs). Image representing the schematic CAR structure of the five generations of CARs. In the first generation the CAR comprise the ScFv antibody portion and the CD3ζ signaling component. In the second generation a co-stimulatory molecule was added (CD28 or 4-1BB). In the third generation an extra co-stimulatory signal was added. The fourth generation of CARs is equipped with an inducible cytokine (e.g., IL12) that is expressed when the CAR is engaged with the MHC of a tumor cell. The fifth generation is based on the 2nd generation with the incorporation of the intracellular cytokine receptors domain. Image adapted from: Umut et al., 2021 [69].

1.4.2.4 Overview on clinical applications

CAR T cell therapy has been a revolutionary treatment with remarkable clinical responses, in the treatment of haematological malignancies. In 2011, a significant milestone was achieved when a clinical trial conducted by Carl June and his team utilized CAR T cell therapy targeting the CD19 B-cell antigen, leading to complete and sustained tumor remission in three patients with chronic lymphoid leukaemia (CLL) [70]. Although CAR T cells are still undergoing development for solid tumors, the first therapeutic products for haematological malignancies have been successfully introduced into clinical practice. In 2017, the success of the trial and the remarkable efficacy of anti-CD19 CAR T cell therapy led to its approval by the US Food and Drug Administration (FDA) [71]. Novartis' Kymriah® was initially approved for acute lymphoblastic leukemia (ALL) and the diffuse large B cell lymphoma (DLBCL). Following shorter, Gilead-Kite Pharma's Yescarta® was then approved for DLBCL. In 2018, both products also received approval by the European medicines agency (EMA). To date, three additional CAR T cell products have received approval. The Anti-CD19 Tecartus® (Gilead-Kite) and in the Breyanzi® (Juno Therapeutics, Inc., a Bristol-Myers Squibb Company) were commercialized respectively

in 2020 and 2021 to treat mantle cell lymphoma (MCL) and ALL (Tecartus) and different types of B cell lymphoma (Breyanzi). In 2020 also the anti-B cell maturation antigen (BCMA) ABECMA® (Celgene) was approved to treat patient with multiple myeloma (MM). In early 2022 Breyanzi® underwent regulatory review in Europe, Switzerland, and Canada for regulatory approval. Shortly following that, the FDA granted authorization to the anti-CD38 Carvykti™ (ciltacabtagene autoleucel), for the treatment of MM [72].

Several factors have contributed to this success. Firstly, CAR T cells demonstrate a greater capacity to migrate and infiltrate in the bone marrow and lymph nodes when compared to solid tumors. Additionally, CD19-positive B cells play an important role in providing co-stimulation to T cells by expressing CD80/CD86, facilitating their long-term persistence after infusion into patient [73]. Moreover, the microenvironment of haematological tumors is less immunosuppressive than solid tumors [74]. Clinical trials are currently ongoing to evaluate the effectiveness of CAR T cell therapy in solid tumors. Although there have been some observed tumor responses, it is evident that the application of CAR T cell therapy to treat solid tumors will necessitate further optimisation of the CAR in order to enhance effectiveness and achieve the clinical outcomes seen in haematological malignancies [75].

1.4.2.5 TCR versus CAR T cell therapy

TCR based therapy is limited by several factors such as: I) HLA restriction which limits its broad clinical applicability II) common mechanism of tumor escape III) low-affinity TCR resulting from the central and peripheral tolerance [76]. Patients selected for TCR T therapy need to fulfil the requirement of expressing both the specific targeted antigen and the corresponding antigen-restricting HLA allele, which is not necessary in CAR T therapy. As a result, TCR T therapies often employ TCRs that are specific to frequently encountered HLA alleles, such as HLA-A*02:01. In contrast, CAR T cells offer the advantage of not being limited by HLA restrictions, making them applicable in a wide range of patients who express a specific target antigen [76]. Moreover, CAR T cells have the unique ability to directly recognize the antigen in its naive form, bypassing the need for antigen processing and presentation, and reducing therefore the chances of tumor escape. A major drawback to this is the restriction of their applicability to a reduced range of target antigens [76]. To ensure optimal efficacy and safety, it is crucial for these treatments to specifically target tumor cells while minimizing the potential occurrence of 'on-target off-tumor' toxicity [73].

CARs and TCRs also exhibit significant differences in their functional response to antigen stimulation due to their different signaling mechanisms. In fact, TCRs can trigger a cytotoxic response even with a small number of peptide-MHC molecules, while CARs require a larger quantity of target antigens for an effective response [77][78]. CARs, in comparison to physiological TCRs, mediate a stronger activation that results in increased cytokine production and a higher risk of patients to develop cytokine release syndrome (CRS) [79]. Given the unsatisfactory responses of CAR T cells and promising clinical outcomes on TCR T cell therapy in the treatment of solid tumor, TCR T cell therapy is considered a more suitable approach for the treatment of this cancers.

1.5 Genetic modification of T cells

Several factors need to be taken into consideration when selecting the appropriate method for the generation of therapeutic T cells. One important aspect is the safety and the translatability of the chosen methodology, along with its ability to provide efficient expression of a TCR. The overall treatment duration is another crucial aspect, as T cells can be modified to express a gene either permanently or transiently [80]. The size of the desired insert also plays an important role, as different vector types may have limitations in accommodating larger genetic material. Other factors include potential side effects, such as immune responses, as well as the manufacturing cost and time [72].

In this section, several approaches will be discussed, with a specific focus on non-viral vector gene transfer techniques that have evolved in recent years. These techniques aim to overcome the limitations and drawbacks associated with classical viral vectors and improve the overall outcome in patients treated with therapeutic T cells.

1.5.1 Viral vectors

The inherent ability of viruses to cross the cell membrane, deliver their genetic material, and integrate into cells makes them a traditional tool for gene engineering.

1.5.1.1 Retroviral Vectors

Retroviruses (RV) are enveloped viruses containing a single-stranded RNA genome. To replicate, they rely on a reverse transcriptase enzyme, which is included within the virus itself. This enzyme facilitates the transcription of the viral RNA into complementary DNA

(cDNA), which can subsequently integrate into the host genome [81]. Two important viral vectors used for T cell engineering, gamma retrovirus (γ-RV) and lentivirus (LV), belongs to this virus family[80].

Gamma-RV have a simple genome and can integrate their genetic material into the host genome and permanently express the gene of interest, which makes them convenient to be used as a genetic tool. Gamma-RV vectors are capable of transducing only mitotically active T cells and derive from the replication-incompetent moloney murine leukaemia virus (Mo-MLV) [82]. In order to integrate into the genome, specific gene sequences, known as long terminal repeats (LTRs) and a viral integrase are required. The U3 region is also needed to facilitate retroviral RNA transcription. Other viral coding sequences are replaced with the transgene of interest, such as a CAR or a TCR, which are flanked by the LTR sequences [83]. Moreover, genes encoding the capsid protein (*gag*), the replication enzyme (*pol*), and the envelope (*env*) are also needed. Typically, these genes are provided in trans in a helper plasmid to avoid the generation of replication-competent retro or lenti virus (RCR/L) caused by recombination events that may occur during manufacturing or in patients [83].

Lentiviral vectors derive from the replication-incompetent human immunodeficiency virus (HIV). They have a more complex genome and opposite from γ-RV vectors have the ability to transduce also quiescent cells [84]. Besides *gag*, *pol* and *env*, they require several other genes: the central polypurine tract (*cPPT*), the central termination signal (*CTS*), the psi packaging element (*Y*) essential for efficient packaging of genetic material into the virions, and *rev* gene for enhanced nuclear export and expression which confers them in theory the capability in transducing non dividing cells [84]. Gamma-RV vectors are reported to integrated semi-randomly into the host's genome, in fact they have preferential integration sites near transcriptional start sites and CpG islands of active genes, including enhancer and promoters. In contrary, LV vectors prefers introns or transcriptionally active genes [85]. When using RV there is a risk of genotoxicity if integration occurs near a proto-oncogene or a tumor suppressor gene, which can lead to malignant transformation. However, the risk is relatively lower in LV. Insertional mutagenesis can occur through three different mechanisms: transcription of a proto-oncogenes driven by I) viral strong promoter II) viral enhancer elements that activates proto-oncogene's promoters or III) disruption of a gene resulting from the integration of the transgene [86].

One strategy to improve safety is by introducing deletions in the region responsible for the promoter/enhancer activity, the U3 LTR. During reverse transcription this deletion is transferred to the 5' LTR leading to the inactivation of the pro-virus transcription. Therefore, the virus will become "self-inactivating" (SIN) after it integrates into the host genome [87]. However, 3' LTR deletion in the vector reduce the production of high-titre vectors in cell lines that are frequently employed for manufacturing under good manufacturing practice (GMP), restricting the clinical use of γ-RV SIN vectors.

1.5.1.1 Retroviral vectors, clinical applications

Gamma-RV and LV vectors are extensively used to generate transgenic T cells, and several approved and commercialized therapies in the treatment employ these viruses (Yescarta®, Tecartus®, Kymriah®, Breyanzi®, and Abecma®).

So far, no cases of malignant transformation have been observed in HIV patients treated with T cells genetically modified using γ-RV vectors nor in treatment with Yescarta® [88][89]. Although, lymphocytes have been reported to be less predisposed to transformation due to epigenetic and pro-apoptotic mechanisms that prevent clonal outgrowth, there is still a theoretical risk of genotoxicity due to their pattern for integration sites [90].

In fact, the potential impact of the transgene integration in the host genome remains a significant area of investigation. Integration can indeed not only cause potential malignant transformation and clonal expansion, but also variation in the transgene expression levels, which might influence the clinical outcome. In accordance with this, recent findings highlight the influence of lentiviral vector integrating sites on the proliferation of T cells [91]. An analysis of a clinical study in leukaemia patients revealed that integration of the anti-CD19 CAR transgene into the TET2 locus in a patient with a hypomorphic mutation in the second TET2 allele, led to an unusual and significant expansion of a specific CAR-T cell clone, resulting in a complete response. A follow-up study in CD19 CAR T therapy targeting demonstrate that the distribution of integration sites could be used as a marker for the positive or negative outcome of the therapy [91].

The main limitation of viral vector in T cell therapy include the manufacturing time and costs associated with the GMP manufacturing process as well as the stringent regulatory requirements. In fact, the use of RV vectors derived from pathogenic virus such as HIV,

require the implementation of rigorous safety measures. These measures are necessary to prevent the formation of replication-competent viral particles [92]. Therefore, all products developed using viral vectors must undergo extensive testing to ensure compliance with clinical safety guidelines.

Another major drawback is the limited cargo capacity of around 8-10 kb, which restricts the size and number of transgenes that can be accommodated [83][84].

In summary, retroviral vectors for T cells modifications presents several challenges for T cell therapy, particularly for end-stage cancer patients who urgently require treatment. As a result, alternative non-viral gene transfer methods are being investigated, such as transposon systems, genome editing tools, mRNA, and episomal S/MAR DNA vectors.

1.5.2 Non-Viral vectors

1.5.2.1 Sleeping Beauty and PiggyBac Transposons systems

Transposable elements (TE), commonly known as "jumping genes," were originally discovered by Barbara McClintock in 1948 [93]. These DNA sequences have the remarkable ability to move within the genome, making them a valuable tool for genetic engineering. A transposon system consists of a transposase enzyme and a gene of interest flanked by terminal inverted repeats (TIRs) [94]. The transposase gene and the gene of interest are incorporated into separate plasmids, which are delivered to the target cell together. Once inside the nucleus, the transposase facilitates the excision of the gene of interest at the TIRs, enabling its integration into the genome (**Figure 3**) [94]. This system combines the advantageous features of non-viral vectors and viral vectors, combining a simple DNA-based system with persistent gene expression. Opposite to other integrating systems, transposons are typically not subjected to silencing and inherently exhibit low activity levels of promoter and enhancer.

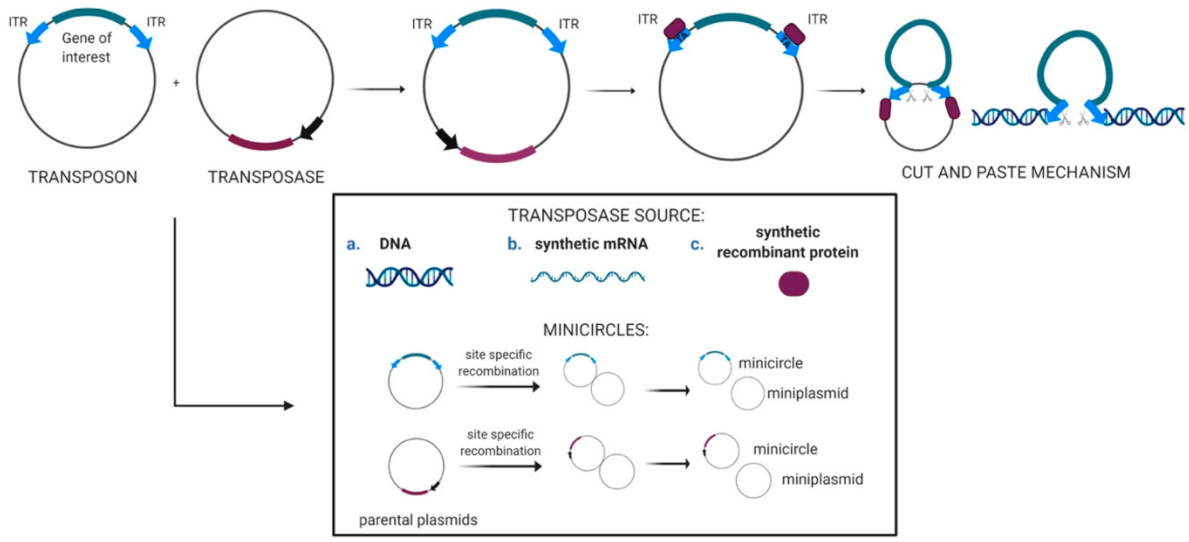

Figure 3 Schematic overview of transposons system. Transposons systems comprise two elements: a plasmid encoding for the gene of interested flanked by ITRs regions containing the transposase binding sites and a plasmid encoding for the transposase. Mechanisms of cut and paste. Image obtained from Magnani F. et al., 2020 [95].

There are two main transposon systems that are used: The PiggyBac (PB) transposon and the sleeping beauty (SB) transposon.

- PB transposon was originally discovered in the cabbage looper moth in 1980. It possesses the ability to transfer cargos up to 150 kb in size. PB has shown successful application in the engineering of human cells. However, it is important to note that PB exhibits a genome-wide integration profile like that of MLV γ-retrovirus, displaying a preference for integrating near transcriptional start sites of genes. This characteristic raises safety concerns in its use [96].
- SB transposon originally derived from salmonid fish, had been inactive for 10-15 million years before it was reconstructed and reactivated earning the name Sleeping Beauty [97]. Two hyperactive transposase variants, SB11 and SB100X, coming from molecular evolutionary processes are currently the most used for gene therapy [98]. The integration profile of SB is highly favourable compared to PB, as it does not exhibit any preferences for regulatory elements or active genes. This characteristic significantly reduces the risk of insertional mutagenesis associated with SB.

1.5.2.2 Sleeping Beauty and PiggyBac Transposons systems, clinical applications

In 2011, SB has been shown to be successful for the generation of CD19 targeting CAR T cells for treating NHL and ALL following hematopoietic stem cell transplantation (HSCT).

Several clinical trials are currently ongoing and unfortunately, one of these, the CARTELL study encountered unforeseen serious adverse events following the infusion of anti-CD19 CAR T cells engineered with PB. Two patients developed T cell lymphoma, leading to the unfortunate death of one patient [99][100]. Further analysis, shown transcriptional alterations, likely influenced by the transgene promoter rather than the specific insertional sites [99].

However, the adverse reactions founded highlight the need for further investigation into the underlying mechanisms and potential implications of these transcriptional changes in relation to the observed adverse events.

1.5.2.3 Genome editing technologies: CRISPR/Cas9

The CRISPR/Cas9 was discovered in 2012 by Charpentier, Doudna and colleagues. It derives from a bacterial natural defence mechanism which enables the cleavage of nucleic acid during bacteriophage infection, providing an acquired immunity mechanism [101]. Due to its features such as, the ability to simultaneously editing multiple genes and its practicality this system has been revolutionary in the field of gene therapy and offers potential also on cell therapy.

CRISPR/Cas9 system consist of two primary elements: the single guide RNA (gRNA) and the Cas9 endonuclease [102]. In gene therapy applications, the same principle of targeted DNA cutting, as in bacterial immunity is employed. Briefly, the gRNA, composed by a fusion of crRNA and tracrRNA connected by a tetraloop, forms a stem loop structure that interacts with the Cas9 protein, facilitating the precise cleavage of the desired DNA sequence (**Figure 4**) [102]. DNA repairing pathways will then be responsible of the genome editing; DNA sequences can then either be inserted via the homologous recombination end joining (HDR) correction mechanism or by disrupted or deleted via non-homologous end joining (NHEJ) into the genome (**Figure 4**).

Despite the excitement, first attempt is using this technology for T cells engineering showed unwanted off-target and toxicity effects [103]. In fact, the system can work with 3–5 base pair (bp) mismatches. In order to improve CRISPR/Cas9 safety and target specificity, several strategies have been employed. These strategies include the use of other Cas endonucleases, modifications of the gRNA, and screening of potential off-target sites [104].

In a recent application of CRISPR/Cas9, Sadelain, Eyquem, and their colleagues demonstrated the system's effectiveness for T cell engineering. They integrated the donor DNA encoding the CAR into the TRAC locus, resulting in the knockout (KO) of the native TCR and its subsequent replacement with the CAR. This modification led to a more physiologically CAR expression that subsequently resulted to CAR T with less differentiated phenotype and with postponed exhaustion, enhancing *in vivo* anti-tumor activity when compared to retroviral vectors [105].

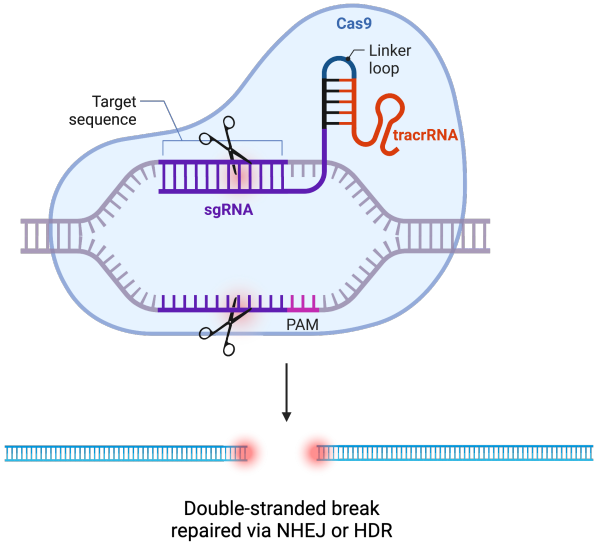

Figure 4 Scheme of the CRISPR/Cas9 genome editing technology. A specific sgRNA form a complex and directs the Cas9 nuclease to target a specific genome region. The generated DSB will then be repaired either by NHEJ or HDR. Generated with BioRender.com

1.5.2.4 CRISPR/Cas9 system, clinical applications

Since 2020, several ongoing clinical trials involving CRISPR/Cas9 have been conducted in T cell therapy; one study reported no major toxicities, and the engineered T cells demonstrated persistent long-term engraftment however, no approved therapy currently exists [106] [104] [107]. Traditionally, Cas9 was introduced with classical viral vectors or plasmids, however it has been observed that by replacing these with a ribonucleoprotein (RNP)-based approach, high efficiency can be achieved [108]. This offers an advantage since manufacturing viral vectors in compliance with GMP can be costly and time-consuming. Despite several efforts to improve safety, the off-target effects and the subsequent risk of mutations remain still a major concern for the clinical translation of this

technology. Of note, this are lower when compared with TALEN or ZFNs, which will be described in the next session [109].

1.5.2.5 Genome editing technologies: Zinc-finger nucleases (ZFNs) and transcription activator-like effector nucleases (TALENs)

In 1985, Miller, McLachlan Klug and co-workers discovered a binding motif in Xenopus called Zinc-finger nucleases (ZFNs), which have the ability to bind to various target molecules, including DNA [110]. In genome editing, tandem repeats of ZFNs are employed together with the nuclease FokI to target specific DNA sequences; however, several off-target effects have been observed. To minimize off-target effects and enable site-directed cuts, the ZF domain is often fused to the FokI DNA cleavage domain (**Figure 5**) [109]. Bosh and colleagues in 2009, reported for the first time the discovery of a transcription activator-like effector nucleases (TALENs) [111] [112]. TALENs consist of a DNA-binding domain derived from bacteria called transcription activator-like effectors (TALE) that can specifically bind to a target sequence, along with a DNA cleavage domain of a nuclease, such as FokI. TALENs enable the targeting of specific sites in the genome, and when the FokI dimer is formed between two TALEN monomers, DNA cleavage occurs within the targeted region (**Figure 5**) [112].

1.5.2.6 Zinc-finger nucleases (ZFNs) and transcription activator-like effector nucleases (TALENs), clinical applications

Several ongoing trials are investigating the feasibility of TALEN-mediated engineering of CAR T cells. Anti-CD19 CAR T cell studies have shown promising clinical outcomes, with no major toxicities observed [113]. However, and increased number of patients and more long-term follow-up analysis are still required.

The major challenges for their clinical approval include improving the efficiency of gene editing, ensuring accuracy, and addressing delivery-related issues.

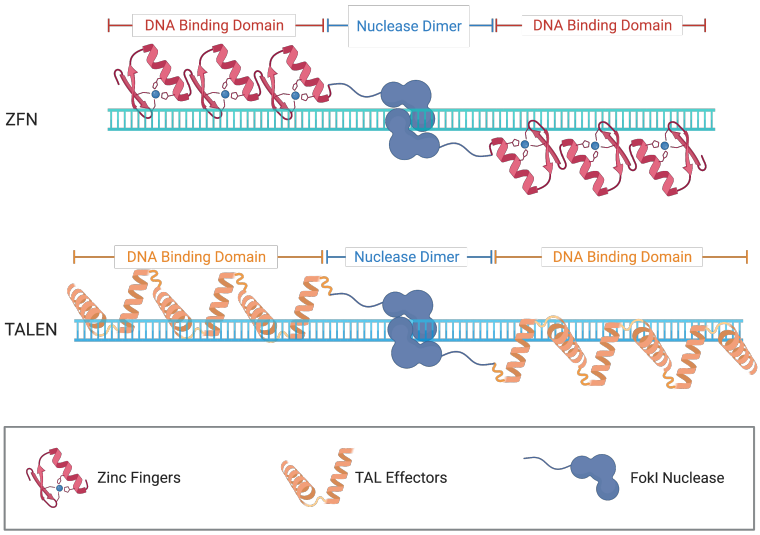

Figure 5 Schematic of the ZFN and TALEN nucleases. DNA binding domain of the ZFN and TALEN are combined with a cleavage domain (FokI) nuclease to direct and generate DSB in specific sites of the genome. Image generated with Biorender.

1.5.2.7 Synthetic messenger RNA (mRNA)

Applications of synthetic mRNA has been explored in the past years as a technique to obtain therapeutic T cells. There are substantial pre-clinical and clinical data demonstrating its in feasibility in transfecting human CAR T cells with effective anti-tumor activity [114]. However, this technology has both advantages and disadvantages. On one hand, it offers reduced toxicity. On the other hand, RNA-based electroporation can result in an unstable expression of the CAR or TCR for a maximum a week, limiting the long-term anti-tumor effect [115]. To overcome this limitation, multiple administrations can be performed [116]. Several modifications have been investigated to increase the CAR or TCR long-term expression, including modifications of open reading frames (ORFs) and the 3' and 5' untranslated regions (UTRs) [117][118]. These modifications have been conferred higher CAR or TCR expression, but not sustained expression. In a proof-of-concept study using a pre-clinical large animal model, CAR T cells transfected with mRNA were tested. Canine T cells were electroporated to express an anti-CD20 CAR for the treatment of B cell lymphoma in dogs [119]. CAR T cells demonstrated the ability to proliferate, produce cytokines, and eliminate tumor cells, thus indicating their safety and temporary anti-tumor activity.

1.5.2.8 Synthetic messenger RNA (mRNA), clinical applications

Synthetic RNA technology has already been tested in the clinic for solid and hematologic tumors that resulted in a safe treatment but with moderate effect. In a first study, CAR T cells targeting CD123 showed no toxicity however, no *in vivo* expansion and disease remission was observed too, pointing out the importance of the quality of the product [120]. In an anti-CD19 CAR T cell clinical study also transient response with no toxicity was observed [121].

1.5.3 Limitations of currently used system in clinical trials

Viral and non-viral-based genetic engineering tools described above, that can result in permanent or transient transgene expression, have been used to generate recombinant T cells. Most of the current clinical trials for adoptive T cell therapy commonly use the latest generation of retroviral (gamma retroviral and lentiviral) integrating vectors. Although the safety levels of viral vectors have been improved, they still represent a potential risk for genotoxicity and insertional mutagenesis. Moreover, the viral capsid packaging limits vector size, and thus the capacity of the expression cassette they can accommodate. Also, currently employed protocols for the generation of viral products are expensive and time-consuming. Novel, non-viral transposon systems such as Sleeping Beauty are currently under investigation in the clinic as an alternative transgene delivery vector system (ClinicalTrials.gov: NCT04102436), however the main downside effect of this approach is its requirement for a long expansion protocol that can result in T cell differentiation and poor persistence of the therapeutic T cells.

1.5.4 A novel non-viral non integrating approach: Scaffold-Matrix Attachment Region (S/MAR) Vectors

An alternative system for the stable genetic engineering of T cells are DNA vectors containing Scaffold/matrix-associated regions (S/MAR). S/MAR DNA elements are present in the mammalian genome and are understood to have both a structural and regulatory function; they tether to the nuclear matrix via the SAF-A protein and organize the eukaryotic genome into independent loops that are involved in several regulatory functions such as DNA replication and repair and regulation of gene expression (**Figure 6**) [122][123].

In 1999, pEPI, the first S/MAR-based vector based on the β-interferon (IFNβ) gene locus was developed by Piechaczek and colleagues [124]. Vectors containing S/MAR elements have two notable features: they can replicate episomally and thus be maintained in a wide range of cells, including human T cells, and provide sustained gene expression [125][126]. MAR elements have been shown to localize preferentially in actively transcribed regions, within promoter sequences and transcription start sites, allowing the vector to replicate generating associations with the origin of replication complexes (**Figure 6**) [127][128]. However, the process of establishment of an S/MAR vector as an episome is thought to be a partially stochastic process that depends on which nuclear compartment the vector settles after it reaches the nucleus; after transfection, the majority of the DNA molecules are subsequently lost within a few days and only the vectors that reach a nuclear compartment favourable for transcription and replication can be retained as episomes and therefore, be maintained through limitless cell divisions.

pEPI presented several limitations and draw backs, such as a backbone rich in CpG motifs that can trigger an innate immunity response that can subsequently result in silencing of the vector, and have poor establishment effect rate [129]. Several efforts have been made to overcome these limitations. A new vector class called pEPito was developed. pEPito was characterized by a reduced CpG island content, to minimize silencing effects and the activation of an immune response, and a chimeric hCMV/EF1α promoter, resulting to an enhanced establishment efficiency rate compared to pEPI [129]. Another advancement arrived with the development of minicircles, which are episomal vectors completely lacking any residual bacterial sequence. Minicircle showed increased expression of the transgene and higher establishing rates both *in vitro* and *in vivo* [130][131]. However, minicircle also present limitations; the production process involves recombination of the vector and is very laborious.

Our group is also actively involved in the development of a next generation class of vectors, leading to the development of a next-generation class of vectors, the nanoS/MAR (nS/MAR) platform.

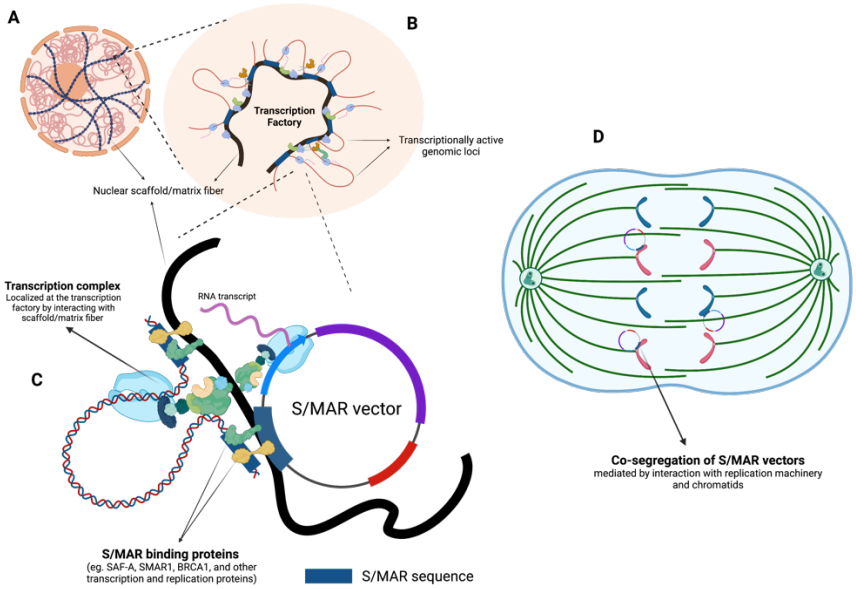

Figure 6 Schematic of S/MAR DNA Vectors. A) S/MAR DNA vectors are tether to the nuclear matrix through interactions with TFs and the SAF-a protein. **B)** S/MAR sequences have a structural function and helps the formation of loops. S/MAR DNA vectors are associated with transcriptionally active regions. **C)** Model proposing the replication of an S/MAR DNA vector during cell division in a S. Cerevisiae model. Image adapted from Toros Tasgin.

1.5.4.1 Towards the development of a next generation of S/MAR DNA vectors

Several features have been modified to develop the latest generation of vectors. In pEPI, the transgene was physically distant from the Kanamycin/G418 selection marker that was placed in the bacterial backbone. The initial modification involved the replacement of the eukaryotic selection marker G418 with Puromycin and its link with the transgene [132]. Additionally, an insulator, such as UCOE or Element40, was placed before the promoter to prevent silencing.

Variations of the S/MAR were also performed. The classic 2Kb IFNβ-S/MAR was replaced with the 800 bp sequence of the apolipoprotein cluster (ApoL) (**Figure 7**). Subsequently, a core version of this sequence, 500 bp, was used known as coreApoL (C/MAR) (**Figure 7**) [132][133]. This modification also decreased further the vector size and resulted in enhanced transgene expression and establishment rates. In order to improve S/MAR RNA stability, which is necessary for conferring mitotic stability and keeping the vector in an episomal state, the S/MAR region was flanked by splice sites [133]. This resulted in enhanced establishment efficiency and transgene efficiency.

Finally, the kanamycin bacterial backbone was substituted with a nano-sized bacterial backbone known as NTX™ RNA-out, enabling antibiotic free selection (**Figure 7**)

[133][134]. The NTX™ RNA-out backbone offers several advantages. This technology is based on a small RNA interference strategy [135]. In the context of gene therapy vectors, it is desirable to avoid the use of resistance markers that encode proteins, as this can affect cell viability and disrupt normal cellular functions. Moreover, this replacement not only completely eliminated any CpG islands from the vector, minimizing silencing events, but also reduced the backbone size from 1725 bp to 458 bp [133]. As a result, it led to higher levels of transgene expression and stability, while also reducing immunogenicity and toxicity. Overall, this class of plasmids offers improved safety and efficiency compared to traditional plasmids. In fact, instead of the classical pUC origin of replication, the backbone contains a bacterial origin called R6K, which renders them replication-incompatible with other organisms [135].

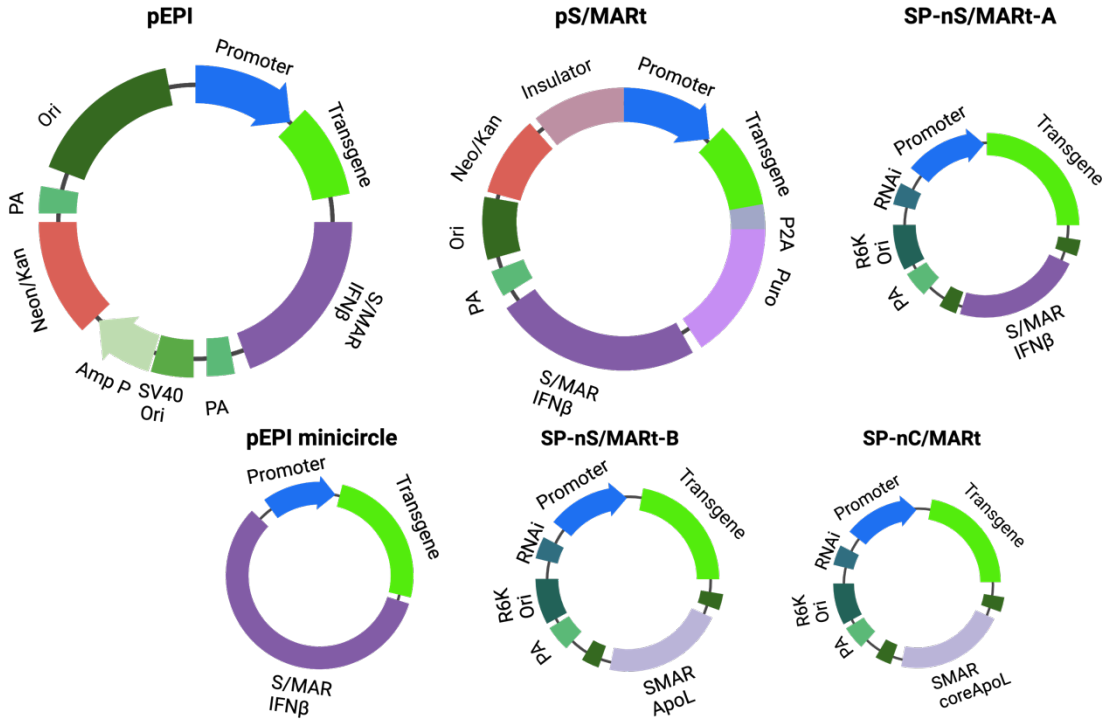

Figure 7 Schematic of the S/MAR DNA Vector development. Steps of the development of the S/MAR DNA Vector platform. Modification in the bacterial backbone, the S/MAR sequence and the addition of insulator elements brought to the next generation of vectors: the nSP S/MAR Vectors. Image created with Biorender .

Different generations of these vectors were employed to successfully engineered different cell types, such as several tumor cells including the pancreatic tumor cells (PaCo) which have shown stability in restoring gene function both *in vitro* and *in vivo* models as wells as human and mouse ESCs and iPSC [134][136].

2. Aim of the thesis

The overall goal of this thesis is to explore the potential of the nS/MAR DNA platform in modifying T cells for Adoptive Cell Therapies (ACT). Specifically, the aim is to investigate the applicability of this technology in generating CAR and TCR transgenic T cells for both hematological and solid tumors, with the ultimate goal of clinical translation.

Furthermore, this research seeks to refine the nS/MAR DNA vectors to optimize their effectiveness as delivery vectors for personalized immunotherapies targeting brain tumors. Given the existing limitations of current ACTs in effectively targeting solid tumors, particularly those in the brain, this project aims to enhance the non-viral S/MAR DNA vectors to generate recombinant T cell that can augment T cell-mediated tumor killing by enhancing immune responses, such as the expression of pro-inflammatory cytokines like hIL12, drawing inspiration from the TRUCK paradigm (T cells redirected for universal cytokine-mediated killing).

Finally, this thesis investigates the potential of the developed technology to establish a manufacturing protocol capable of rapidly producing TCR T cells at clinical scale. This protocol offers several advantages over current methodologies, providing a streamlined and efficient process for generating therapeutic T cells.

3. Material and methods

3.1 Materials

Table 1. Cell lines used in this study.

Name	**Description**
MeWo	Human malignant melanoma cells, derived from melanoma skin cancer
Mel264	Human malignant melanoma cells, derived from melanoma skin cancer
Jurkat 76	Human T cell line derivative, deficient of endogenous CD8 expression
HT-29	Human colon cancer cells, derived from primary tumor
MCF-7	Human breast cancer cells, derived from metastatic tumor
U87	Human glioma cells, derived from primary tumor
Nalm-6	Human B cell precursor leukemia cells, derived from acute lymphoblastic leukemia
Nalm-6	Human B cell precursor leukemia cells, derived from acute lymphoblastic leukemia

Table 2. Culture media used in this study.

Reagent	**Company**
DMEM	Sigma
RPMI	Sigma
TexMACS	MACS

Table 3. Reagents and components used for cell culture.

Reagent	**Company**
β-mercaptoethanol	Gibco
Fetal Bovine Serum	Gibco
HEPES buffer	Panreac
L-Glutamine (x100)	Gibco
Penicillin/Streptomycin (x100)	Sigma-Aldricht
Phosphate Buffered Saline (1xPBS)	Gibco
Trypsin EDTA (x1)	Sigma-Aldricht
Penicillin/Streptomycin (x100)	Sigma-Aldricht
Phosphate Buffered Saline (1xPBS)	Gibco
Trypsin EDTA (x1)	Sigma-Aldricht
Transact	Miltenyi Biotec
hIL7	Miltenyi Biotec
hIL15	Miltenyi Biotec

Table 4. Vectors used in this study.

Vector	**Promoter**	**Transgene**	**S/MAR**
SP-nC/MARt sEF1α MART-1 TCR	sEF1α	MART1 TCR	cApoL 500 bp
SP-nC/MARt hPGK MART-1 TCR	hPGK	MART1 TCR	cApoL 500 bp
SP-nC/MARt hWASP MART-1 TCR	hWASP	MART1 TCR	cApoL 500 bp
SP-nC/MARt hCD3 MART-1 TCR	hCD3	MART1 TCR	cApoL 500 bp
SP-nC/MARt hTCR MART-1 TCR	hTCR	MART1 TCR	cApoL 500 bp
SP-nC/MARt sEF1α GB TCR	sEF1α	GB TCR	cApoL 500 bp
SP-nC/MARt sEF1α ft ct10 A1	sEF1α	TCR 1	cApoL 500 bp

SP-nC/MARt sEF1α ft 39 ct 27	sEF1α	TCR 2	cApoL 500 bp
SP-nC/MARt sEF1α ft 346 ct 246	sEF1α	TCR 3	cApoL 500 bp
SP-pC/MARt sEF1α MART1 NFATTATA^{syn}-hIL12	sEF1α and TATA^{syn}	MART1 TCR and HIL12	cApoL 500 bp
SP-pC/MARt sEF1α MART1 NFATIL12minip-hIL12	sEF1α and IL2minp	MART1 TCR and HIL12	cApoL 500 bp
SP-pC/MARt sEF1α GFP-P2A-dTomato	sEF1α	GFP and dTomato	cApoL 500 bp
SP-pC/MARt sEF1α GFP	sEF1α	GFP	ApoL 800 bp
SP-nS/MARt-A GFP	EF1α	GPF	ApoL 800 bp
SP-nS/MARt-B GFP	EF1α	GFP	ApoL 800 bp
SP-nS/MARt-B anti-CEA CAR	hPGK	CEA CAR	ApoL 800 bp
SP-nS/MARt-B anti-CD19 CAR	hPGK	CD19 CAR	ApoL 800 bp
pEPI	CMV	GFP	IFNβ 2 kb

Table 5. Kits used in this study.

Kit	**Company**
Amaxa SE Nucleofection Kit	Lonza
Amaxa P3 Primary Cell Nucleofection Kit	Lonza
CD8a T Cell Isolation Kit Miltenyi	Miltenyi Biotec
Pan T Cell Isolation Kit Miltenyi	Miltenyi Biotec
DNeasy Blood & Tissue Kit	Qiagen
TempliPhi Amplification Kit	GE Healthcare
Life Technologies Cell Trace Violet Proliferation	Theermo Fishher Scientific
DNeasy Blood & Tissue Kit	Qiagen
TempliPhi Amplification Kit	GE Healthcare
Wizard Genomic DNA Purification Kit	Promega
LDH-Glo® Cytotoxicity assay Kit	Promega
Clone Amp HiFi PCR preMix	Takara

Human IL-12 p70 DuoSet ELISA	R&D Systems
ELISA MAX™ Deluxe Set Human IFN-γ	BioLegend

Table 6. Antibodies used for FACS staining.

Name	**Host**	**Clone**	**Company**
APC anti-human CD3	Mouse	SK7	BioLegend
APC anti-human CD8	Mouse	SK1	BioLegend
FITC anti-human CD8	Mouse	SK1	BioLegend
Alexa Fluor® 700 anti-human CD3	Mouse	UCHT1	BioLegend
PE anti-mouse TCR β chain	Armenian Hamster	H57-597	BioLegend
APC anti-mouse TCR β chain	Rat	QA18A18	BioLegend
FITC anti-mouse TCR β chain	Armenian Hamster	H57-597	BioLegend
BUV737 anti-human CCR7	Rat	3D12	BD
PerCPCy5.5 anti-huma CD45RA	Mouse	HI100	BD
APC anti-human CD137	Mouse	4B4-1	BioLegend
PE anti-human IgG CAR	Mouse	AffiniPure F(ab‘)$_2$ Fcγ fragment	Jacksonimmunogy

Table 7. Reagents and chemical compounds used in this study.

Reagent	Company
Agarose	Sigma Life Science

Dimethylsulfoxid (DMSO)	Carl Roth
Ethanol	Sigma-Aldrich
Isopropanol	Sigma-Aldrich
Luciferin	BIOMOL
PeqGreen DNA/RNA Dye	PeqLab
Trypan Blue Stain 0.4%	Logos
PeqGreen DNA/RNA Dye	PeqLab
Trypan Blue Stain 0.4%	Logos

Table 8. Primers used in this study.

Name	**Sequence**
ct27.FOR	CTCTCCACAGGCTAGCATGGGCCCCCAG
ct27.REV	TCTGCATGCATGTCGACTCAGCTGGACCACAGTCTCAGG
ct10.FOR	CTCTCCACAGGCTAGCATGAGCAACCAGGTG
ct10.REV	TCTGCATGCATGTCGACTCAGCTGGACCACAGTCTCAGG
ct246.FOR	CTCTCCACAGGCTAGCATGGGCCCCCAG
Ct246.REV	TCTGCATGCATGTCGACTCAGCTGGACCACAGTCTCAGG
GFP.FOR	CTCTCCACAGGCTAGCATGCCCGCCATGAAGATCGAG
GFP.REV	TCTGCATGCATGTCGACTCAGGCGAAGGCGATGG
GFP-P2A-dTomato.FOR	CTTTCTCTCCACAGGATGCCCGCCATGAAGATCG
GFP-P2A-dTomato.REV	CCCTTGCTCACCATGGGCCCAGGGTTT
minipIL12.FOR	GCGTAGATCTGGCCTTCTGCAGGACATGTGTAG
minipIL12.REV	ACTCATCGAGCTCGAGATAAAAATCATTAGGTACCTTAGC
TATA^{syn}hIL12.FOR	AATCATTAGGACTAGTAAGCTTCTCGAGGCCTACCGGAG

TATA^{syn}hIL12.FOR	GAAGAATTATTTAAGTAACAGAATAAAAATGGAAAC GGAGAAATTATGGAG

Table 9. Markers used for gel electrophoresis.

Marker	**Company**
100 bp DNA ladder	New England Biolabs (NEB)
1 kb DNA ladder	New England Biolabs (NEB)

Table 10. Equipment used in the laboratory.

Equipment	**Company**
Amaxa 4DNucleofector	Lonza
Centrifuge 5424R	Eppendorf
Centrifuge 5430R	Eppendorf
Centrifuge 5810	Eppendorf
FusionSL Vilber Lourmat	PeqLab
Horizontal Gel Electrophoresis System	Horizon
Light Cycler 96	Roche
NanoDrop 2000c	Thermo Fisher
NUARE incubator	Tecnomara
Thermomixer Comfort	Eppendorf
4D-Nucleofector®	Lonza Bioscience
MaxCyte ExPERT GTx™	MaxCyte

Table 11. Software used in this study.

Name	**Description**
FlowJo 10	Platform for flow cytometry analysis
FUSION-CAP Software	Software for luminescent image acquisition and analysis
Biorender	Software for graphic design
Zotero	Software for references

GraphPad Prism 8	Software for statistical analysis

3.2 Methods

3.2.1 Cloning

3.2.1.1 Digestion with restriction enzymes

Restriction digestions were performed according to the manufacture instructions. For the production of pS/MAR vectors the base vectors Ele40-500bp ApoL dTomato with sEF1α promoter was used while for nS/MAR vectors the JP4.17 NTX as backbone. The vectors were cut with one or two specific restriction enzymes to linearize the plasmid either to remove the transgene or to insert a second transgene or an expression cassette. Restriction digestions were carried out for 20 minutes at 37˚C and according to the table below:

DNA vector	2-4 µg
Enzyme 1	1 µl
Enzyme 2	1 µl
10x FD Green Buffer	2 µl
H_20	x µl
Total	**20 µl**

Subsequently the desired fragments were run in an agarose gel 1% and then purified with gel extraction kit form Qiagen according to the manufacture instructions.

3.2.1.2 Polymerase chain reaction (PCR)

Insert of interest was amplified by PCR reaction with the CloneAmp™ HiFi PCR Premix following the manufacture instructions. Cloning and primers design was done with the SnapGene software. 0.5-1 ng of DNA template was amplified according to the manufacture instruction following the table below:

CloneAmp™ HiFi PCR Premix	12.5 µl
Forward Primer (10 µM)	0.75 µl
Reverse Primer (10 µM)	0.75 µl
Template DNA	0.5-1 ng
H_20	x µl
Total	**25 µl**

The reaction was carried out in a thermocycler (PeqStar) according to the the table below:

Step	Temperature - Time
1. Denaturation	95 ˚C – 2 min
2. Denaturation	98 ˚C – 10 sec
3. Annealing	Primer Tm ˚C – 10 sec
4. Extension	72 ˚C – 5 sec/Kb
5. Final Extension	72 ˚C – 10 min
6. Storage	8 ˚C

Step 2 and 4 were repeated for 35x cycles.

3.2.1.3 Agarose gel electrophoresis

Agarose gel electrophoresis was performed on 1% agarose. 4 µl of the dye PeqGreen DNA/RNA were added into 50 ml of agarose solution. DNA and appropriate loading marker were then loaded into appropriate wells. Electrophoresis was normally run at 100 V and then gel visualized in a UV-Transillumiator; images were then analyzed with the FusionSL Lourmat.

3.2.1.4 DNA Gel extraction

Desired DNA fragments, from either restriction digestions or PCRs, were excised from 1% agarose gel with a scalpel blade. DNA was then extracted using the QIAquick Gel extraction (Qiagen) according to the manufacture instructions. 1 volume of gel was mixed with 3 volumes of solubilisation for 10 min at 50˚C until gel dissolution. Then, 1 volume of isopropanol was added and subsequently transferred into a Spin column and centrifuged at max speed for one minute. A washing step with washing buffer was then performed and DNA solution eluted in 25 µl of TE Buffer.

3.2.1.5 In-Fusion® cloning

DNA insert, previously amplified by PCR, was cloned into linearized plasmid DNA, previously digested, through homologous recombination using the In-Fusion® cloning (Takara) kit following the manufacture instruction and the following table:

PCR template	100 ng
Linearized vector	50 ng
5x In-Fusion® HD Enzyme Premix	2 µl
H_20	x µl
Total	**10 µl**

3.2.2 Bacterial methods

3.2.2.1 Bacterial culture

E. coli strain Stellar Super competent cells were cultivated in sterile Luria-Bertani (LB) broth supplemented with Amplicillin. The volume of the cultures varied based on the specific experiment requirements and ranged from 5 ml for extracting plasmids using a Miniprep kit to 250 ml for generating larger quantities of pDNA using a Maxiprep method. To obtain isolated bacterial colonies derived from a single cell, the cultures were spread onto solid agar plates and incubated overnight at 37°C. After incubation, separate colonies were visible and could be picked for further analysis or experiments.

3.2.2.2 Bacterial transformation

The stellar super competent commercially available bacterial cells, were thaw on ice and subsequently aliquoted in pre-chilled 1.5 ml Eppendorf tubes. Each tube contained 2.5 µl In-fusion reaction. Bacteria were then incubated for 30 minutes on ice, then a 45-second heat shock at 42°C was performed, followed by a 2-minute recovery on ice. Next, 450 µl of pre-warmed SOC medium was added, and the cultures were incubated with 200 rpm shaker for 1 hour. Subsequently, 50 µl of bacterial cells were spread onto pre-warmed LB agar plates supplemented with Ampicillin for transformants selection.

3.2.2.3 *RNA-out RK6 Bacterial culture and transformation*

RNA-out RK6 bacterial culture and transformation was performed following the manufacture instruction of Nature Technology.

3.2.3 Plasmid DNA isolation

3.2.3.1 Miniprep: small scale isolation

To perform a small-scale plasmid isolation, 5 ml cultures of E. coli were cultivated in LB medium with Ampicillin and the plasmid DNA subsequently isolated using the Miniprep spin column kit provided by Qiagen according to the manufacture instructions. First, the bacterial cells were centrifuged at 15,000 rpm for 1 minute using an Eppendorf 54324 R Centrifuge. The pellet was then resuspended in a resuspension buffer containing RNase A, and subsequently the cells were lysed using the provided lysis buffer. To precipitate proteins and neutralize the lysate, neutralization buffer was added. Cellular debris were removed by centrifugation at 15,000 rpm for 10 minutes, and the supernatant, containing

the target pDNA, was carefully transferred to a spin column and centrifuged at 15,000 rpm for 1 minute. The pDNA selectively bound to the column matrix during this step. Following two wash steps to remove impurities, the pDNA was eluted from the column using 30 µl of elution buffer allowing the isolation of 100-200 ng/ µl of pDNA,

3.2.3.2 Maxiprep: large scale isolation

Larger quantities of DNA were isolated using the EndoFree Plasmid Maxiprep kit supplied by Qiagen, according to the manufacture instructions. 5 ml from a positive clone culture was used to inoculate 250 ml of fresh LB medium supplemented with Ampicillin in a 1-liter flask and incubated overnight in a shaker 200 rpm at 37 C. Then bacterial cells were centrifuged using a Sorvall RC6+ centrifuge for 15 minutes at 6,000 rpm. The resulting pellet was resuspended in a resuspension buffer supplemented with RNase A by vortexing. Subsequently, the cells were incubated with lysis buffer at RT for 3 minutes. Neutralization buffer was the added, and the resulting lysate was incubated in an endotoxin-removal buffer. The lysate was then applied to a column containing an ion-exchange resin. Under conditions of pH 7 and ionic strength of 750 mM NaCl, the DNA selectively bound to the resin. Afterward, the DNA was eluted from the column. 0.7 volumes of isopropanol were then added, and 30 minutes centrifugation at 15,000 rpm using a Sorvall RC6+ centrifuge performed. The resulting pellet was washed with 70% ethanol and subsequently resuspended in 100-250µl of endotoxin-free elution buffer, depending from the size of the pellet.

3.2.3.3 DNA concentration and purity

NanoDrop 2000c spectrometer (Thermo Fisher) was utilized to measure the DNA concentration and purity of the recovered plasmid DNA. The purity can be estimated via absorbance ratio of A260/A280; decent levels of DNA purity typically exhibit ratios ranging from 1.7 to 1.9. RNA contaminations will result in higher ratio, while a lower ratio indicates the presence of protein contaminants. To serve as blank controls for the OD measurements, elution buffers specific to each protocol were used.

3.2.4 Southern Blot

For the detection of episomal pDNA, total DNA was isolated using the DNA Blood&Tissue Extraction kit from Qiagen. 10-15 µg of DNA were digested overnight using appropriate restriction enzyme(s). The digested DNA was mixed with 10x Loading Dye (LD) and

separated on a 0.8% agarose gel at 20 mV overnight. Then the gel was immersed for 10 minutes in 0.25 M HCl and subsequently underwent two 15-minute incubations in depurination buffer, followed by incubation in neutralisation buffer for 15 minutes. DNA was then transferred, using capillary action, into a nylon membrane. Whatman 3MM paper was placed into a tank containing 20x SSC nucleic acid transfer buffer and the gel placed on a layer of the paper. Then a nylon membrane from Amersham Bioscience, Hybond XL, was immerse in buffer and put on top of the gel, ensuring the removal of any bubbles. Paper towels were then arranged, and a weight was put on top of the apparatus. The transfer process was the performed overnight. The day after, the nylon membrane was exposed to UV radiation for one minute in order to permanently cross-link the DNA fragments to the membrane, ensuring their stable attachment. To generate DNA fragments for probing, the GFP gene reporter was used. The fragments were labeled with 32P using the Prime-It II Random Primer Labelling kit from Agilent Technologies. Subsequently, a hybridization process was carried out in Church buffer at a temperature of 65°C for a duration of 16 hours.

3.2.5 Rolling Circle Amplification (RCA)

DNA Blood and Tissue Extraction kit (Qiagen) was used to isolate total DNA and the TempliPhi Amplification Kit from GE Healthcare, was used to detect episomal state of the vector. 20 ng of DNA were used for the RCA reaction. DNA was denaturated at 95°C for 3 minutes, followed by immediate transfer to ice. Subsequently, the master mix was";/ added, and the reaction was incubated at 30°C for 18 hours. Then, the reaction was incubated for 2 minutes at 65°C, and subsequently cooled down to 37°C. Then digested with the BamHI single cutter (Thermo Fisher Scientific), for 30 minutes and resolved on a 0.8% agarose gel.

dead cells. Samples were acquired, using BD LSR Fortessa and the resulting data was analyzed with FlowJo V10.

3.2.6 Human cell culture methods

3.2.6.1 Human adherent cell lines

Human adherent cell lines were cultured according to the recommended manufacture instruction provided by the American Type Culture Collection (ATCC). Specifically, the

cells were cultured in Dulbecco's Modified Eagle's Medium (DMEM) or Roswell Park Memorial Institute (RMPI) supplemented with 10% heat-inactivated Fetal Bovine Serum (FBS), penicillin (5 U/ml), and streptomycin (50 mg/ml). Cell monolayers were grown in sterile Petri dishes until they reached 80%-90% confluence. At this stage, the growth medium was replaced. To accomplish this, the existing medium was aspirated, and the cell monolayer was gently washed with phosphate-buffered saline (PBS). Subsequently, a Trypsin-EDTA solution was added to the cells and incubated at 37°C for 3-5 minutes and subsequently trypsin activity was neutralized by adding two volumes of growth medium. A portion of the detached cells was transferred to a new dish containing fresh growth medium and cells were then cultured in a NUARE incubator (Tecnomar) at 37°C in a 5% CO2 atmosphere. Cell passaging was performed twice a week, typically at a ratio of 1:6 - 1:10, depending on the experimental requirements.

3.2.6.2 Human suspension cell lines

Mammalian suspension cells were cultured in RPMI growth medium, following the ATCC instructions. The medium was typically supplemented with 10% heat-inactivated fetal bovine serum (FBS), penicillin (5 U/ml), and streptomycin (50 mg/ml). Cell lines were cultured in appropriately sized flasks based on the cell number at a $1x10^6$/ml concentration. When the cells reached 80%-90% confluence, were centrifuged at 350 rcf for 5 minutes, old medium was replaced with fresh one and then cells were transferred to a new flask at a concentration of $1x10^6$/ml. Cell passaging was performed three times a week to maintain cell viability and growth. The cells were passaged at a ratio of 1:3 - 1:10, depending on the experimental requirements. The cells were cultured in a NUARE incubator (Tecnomar) at 37°C in a 5% CO2 atmosphere.

3.2.6.3 Freezing and thawing of cells

To preserve cell lines for long-term storage, cryopreservation techniques were employed. Upon collection, cells were centrifuged and resuspended in freshly prepared "frozen medium" consisting of 90% fetal bovine serum (FBS) and 10% dimethyl sulfoxide (DMSO). The cell suspension was then aliquoted into cryotubes and placed in a -80°C freezer for two days and then moved to N2 tank for long-term storage. For cell revival, frozen cells were quickly thawed by immerging the cryotubes in a 37°C water bath for approximately 2-3 minutes. Once completely thawed, the cells were diluted in fresh medium, centrifuged at low speed (150 rcf for 7 minutes), and subsequently resuspended

with fresh medium and then seeded into a new culture flask. To ensure the removal of any remaining traces of DMSO, the growth medium was changed the following day after cell seeding. This step helped maintain optimal culture conditions for the cells without the presence of cryoprotective agents.

3.2.6.4 Dead cells removal

Dead cell removal was carried out using the Dead Cell Removal Kit from MACS-Miltenyi Biotech according to the manufacture instructions. Cells were first labelled with MicroBeads and then passed through a LS magnetic separation column. Cell debris, dead cells, and dying cells were magnetically labeled with the MicroBeads solution were retained within the column, while the unlabelled living cells passed through in the flow-through.

3.2.6.5 Jurkat 76 transfection

T cells were transfected using the Amaxa 4D-Nucleofector electroporator (Lonza). User guidelines and nucleofection solutions were obtained from Lonza. Jurkat 76 T cells were collected, counted and the desired number centrifuged at low speed, 100 rcf for 10 minutes. A washing step with plain TexMacs medium was performed and then cells resuspended in electroporation (EP) buffer. Strip or cuvette devices were used, depending on the desired number of cells to be transfected. For strip devices, $2x10^6$ cells along with 1 µg of DNA were used, while for cuvettes $1x10^7$ cells and 5 µg of DNA were used. Cells resuspended in EP buffer were mixed with DNA immediately electroporated with CL-120 program. After EP cells were then recovered in strips/cuvettes at room temperature for 10 minutes and then transferred to the appropriate vessel (according to the cell number) containing pre-warmed plain RPMI medium. Six hours after transfection, medium was replaced with 10% RPMI.

3.2.6.6 Generation of GFP expressing MeWo cell line

MeWo cells were transfected using the Amaxa 4D-Nucleofector electroporator (Lonza). User guidelines and nucleofection Amaxa 4D Nucleofector SF Kit were obtained from Lonza. MeWo cells were collected, counted and the desired number centrifuged at low speed, 100 rcf for 10 minutes. A washing step with PBS was performed and then cells resuspended in 100 µl of electroporation (EP) buffer. $1x10^6$ cells were mixed with 1.6 µg of GFP-P2A-Puro nS/MAR DNA and immediately electroporated. After EP cells were then

recovered in the cuvette at room temperature for 10 minutes and then transferred to the a 6 well plate contained 2 mL of pre-warmed DMEM 10% medium. 24 hours after transfection, medium was replaced with fresh DMEM 10%. 72 hours post transfection, medium was replaced with fresh DMEM 10% supplemented with 1 µg/mL of Puromycin; cells were cultured in the presence of puromycin for approximately one month, GFP expression was then assessed by flow cytometry analysis and once the expression was stable cells and aliquote of cells was used for further experiments while other aliquote was stored in liquid nitrogen for future experiments.

3.2.7 Primary T cells cell culture methods

3.2.7.1 Peripheral Blood Mononuclear Cells (PBMCs)

PBMCs were isolated using Ficoll-Paque density gradient centrifugation method. Healthy donors buffy coats were obtained from the Blood Bank of Heidelberg Hospital. To begin, the received buffy coat was diluted 1:1 with PBS and carefully layered on top of the Ficoll gradient in a 50 ml Falcon tube. Then, a gentle centrifugation step at 350g for 30 minutes without brakes or and low acceleration was performed. This centrifugation allowed for the separation of mononuclear cells from other blood components, resulting in the formation of distinct layers. The layer containing the PBMCs was carefully collected with a Pasteur pipette. PBMCs were then washed with PBS three times and then resuspended in Red Blood Cell Lysis Buffer RBC (1X) diluted with sterile distilled water and incubated for 10 minutes at 37°C. The cells were then washed two more times with PBS and finally resuspended in TexMACs growth medium and plated into flasks based on the harvested cell quantity. The flasks were incubated overnight at 37°C with 5% CO2 before proceeding with T cells isolation.

3.2.7.2 CD3+ isolation

CD3+ T cells were isolated using the Pan T Cell isolation kit from MACS-Miltenyi Biotech, following the manufacture istructions. Cells were first labelled with a biotin-conjugated antibody cocktail and then with MicroBeads. PBMCs were then passed through a LS magnetic column, where labelled cells were retained while unlabelled cells, representing the desired cell population, were collected in the flow-through. After isolation, the T cells were resuspended in TexMACS growth medium supplemented with IL7 (10 ng/µl), IL15 (10 ng/µl), and TransAct (10 µl/ml). T cells were then seeded at a density

$1x10^6$/ml and incubated at 37°C with 5% CO2 for three days before proceeding with transfection.

3.2.7.3 CD3+ transfection

T cells were transfected either with the Amaxa 4D-Nucleofector or the Maxcyte GTx electroporators. User guidelines and nucleofection solutions were obtained from Lonza or Maxcyte for the transfection procedures. T cells were collected, counted and the desired number centrifuged at low speed, 100 rcf for 10 minutes. A washing step with plain TexMacs medium was performed, and then CD3+ cells resuspended in electroporation buffer (EP). For the Lonza, strip or cuvette devices were used depending on the desired number of cells to be transfected. For strip devices, $2x10^6$ cells along with 2 µg of DNA were used, while for cuvettes $1x10^7$ cells and 10 µg of DNA were used. For Maxcyte, a concentration of 1 $x10^8$ CD3+ T cells/ml with 250 µg/ml was used. Cells resuspended in EP buffer were mixed with DNA immediately electroporated with the programs F-115 for Lonza or Expanded T cells 4 for Maxcyte. Cells were then recovered in strips/cuvettes for Lonza at RT for 10 minutes while with Maxcyte were transferred in a 96-well plate and recovered for 20 minutes at 37°C with 5% CO2. CD3+ cells were transferred to the appropriate vessel (according to the cell number) containing pre-warmed plain TexMacs medium. Six hours after transfection, medium was replaced with TexMacs medium supplemented with IL7 (10 ng/µl), IL15 (10 ng/µl).

3.2.8 Spheroids formation and co-culture assays

For the formation of tumor spheroids 2000 MeWo GFP+ tumor cells were co-cultured with 3000 MRC-5 fibroblast in 150 µl of TexMacs medium in 96 well ULA plates. Plate were placed at 37°C with 5% CO2 until spheroids formation. After spheroids formation, effector anti-MART-1 TCR T cells were co-culture at a ratio 5:1 with tumor spheroids in a final volume of 300 µ l of TexMacs medium. Spheroids growth and GFP expression was followed for 10 days every 12 hours using the Incucyte Live Cell Imaging® (Sartorius).

3.2.9 Cell Trace Violet (CTV) proliferation assay

The intercalating dye CTV from Thermo Fisher Scientific was used to assess the proliferation rate of DNA and mock-electroporated cells. CTV enables, to trace multiple generations through dye dilution analyzed by flow cytometry by the labelling of cells with

a dye. CD3+ T cells were isolated and activated for 2 days. were centrifuged at 200 rcf, resuspended in PBS and then stained with CTV, at a final concentration of 5 mM, for 20 minutes at 37°C in the dark. Then, culture medium was added, and centrifuged at 200 rcf for 10 minutes. Two washing steps were then performed with PBS containing 5% FCS. Finally, T cells were electroporated and an aliquote analyzed on the flow cytometer to detect generation 0, using a detection channel of 405 to 450/50. 7AAD (7-Aminoactinomycin D) was used to distinguish live/dead cells. At day 3, and day 5 the cells were again recorded.

3.2.10 Cytotoxicity assays

3.2.10.1 Real-time cytotoxicity assay: xCELLigence

In order to assess *in vitro* cytotoxicity and T cell activation, real-time cytotoxicity assays were conducted using the xCELLigence RTCA SP device from ACEA Biosciences. Target cells were initially seeded in duplicate or triplicate on an E-Plate 96 at a density of 2.5-4 × 10^4 cells/well and growth for 24 hours. Impedance readings were taken at 5-minute intervals, and the resulting data was plotted as a cell index. CAR or TCR T effector cells were added to the target cells in a serial dilution, to an effector-to-target (E:T) cell ratio of 2:1 or 1:1 depending on the experiment. The measured cell index was used to evaluate the viability of the target cells, in relation to the untreated control as a reference, and the mean viability ± standard deviation over time was plotted. The RTCA software was used to calculate the EC_{50} values using the with the sigmoidal dose response algorithm. Following a 48-hour co-culture, supernatant was collected from each well and the concentration of IFN-γ recorded using the BD OptEIA Human IFN-γ ELISA kit (BD Biosciences), according to the manufacture instructions.

3.2.10.2 Crystal Violet assay

Cytotoxicity assays were performed using the Crystal Violet Assay. U87-TMG tumor cells were seeded on a 96-well plate (3×10^4 cells per well) and incubated for 24 hours. TCR T effector cells were added at an effector-target cell ratio of 2:1 and co-incubated at 37°C in RPMI 10% medium for 24 hours. After the 24-hour co-incubation, 50 µl of supernatant per well was collected, and the production of IFN-γ was measured using the BD OptEIA Human IFN-γ ELISA kit (BD Biosciences) according to the manufacturer's instructions. Next, the medium was completely removed, and the cells were incubated at room

temperature for 30 minutes with 50 µl of Crystal Violet. The Crystal Violet was then removed by repeated immersion in dH20 and allowed to dry overnight. Finally, 200 µl of methanol was added to dissolve the Crystal Violet, and the absorbance was measured at 570 nm.

3.2.10.3 LDH assay

Cytotoxicity assays were performed using the lactate dehydrogenase (LDH) assay. U87-TMG tumor cells were seeded on a 96-well plate (3×10^4 cells per well) and TCR T effector cells were added at an effector-target cell ratio of 2:1 and co-incubated at 37°C in RPMI 10% medium overnight. Afterwards, 50 µl of supernatant per well was collected, and the production of LDH was measured via LDH-Glo™ Cytotoxicity Assay.

3.2.11 Enzyme-linked immunosorbent assay (ELISA)

3.2.11.1 Human INF-γ ELISA

ELISA MAXTM Deluxe Set Human INF-γ (Biolegend) was used to detect production of IFN-γ after co-culture, following the manufacture instructions. Briefly, after 24-48 hours co-culture supernatant was collected, centrifuged at 350 rcf to remove debris and stored at -80 C until further use. Before proceeding with assay, supernatant was thawn and pre-diluted (1:25-1:100) according to experiment requirments.

3.2.11.2 Human IL12 ELISA

Human IL12p70 DuoSet ELISA (R&D Systems) was used to measure the production of hIL12 after coculture assays, following the manufacture instructions. Briefly, after 48 hours of co-culture supernatant was collected, centrifuged at 350 rcf to remove debris and stored at -80 C until further use. Before proceeding with assay, supernatant was thawn and pre-diluted (1:10) and the ELISA was performed.

3.2.12 Flow cytometry

In accordance with the experimental setup and manufacture instructions, 1-2x10^6 cells were transferred into a 96 v-bottom plate. Cells were centrifuged at 350 rcf for 3 minutes 4°C, washed twice with FACS Buffer and then incubated with appropriate antibodies for 30 minutes at 4°C in the dark. Cells were then washed twice with FACS Buffer and resuspended in 200 µl and DAPI dye at a concentration 200 ng/ml was added to exclude

3.2.13 Animal experiments

3.2.13.1 Anti-CD19 CAR xenograft model

At day 0, 2×10^5 NALM6-luc tumor cells suspended in 100 µl of PBS were intravenously injected into NOD.Cg-Prkdc^{scid}Il2rg^{tm1Wjl}/SzJ mice six to eight weeks old. The tumor growth was monitored by measuring luciferase activity using the IVIS 200 system (Xenogen). For this, mice were anesthetized, and intraperitoneal injections of d-luciferin (15 ng/ml, 200 µl) were administered twice a week. One week after tumor injection, a single injection of 1×10^6 CAR+ T cells per mouse in 100 µl of PBS was delivered via the tail vein. All animal experiments were conducted in compliance with local animal welfare guidelines and were approved by the relevant regional authorities (Regierungspräsidium Karlsruhe).

3.2.13.2 Anti-CEA CAR xenograft model

At day 0, 2×10^6 HT-29 tumor cells in 100 µl of PBS were subcuteneusly injected into NOD.Cg-Prkdc^{scid}Il2rg^{tm1Wjl}/SzJ mice six to eight weeks old. One week after tumor injection and when a palpable tumor was present, a injection of 2×10^5 CAR+ T cells per mouse in 100 µl of PBS was delivered via the tail vein. Every 3 days, tumor size was measured using a caliper, and the equipotential ellipsoids formula was used to calculate tumor volume. All animal experiments were conducted in compliance with local animal welfare guidelines and were approved by the relevant regional authorities (Regierungspräsidium Karlsruhe).

3.2.13.3 Anti-MART-1 and GB TCR tumor models

At day 0, 1×10^6 U87 tandem minigene (TMG) glioma tumor cells in 100 µl of PBS were subcuteneusly injected into NOD.Cg-Prkdc^{scid}Il2rg^{tm1Wjl}/SzJ mice six to eight weeks old. Once a palpable tumor was detectable, to 5 x 10^6 T cells were injected via tail vein. Tumor growth was measured every 2 days, tumor size was measured using a caliper. All animal experiments were conducted in compliance with local animal welfare guidelines and were approved by the relevant regional authorities (Regierungspräsidium Karlsruhe).

3.2.14 Histology

After the necropsy, for histology tumors and organs were embedded using the Tissue-Tek O.C.T. compound (Sakura) and put immediately at -80°C. SuperFrost Plus slides (Thermo Fisher Scientific) was used to prepare 10 µm cryosections. Subsequently, the Bond-MAX device (Leica) was used to perform automatically the CD3 staining, using the NCL-L-CD3-

565 reagent (clone LN10, Leica). For haematoxylin and eosin staining (H&E) tumor and organs were fixed in 4% paraformaldehyde and then stored at 4°C in PBS. Formalin-fixed organs were embedded in paraffin and subsequently sectioned with a microtome at 2 µm. Subsequently a deparaffinization and rehydration steps were performed. Rehydrated slides were stained in hematoxylin and counterstained with eosin. The slides were afterwards acquired with the BZ-9000 microscope and analysed using the ImageViewer software.

3.2.15 Preparation of tissues for flow cytometry

After necropsy, mice were perfused with PBS and organs subsequently dissected and temporarly stored on ice. Tumors and lungs were then incubated at 37°C with Liberase and subsequently passed through a 100µm and then 70µm strainers. Tumors were then washed with PBS and subsequently centrifuged for 5min/500rcf at 4°C and then stained according to the 3.2.12 section with appropriate antibodies. Spleens and livers were passed through a 70µm and then 100µm strainers respectively and then washed with PBS and subsequently centrifuged for 5min/350rcf at 4°C. Spleens were incubated for 90 seconds with 1mL of ACK lysis and then passed again into a 70µm, washed and stained according to the 3.2.12 section. Livers were resuspended in Percoll, vortexed and centrifuged for 10min/500rcf at 4°C. Subsequently incubated for 4 minutes seconds with 5mL of ACK lysis and then washed with PBS and stained according to the 3.2.12 section according to the 3.2.12 section with appropriate antibodies.

3.2.16 Statistical analyses

Data are presented as the mean ± standard deviation (SD), or as single values as specified in figure legends. Sample size (n) and appropriate statistical tests used are also specified in figure legends. GraphPad Prism software version 8 (GraphPad Software) was used for statistical analyses. When comparing multiple groups data were analyzed using the one-way or two-ways analysis of variance (ANOVA) with post hoc tests. When comparing two groups the unpaired, two-tailed Student's t test was used. Data are presented as follows and indicated in figure legends:*$p < 0.05$, **$p < 0.01$, ***$p < 0.001$ and ****$p < 0.0001$.

4. Results

4.1 S/MAR DNA-mediated genetic modification of T cells ensures stable episomal transgene expression

4.1.1 nS/MAR DNA vectors can successfully modify rapidly dividing Jurkat 76 T cell line

In the first set of experiments, I assess the ability of nS/MAR vectors in sustaining episomal expression within rapidly dividing T cells. As a proof of concept, Jurkat 76 T cell line was employed, and the GFP gene reporter, under the control of the EF1α promoter. This was introduced into the so-called SP nS/MARt B, previously developed in the lab that consists of nS/MAR ApoL (800bp) flanked by two splicing sites and the NTX bacterial backbone (**Figure 8A**). Jurkat 76 T cells were transfected and 14 and 30 days after electroporation, GFP+ cells were sorted by fluorescence-activated cell sorting (FACS) (**Figure 8B**).

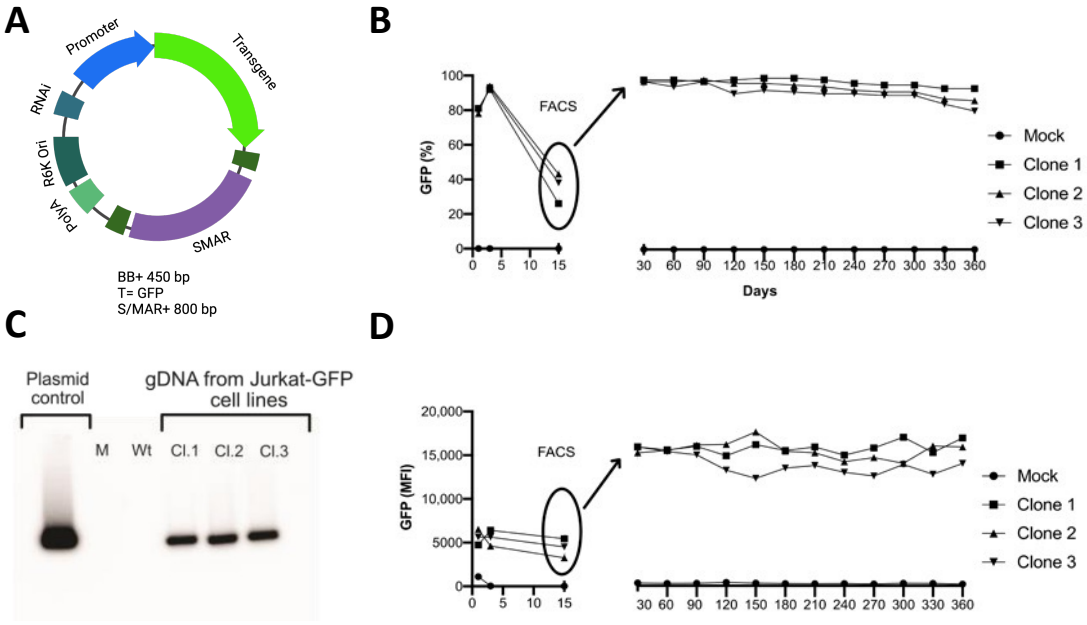

Figure 8 nS/MAR DNA vectors efficiently modify T cells with long-term expression retaining an episomal state. **A)** Schematic of the nS/MAR vector encoding for GFP. The expression of the GFP is under the control of the EF1α promoter. **B) C)** Three independent clones of Jurkat 76 were transfected with nS/MAR vector encoding GFP; 15 and 30 days post transfection GFP+ cells were sorted through FACS. GFP expression and the medium fluorescent intensity (MFI) was followed by flow cytometry for one year. **D)** Southern blot showing the episomal maintenance of nS/MAR vector in nS/MAR transfected single Jurkat 76 clones with DNA probed against GFP. (Figure adapted from my contribution in Bozza et al., 2021 [133]).

Three independent stable cell lines were successfully generated, and the maintenance of GFP expression and median fluorescence intensity (MFI) were monitored for 360 days using flow cytometry (**Figure 8B-D**). Furthermore, Southern blot analysis was performed, confirming the sustained episomal state of the vector (**Figure 8C**), and a copy number of 1.71 copies per cell was determined (data not shown) [133].

4.1.2 nS/MAR DNA Vectors can successfully modify primary T cells

Subsequently, I investigated the capability of nS/MAR vectors to modify primary T cells. For this purpose, three different vectors, encoding the GFP reporter gene, were used: the original pEPI, the SP-nS/MARt-B (800bp), and the SP-nS/MARt-A (2kb) as a control. Primary CD3+ T cells, isolated from healthy donors, were transfected and cultured for 27 days without antibiotics. The expression of GFP was monitored over time using flow cytometry. While a decline in GFP expression was observed after 21 days, a substantial proportion of cells (approximately 40%) exhibited persistent expression for both nS/MAR vectors, whereas the expression was lost 15 days after transfection with pEPI (**Figure 9A**). Subsequently, rolling circle amplification (RCA) was used to confirm the episomal maintenance of both nS/MAR vectors (**Figure 9B**). Next, I aimed to assess whether electroporation could impact T cell proliferation. In fact, in contrast to viral vectors, DNA plasmids lack the ability to transfect cells and must be delivered into the nucleus by electroporation. In order to determine the effects of electroporation on proliferation, a Cell Trace Violet (CTV) proliferation assay was performed. CD3+ T cells were transfected nS/MAR vector (800bp) and subsequently stained with CTV. To detect different generation of proliferating cells, flow cytometry analysis were performed three and five days after electroporation (**Figure 9C**). DNA-transfected T cells proliferated similarly to the unpulsed and mock cells, demonstrating that the proliferation of CD3+ cells treated with SP-nS/MARt vectors remains unaffected.

I concluded that nS/MAR DNA vectors can be used to successfully modify T cells providing long-term episomal transgene expression.

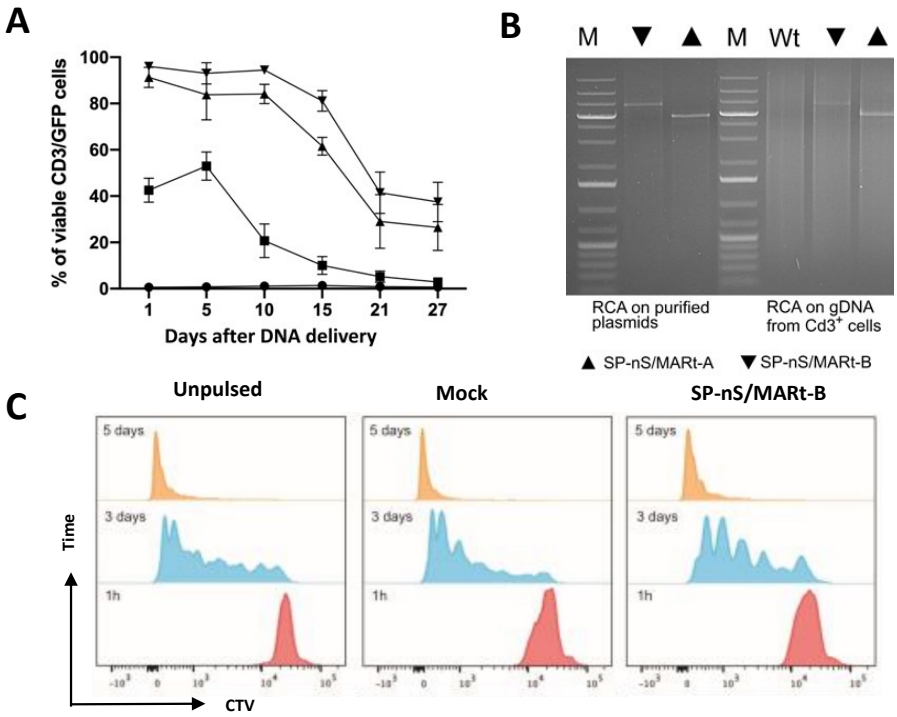

Figure 9 nS/MAR DNA Vectors retain long-term GFP expression in primary CD3+ cells without affecting the cell proliferation. A) Primary human CD3+ cells transfected with the original pEPI and nS/MAR vectors harbouring two different S/MAR (2kb and 800 bp). GFP expression was followed by flow cytometry for a period of 27 days. **B)** Rolling circle amplification (RCA) analysis to detect episomal state of the vectors. **C)** Cell proliferation was monitored by cell trace violet staining (CTV) three and five days post electroporation. Data shown as mean ± SD (n = 3). (Figure adapted from my contribution in Bozza et al., 2021 [133]).

4.2 S/MAR DNA-mediated genetic modification of T cells as a new platform for Adoptive Cell Therapy (ACT)

The complexity of manufacturing, cost, and regulatory constraints associated with generating viral vectors have limited the success of adoptive T cell therapy using CARs and TCRs. After achieving successful results in modifying T cells with a gene reporter using nS/MAR DNA vectors, I aimed to investigate this alternative approach for CAR and TCR gene modification. Implementing nS/MAR genetic modification in T cells offers several advantages over current systems, including a faster and more cost-effective manufacturing and a safer integration profile.

4.2.1 Non-viral nS/MAR CAR T cells successfully eliminate tumor cells in a haematological CD19 model

Next, I sought to investigate the capacity of S/MAR DNA nanovectors in generating CAR T cells. Human primary CD3+ T cells, derived from healthy donors were isolated and then

transfected with an nS/MAR DNA vector harbouring the anti-CD19 CAR. The scFv of the anti-CD19 A3B antibody was cloned in frame with the rest of the CAR-signaling domain, under the control of the hPGK promoter, in the SP-nS/MARt-B backbone (**Figure 10A**). After electroporation, the expression of the CAR CD19 on T cells was confirmed by flow cytometry (**Figure 10C**). Cytotoxicity of nS/MAR anti-CD19 CAR T cells was measured by a co-culture assay with the $CD19^+$ NALM-6 tumor B cell line expressing luciferase. A flow cytometry-based assay was developed in order to quantify the number of viable, $CD19^+$ NALM-6 cells using the apoptotic marker Annexin V and the live/dead marker 7AAD. CAR anti-CD19 T cells were co-cultured with NALM-6 cells for 8 hours at an effector (E) to target (T) ration 1:1. 8 hours post co-culture only 30% of the NALM-6 B tumor cells were still alive; 21,6% of cells were already dead, 18% were undergoing apoptosis and 30,4% were at a stage of late apoptosis (**Figure 10B-D**). In order to assess the specificity of the CAR T cells cytotoxicity, NALM-6 target cells were co-cultured with the Mock control. As expected, only a minor cytotoxicity effect (5,76%) was observed, probably due by alloreactivity. These data together indicate that our nS/MAR CAR anti-CD19 T cells exhibit a potent and specific cytotoxic effect against $CD19^+$ cells in an *in vitro* setting.

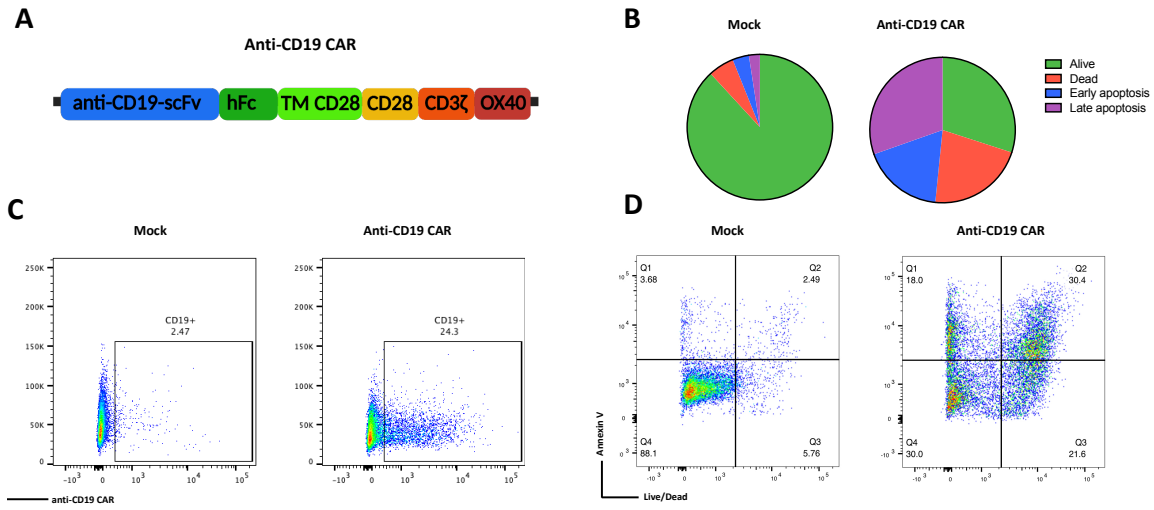

Figure 10 nS/MAR CAR anti-CD19 T cells efficiently kill NALM-6 tumor cells *in vitro*. A) Schematic of the anti-CD19 CAR **B) D)** Annexin V flow cytometry-based *in vitro* killing assay; NALM-6 tumor cells and nS/MAR anti-CD19 CAR T cells were co-cultured at an effector (E) to target (T) ratio 1:1 for 8 hours. Then they were analysed by flow cytometry and alive, dead, early/late apoptotic subpopulations could be distinguished by expression of the Annexin V and Live/Dead markers. **C)** Representative flow plot showing efficient delivery of nS/MAR vector expressing the CAR anti-CD19 into primary human CD3+ T cells (n = 3).

4.2.2 Non-viral nS/MAR CAR T cells efficacy is comparable to the current state-of the art lentivirus-produced CAR T cells in a haematological CD19 *in vivo* model

Next, I further evaluate the efficacy of the anti-CD19 CAR T cells using a CD19 xenograft mouse model in collaboration with Patrick Schmidt from NCT, Heidelberg. To investigate the tumor activity the nS/MAR technology was tested and compared to the state-of-the-art SIN (self-inactivating) lentiviral anti-CD19-CAR vector. At day 0, Luciferase expressing NALM-6 tumor cells were intravenously injected into NOD.Cg-Prkdc^{scid} Il2rd^{tm1Wjl}/SzJ (NSG) mice (**Figure 11A**). Seven days post tumor inoculation, mock T cells or CAR^{+} T cells transfected or transduced were intravenously injected (**Figure 11A**). Bioluminescence imaging data were taken 4 and 11 days after T cell treatment (**Figure 11A**). As shown in (**Figure 11B**), 4 days post treatment, no tumors were detected in any of the mice belonging to the CAR^{+} treated groups. However, after a period of 7 days, disease recurrence was observed in some of the mice belonging to the CAR^{+} treated group (**Figure 11B**). Overall, both nS/MAR and lentiviral-transduced anti-CD19 CAR T cells demonstrated a significant tumor growth delay compared to the control group, with no differences observed between the two CAR^{+} T cell groups (**Figure 11C**). Therefore, I concluded that the nS/MAR DNA vector platform offers a valid alternative for generating CAR T cells with an efficiency comparable to the established SIN Lentiviral platform.

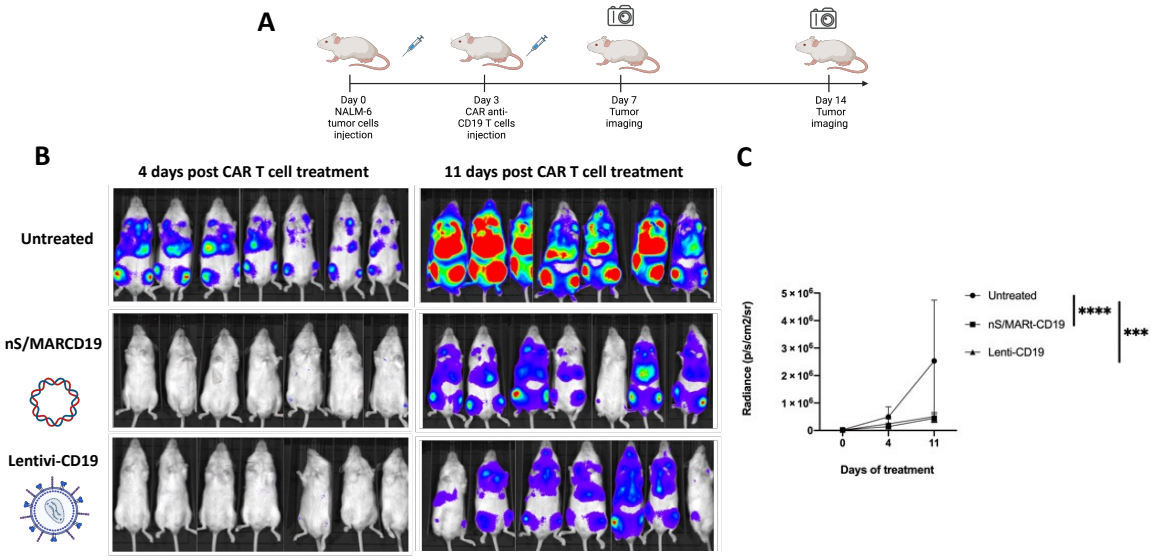

Figure 11 *In vivo* anti-tumor activity of nS/MAR T cells in CD19 model. A) Schematic of the experiment; Luciferase expressing NALM-6 tumor cells were injected intravenously at day 0 in NSG mice. At day 3, effector CAR T cells were injected intravenously, and Luciferase expression was quantified 4 and 11 days post CAR T cells treatment. Tumor growth was determined through bioluminescence imaging. **B)** Images representing non-treated and CAR T cells treated groups (nS/MAR or lentiviral anti-CD19). **C)** Luciferase was measured as the radiance (p/s/cm2/sr). Data shown as mean

± SD. One-way anova test was performed followed by post hoc analysis: *p < 0.05, **p < 0.01, ***p < 0.001 and ****p < 0.0001). (Figure adapted from my contribution in Bozza et al., 2021 [133]).

4.2.3 Non-viral nS/MAR CAR T cells expressing anti-CEA CAR demonstrate superior activity than state-of the art lentivirus-produced in the treatment of solid tumors.

Next, I aimed to investigate the versatility of our S/MAR DNA nanovectors in transferring different chimeric antigen receptor (CAR) genes to T cells, for the treatment of solid tumors. For this purpose, I collaborated with Aileen Berger and Patrick Schmidt from NCT, Heidelberg, and used the CAR against the CEA antigen as a proof of concept. Once again, the efficiency of the nS/MAR CAR T cells was compared to the state-of-the-art SIN lentiviral anti-CEA-CAR T cells. Human CD3+ cells from healthy donors were respectively transfected or transduced with n/SMAR or SIN lentiviral vectors to express the anti-CEA CAR, under the control of hPGK promoter. Both systems showed similar CAR expression efficiencies, but nS/MAR transfected T cells presented a higher MFI, when compared to the lentiviral control (**Figure 12A**).

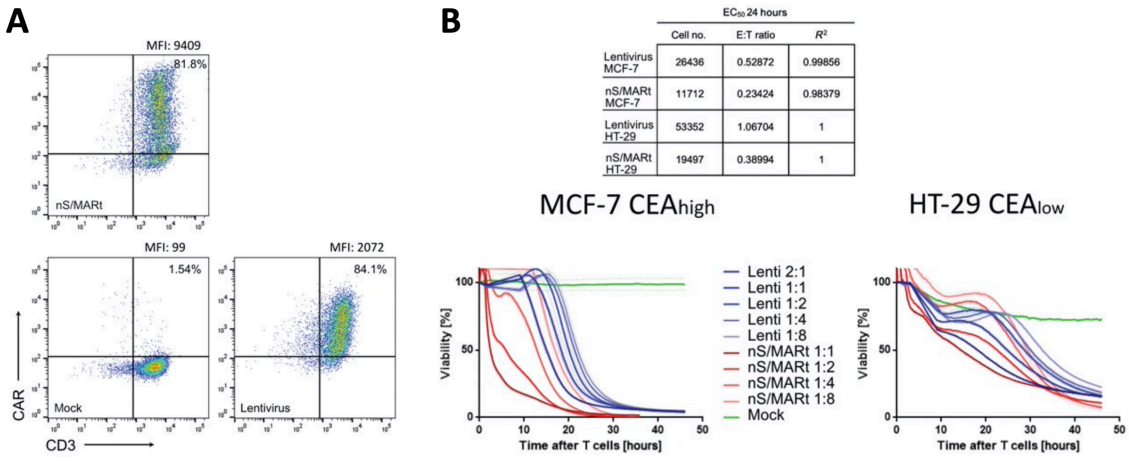

Figure 12 Anti-CEA nS/MAR CAR T cells over-performed anti-CEA Lenti CAR T cells in an *in vitro* setting. A) Representative flow plot showing CAR^+ CD3+ T cells and respective MFI 2 days post transfection. **B)** Real-time killing assay with tumor cells (T) expressing high (MCF-7) or low (HT-29) levels of the CEA target epitope and primary CD3+ T cells expressing the anti-CEA CAR (E). Different E:T ratio were tested, and the EC_{50} was assessed for both nS/MARt and Lenti anti-CEA CAR T cells. Data shown as mean ± SD (n = 3). (Figure adapted from my contribution in Bozza et al., 2021 [133]).

Next, two different human cancer cell lines, MCF-7 and HT-29, expressing respectively high or low CEA target antigen levels, were tested in a real-time killing assay. Irrespective of the level of the CEA target antigen expression, nS/MARt-CEA-CAR-T cells exhibited a higher efficiency in killing tumor cells, when compared to lentiviral transduced T cells

(**Figure 12B**). In particular, lentiviral transduced T cells required an effector to target ratio of 2.5:1 to achieve the same activity of a 1:1 ratio of nS/MAR-CEA-CAR-T cells when co-cultured with MCF-7 target cell line (**Figure 12B**). Similarly, when HT-29 cells were the target, a 2.7:1 ratio of cells lentivirus CEA CAR T cells was needed to achieve equivalent tumor killing as a 1:1 co-culture with cells engineered using nS/MARt vectors (**Figure 12B**). Furthemore, IFN-γ production was measured and produced in similar levels in both lentiviral transduced and S/MAR transfected T cells, suggesting also its role in mediating the tumor cells cytolysis [133].

4.2.4 nS/MARt T cells mediate prolonged survival in a CEA^{+} pre-clinical solid tumor model compared to lentivirus CAR T cells

Next, I investigated in collaboration with Patrick Schmidt from NCT Heidelberg the anti-tumor activity of anti-CEA CAR T cells in a xenograft model using NOD.Cg-Prkdc^{scid}Il2rg^{tm1Wjl}/SzJ mice. HT-29 tumor cells were injected subcutaneously, and upon detection of a palpable tumor, mock or anti-CEA CAR T cells were administered intravenously. The administration of nS/MAR modified T cells in mice resulted in a reduction in tumor size and delayed tumor growth (**Figure 13A**), leading to prolonged survival of this group when compared to the mock or lentiviral CART T cells groups (**Figure 13B**).

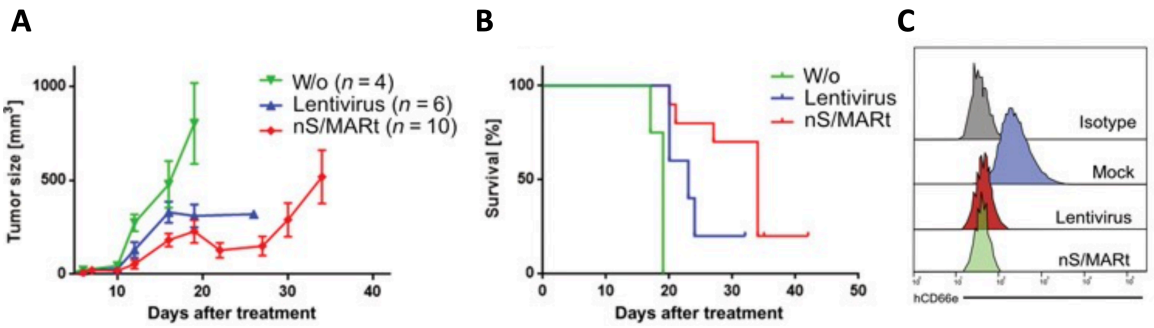

Figure 13 anti-CEA nS/MARt T cells mediate delay in tumor growth and prolonged survival in an *in vivo* CEA+ model. A) B) Graph showing the tumor growth and the survival of NSG mice treated with antiCEA CAR T cells. At day 0 HT-29 tumor cells were injected subcutaneously in NSG mice, and 7 days after tumor inoculation mock, anti-CEA CAR nS/MARt or lenti T cells were injected intravenously. **C)** Histograms showing the CEA target antigen expression in tumors of mock, anti-CEA CAR nS/MARt or lenti CAR T cells. (Figure adapted from my contribution in Bozza et al., 2021 [133]).

Nevertheless, none of the groups reached complete eradication of the tumor; to further investigate the reasons, analysis of the tumors were performed. Flow cytometry analysis

revealed a loss of CEA surface expression in HT-29 tumor cells (**Figure 13 C**), indicating that a frequent escape mechanism employed by tumors during treatment occurred.

4.2.5 nS/MARt T cells retain long-term anti-tumor functionality and episomal maintenance in a pre-clinical in-vivo model

In order to determine further the long-term persistence and activity of nS/MAR T cells I performed further analysis in collaboration with Aileen Berger and Patrick Schmidt on tumors and organs of treated mice.

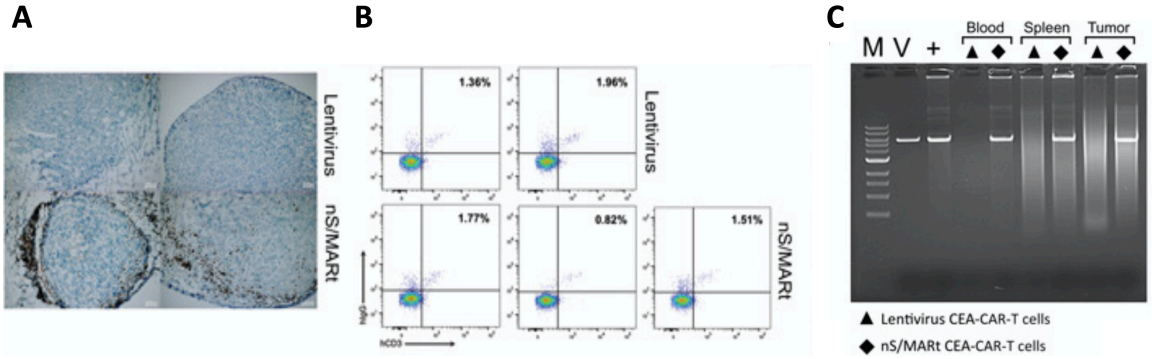

Figure 14 anti-CEA nS/MARt CAR T cells showed high tumor infiltration after treatment and persist in an episomal state. A) Representative immunohistochemistry (IHC) images showing anti-CEA CAR T cells infiltration into the tumors. **B)** Flow plot showing the engraftment of anti-CEA CAR T cells. **C)** Rolling circle amplification (RCA) to confirm the episomal state of the nS/MARt anti-CEA CAR vector performed with total genomic DNA isolated from blood, spleen at tumor. (Figure adapted from my contribution in Bozza et al., 2021 [133]).

RCA analysis performed in DNA extracted from the tumours, spleen and total blood of the groups that received the treatment showed that the vector was still persistent in these cells and was retained in an episomal state (**Figure 14C**). T cells were also still detectable in tumors, as shown by histology (**Figure 14A**), interestingly with an higher infiltration in n/S/MAR treated groups compared to the lentiviral transduced group (**Figure 14A**). However, flow cytometry analysis showed no differences in the infiltration frequencies from both groups in the spleen (**Figure 14B**). In order to determine the long-term activity and the prolonged duration of the treatment splenocytes from nS/MAR CEA CAR treated mice group, were isolated from sacrificed mice and subsequently co-cultured with MCF-7 tumor cells in a real-time killing assay by Aileen Berger and Patrick Schmidt from NCT. 40 days after treatment CAR-T cells were still showing killing capabilities demonstrating their prolonged functionality [133].

4.2.6 Exploring the efficacy of nS/MARt T cells compared to other non-viral systems, such as sleeping beauty (SB) transposons

Next, I aimed to investigate the compatibility of our platform with other state-of-the-art non-viral systems, such as the Sleeping Beauty transposon. The anti-CEA CAR was cloned into an S-100X SB backbone. CD3+ T cells from healthy donors were then transfected with either nS/MARt vectors or SB transposons. The transfection efficiencies of both systems were comparable, with a slight trend towards increased efficiency observed with SB transposons (**Figure 15A**). Subsequently, an *in vitro* real-time killing assay was conducted to evaluate any differences in the killing capabilities between the two systems. CEA^+ HT-29 tumor cells were co-cultured in a 1:1 E:T ratio with nS/MAR or SB-transfected anti-CEA CAR T cells (**Figure 15B**). No discernible differences were detected in terms of anti-tumor activity, as well as IFN-γ production, which is responsible for tumor cell cytolysis (**Figure 15B-C**).

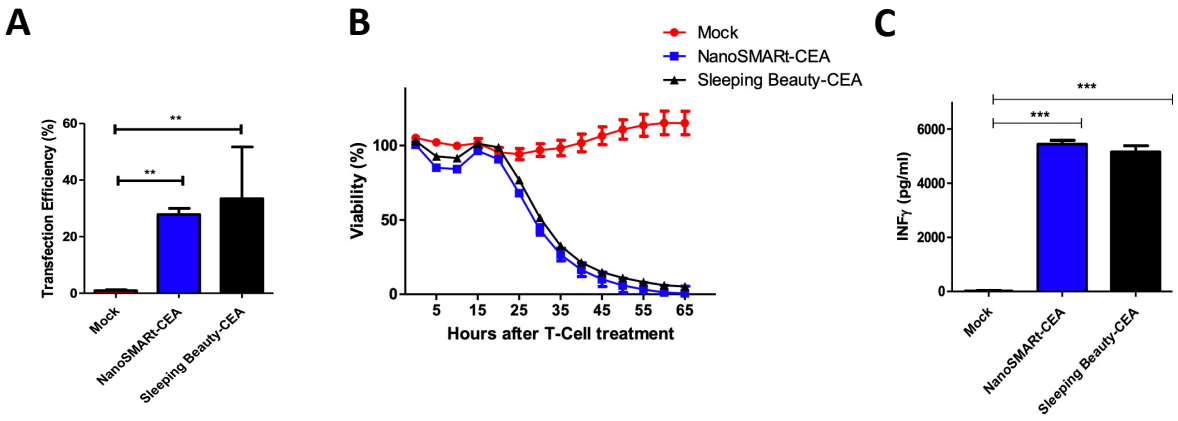

Figure 15 nS/MAR anti-CEA CAR T cells killing activity is comparable to Sleeping Beauty (SB) CAR T cells. A) Histogram showing transfection efficiency of non-viral DNA delivery for nS/MARt or SB anti-CEA CAR T cells. **B)** Real-time killing assay with target HT-29 tumor cells and effector anti-CEA CAR nS/MARt or SB CAR T cells at a ratio 1:1. **C)** Histogram showing IFNγ production of anti-CEA CAR nS/MARt or SB CAR T cells after co-culture. Data shown as mean ± SD (n = 3). One-way anova test was performed followed by post hoc analysis:*p < 0.05, **p < 0.01, ***p < 0.001 and ****p < 0.0001).

Therefore, I conclude that our nS/MAR DNA vector platform is a valid non-viral alternative for the generation of CAR T cells for targeting both haematological and solid tumors. In pre-clinical models of solid tumors, it exhibited sustained anti-tumor activity *in vivo*, over performing the state-of-the-art SIN lentivirus. It also demonstrated comparable efficacy to other non-viral systems, such as Sleeping Beauty transposon.

4.2.7 nS/MARt vectors for the generation of therapeutic TCR T cells

Next, I sought to explore the potential of utilizing this platform for transgenic TCR therapy, with the final aim of translating it for personalized therapy. To validate this concept, I conducted initial tests using the high-affinity anti-MART1-specific TCR, which has been already used in clinical Phase I and II trials [137][48], subsequently I moved to patient-derived TCRs.

4.2.7.1 Unravelling the best promoter for driving transgenic TCR Expression

Previous data from the laboratory have shown the ability of nS/MAR T cells in generating a Jurkat 76 T cell line providing prolonged TCR expression for over 4 months (data not shown). Recent publications suggest the role of the promoter controlling the CAR expression in mediating T cells functionality [138][139].

Therefore, I sought to refine the previous vector backbone tested with CARs transgenes by testing five different strong or weak promoters (sEF1α, hPGK, hWASP, hCD3 and hTCR) driving the expression of the MART-1 TCR and a new shorter version of the coreApoL (500bp) S/MAR (**Figure 16A**). Initially, I considered the impact of the internal promoter on cell viability and transfection efficiency following electroporation. Primary human T cells were transfected with the five constructs, and flow cytometry analysis conducted two days post-electroporation revealed that the highest level of transfection efficiency was achieved with the strong sEF1α promoter, and the highest mean fluorescence intensity (MFI) levels as well (**Figure 16C-D**). Opposite, the weak hTCR promoter exhibited the lowest transfection efficiency and MFI levels (**Figure 16C-D**).

Next, to establish a correlation between MFI and TCR density on the surface of the T cells, an antibody-binding capacity (ABC) flow cytometry beads assay was performed. Four known ABC beads standards were labelled with the mTCR antibody, and a standard curve was generated. According to the MFI levels, the highest number of TCR molecules on the cells was observed with sEF1α-driven TCR expression, while the lowest was observed with hTCR-driven TCR expression (**Figure 16F**).

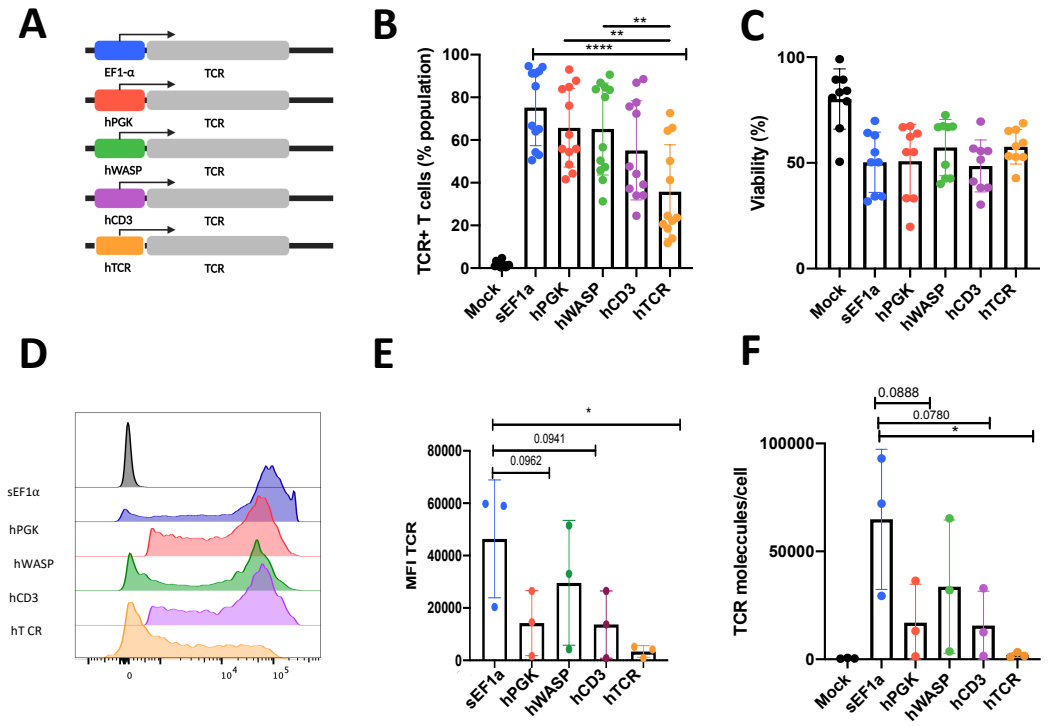

Figure 16 sEF1α mediates highest transfection efficiency and transgenic TCR density on the T cells surface. A) Schematic of the anti-MART-1 DM5F TCR nS/MAR bearing five different promoters (sEF1α, hPGK, hWASP, hCD3, hTCR). **B) C)** Bar graphs showing viability and transfection efficiency of the five nS/MAR vectors on CD3+ T cells from healthy donors. TCR expression was detected by flow cytometry; dead cells were excluded by DAPI gating and alive TCR+ cells were gated (n=12) **D) E)** MFI assessment of TCR for three individual donors are shown as histograms and bar graphs. **F)** Bar graph showing the number of TCR/molecules in the T cell surface of three individual donors. The results are expressed as the mean ± SD (n=3). One-way anova test was performed followed by post hoc analysis:*p < 0.05; **p < 0.01; ***p < 0.001 ****p < 0.0001.

4.2.7.2 Electroporation of nS/MARt DNA vectors does not affect T cells immunophenotype

I then investigated whether electroporation with vectors harbouring different promoters-driving TCR expression could impact the phenotype and proliferation of the cells. To assess the impact on T cell expansion, a crucial factor for *in vivo* applications, I conducted a CTV assay to measure cell proliferation for four days following electroporation. Comparing the mock T cells with those electroporated with DNA, the mock control exhibited two additional cell divisions, while the sEF1α group displayed a proliferation pattern similar to the mock control (**Figure 17D**). Furthermore, I determined the cell phenotype using flow cytometry. The nS/MAR DNA-transfected T cells exhibited a phenotype similar to the mock control, characterized by a higher percentage of naïve T cells, which are known to mediate a more potent anti-tumor effect (**Figure 17A-C**). Additionally, there was no observed difference in the CD4 CD8 ratio compared to the mock control, suggesting that the transfection process does not affect the T cell phenotype (**Figure 17A-E**).

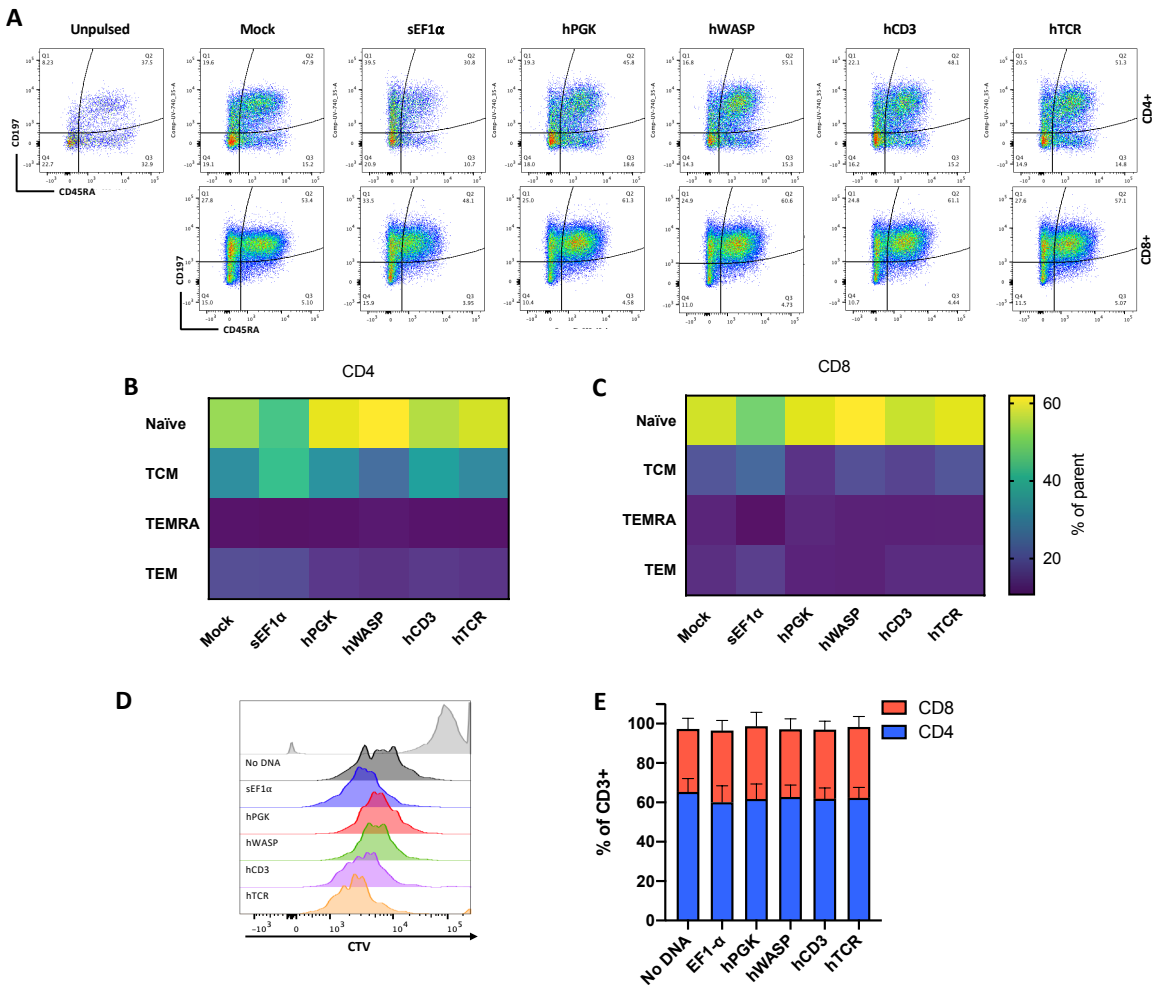

Figure 17 Immunophenotypical characterization of transgenic T cells. **A) B) C)** Stratification of transfected T cells into differentiation status- Naïve (TN), central memory (TCM), effector memory (TEM), and effector memory RA+ (TEMRA). T cell subsets were defined using CD45RA and CD197 by flow cytometry two days post transfection. **D)** T cells were labelled with CTV after transfection to determine their proliferation capacity. CTV dilution was determined by flow cytometry on $CD3^+$ T cells by six days post transfection. **E)** Percentages of $CD4^+$/$CD8^+$ subpopulations after transfection on day two. The results are expressed as the mean ± SD. N=3.

4.2.7.3 Enhanced IFN-γ Secretion in sEF1α Promoter-Driven antiMART-1 Transgenic TCR

Next, I sought to investigate whether different promoters and different TCR densities could modulate the antigen recognition and subsequent cytotoxic activity against the targeted antigen (**Figure 18A**). CD3+ T cells from HLA-$A2^+$ healthy donors were transfected with the five different constructs and subsequently, a real-time killing assay with xCELLigence was performed. Anti-MART1 TCR effector T cells were co-cultured at an E:T ratio 1:1 with either HLA-$A2^+$ $MelanA^{low}$ (MeWo) or $MelanA^{high}$ (Mel264) expressing tumor cell lines (**Figure 18B-C**).

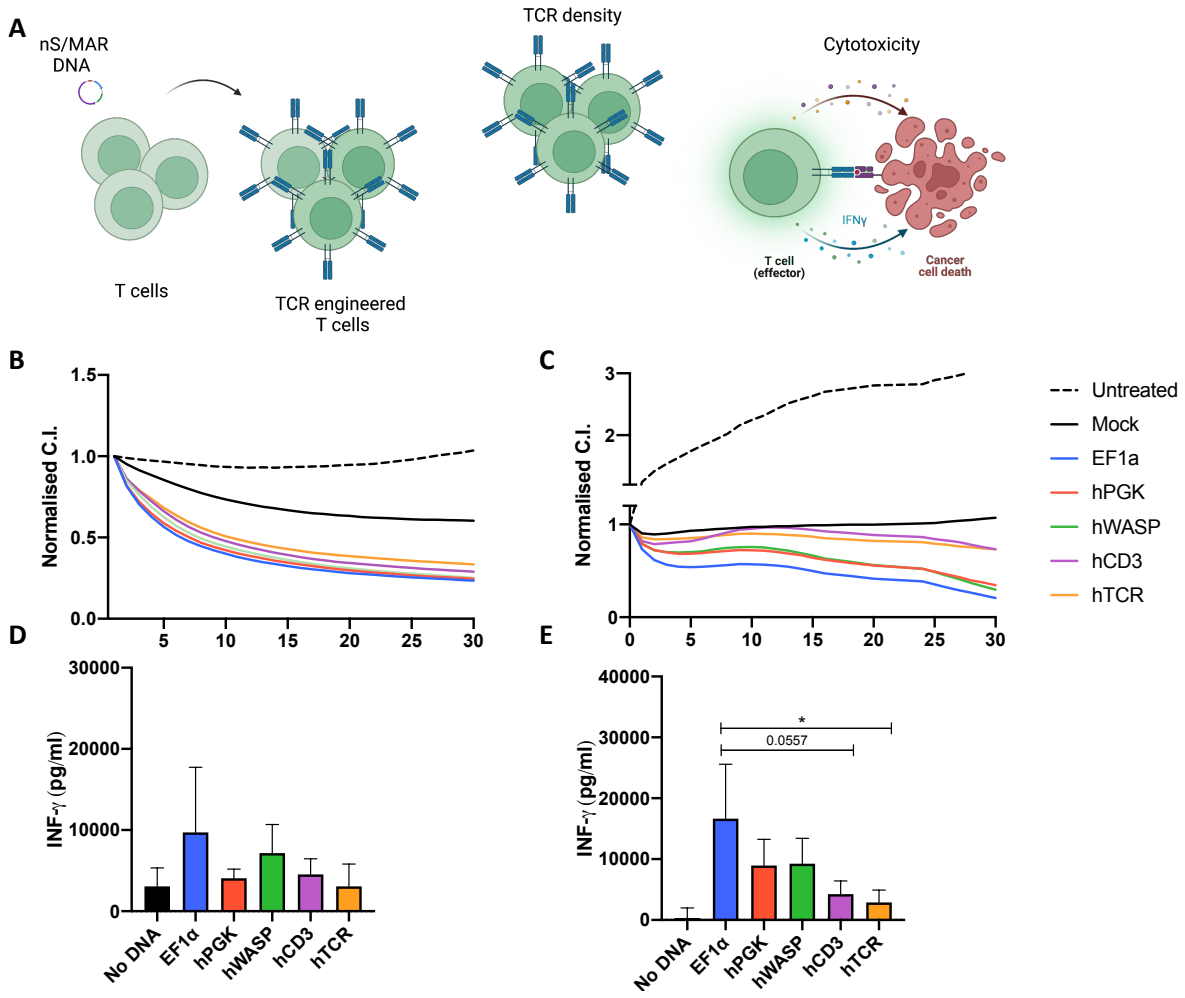

Figure 18 sEF1α promoter driven expression of MART-1 targeting transgenic TCR enhances IFN-ɣ secretion in real-time *in vitro* cytotoxicity assays using n/SMAR vector. A) Schematic of the TCR density and efficacy analysis of TCR T cells. **B) C)** Respectively MeWo^{Low} and Mel264^{high},expressing the target (T) antigen MelanA, target cells were seeded at day 0 and 24 h later effector T cells were seeded with an E:T (1:1) (n = 3). **D) E)** Respectively MeWo^{Low} and Mel264^{high} supernatant was collected 30h after co-culture and IFN-ɣ production was measured by ELISA. The results are expressed as the mean ± SD (n=3). One-way anova test was performed followed by post hoc analysis:*p < 0.05; **p < 0.01; ***p < 0.001 ****p < 0.0001.

sEF1α showed higher IFN-γ production after co-culture with Mel264 and a trend of increased with the MeWo, when compared to hTCR driving antiMART-1 TCR expression T cells (**Figure 18D-E**). Real-time killing assay showed similar cytotoxicity capabilities when the TCR engaged with the MART-1^{low} MeWo cell line, whereas a trend of increase was observed when TCR T cells were engaged with the MART-1^{high} Mel264 cell line in sEF1α when compared to hTCR and hCD3 TCR-driving promoters (**Figure 18B-C**). I conclude that TCR T cells driven by the sEF1α promoter exhibit higher production of cytokines, such as IFN-γ, but demonstrate similar killing capabilities in a bulk assay.

4.2.7.4 Continue antigen exposure model

I then sought to investigate whether T cells transfected with different promoters would behave differently when challenged in a re-stimulation assay. For this purpose, a continue antigen exposure model was used, where TCR T cells were challenged in four consecutive rounds of killing assays. CD3+ T cells from HLA-$A2^{+}$ healthy donors were transfected with the five different constructs and subsequently, four days after electroporation, co-cultured with MeWo cell line at an 1:1 effector to target (E:T) (**Figure 19A**). After 24 hours of co-culture, TCR-T cells were restimulated with freshly seeded MeWo cells, and cocultured at 1:2 E:T ratio for another 24h hours (**Figure 19A**). TCR T cells were then rested for 24 hours and then two more rounds of killing assay were performed, at day 7 and 9 post co-culture (**Figure 19A**). TCR-T cells showed killing abilities until round three (**Figure 19B-D**), even though their anti-tumor activity decreased after round two (**Figure 19B-E**). At day 9, TCR-T cells were then stained to evaluate TCR expression on the T cell surface. Killing capabilities were decreasing together with TCR expression similarly in all groups; indeed, TCR levels were reduced between 2% and 4%, despite initial transfection efficiencies were different (**Figure 19F-G**).

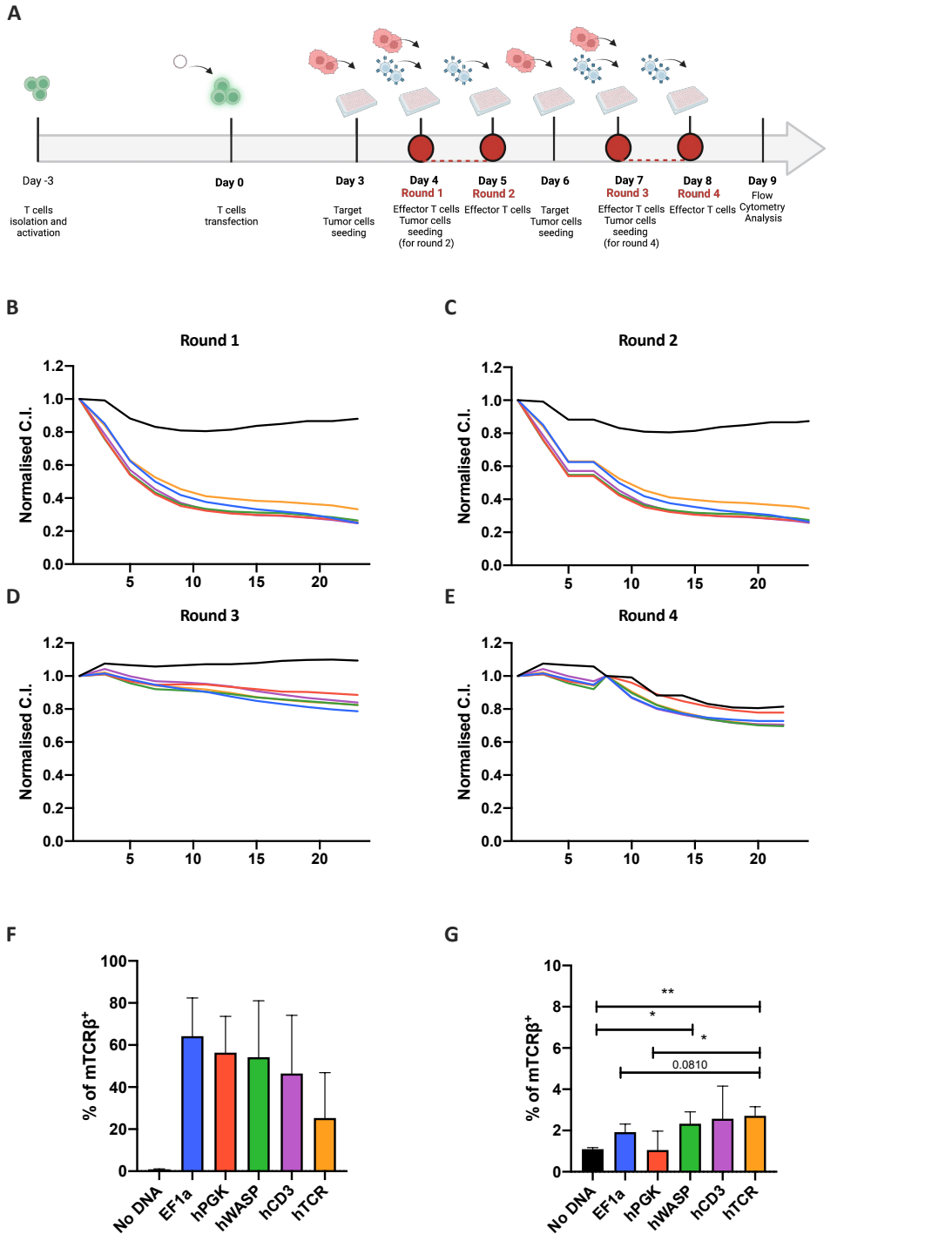

Figure 19 nS/MAR transgenic TCR T cells present killing capacity after several rounds of killing. A) Schematic of the *in vitro* stress test for the analysis of TCR T cell functional status upon repetitive stimulation with MeWo tumor cells. MeWo Target cells, expressing the MART-1 target epitope were seeded at day 5 and 6. The effector DM5F TCR T cells were added at **B)** day 4 (Round 1), **C)** day 5 (Round 2) **D)** day 7(Round 3) and **E)** day 8 (Round 4) at a 2:1 E:T ratio (n = 3). Bar graphs showing TCR expression **F)** before and **G)** after the co-culture. The results are expressed as the mean ± SD (n=3). One-way anova test was performed followed by post hoc analysis: *p < 0.05; **p < 0.01; ***p < 0.001 ****p < 0.0001.

4.2.7.5 nS/MARt TCR T cells mediate cytotoxicity in a 3D model

I then wanted to further test the cytotoxicity of the candidate sEF1α driving TCR expression in a three-dimensional (3D) system. MART-1 targeted TCR T cells were tested against MeWo spheroids. Stably expressing GFP MeWo cell line were co-cultured with MCF5 fibroblast in ultra-attachment plates for three days, allowing the formation of the spheroids (**Figure 20A**). At day 3 of spheroids formation, CD3+ MART-1 TCR-T cells, derived from HLA-A2^{+} healthy donors, were co-cultured with spheroids at a 5:1 E:T ratio. Continued spheroids growth was observed in the no treatment control and mock while a decrease in GFP and disruption of the spheroid was observed in the anti-MART1 TCR treated group (**Figure 20B**). Concluding that nS/MAR vectors are show kill abilities in 3D models.

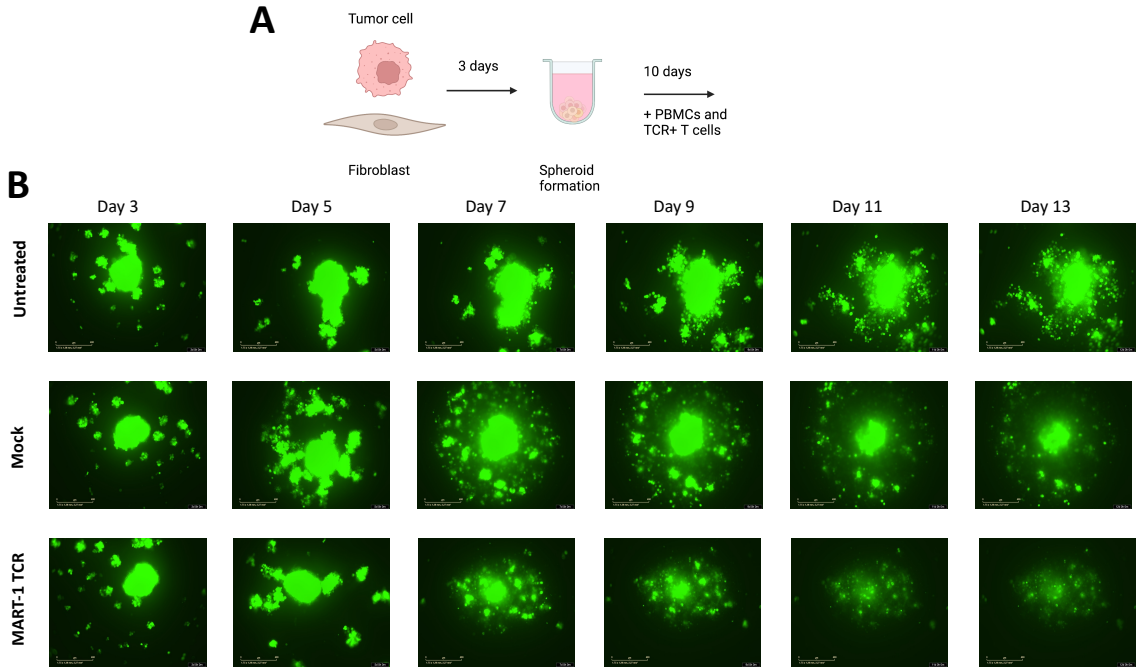

Figure 20 Transgenic antiMART-1 TCR T cells efficiently kill tumor spheroids. A) Schematic of the spheroid's formation and co-culture with effector T cells. After spheroids formation, at day 3, Effector anti-MART-1 TCR T cells were co-culture at a ratio 5:1 with tumor spheroids. Spheroids growth and GFP expression was followed for 10 days. **B)** Representative images of GFP+ tumor spheroids, consisting of MART-1^{+} MeWo cell line and MCF-5 fibroblasts untreated or co-cultured with effector cells (n=3).

4.2.8 nS/MARt TCR T as a platform for personalized therapy

To assess the potential of this system for personalized TCR-T cell therapy in brain tumors, I collaborated with Yu-Chan Chin and Katharina Lindner to utilize the nS/MAR technology

with patient-derived TCRs, from patients with glioblastoma (GB) and brain tumor metastasis.

4.2.8.1 nS/MAR transgenic vaccine-induced Glioblastoma (GB) patient-derived TCR

In the first model of GB, a vaccine-induced TCR specifically targeting a non-mutated glioma-associated antigen coming from a patient with favourable clinical outcome, enrolled in the Glioma Actively Personalized Vaccine Consortium (GAPVAC) study was used [140]. In this study, patients were treated with personalized multi-peptide vaccination for glioma-associated antigens HLA-A2$^+$ restricted.

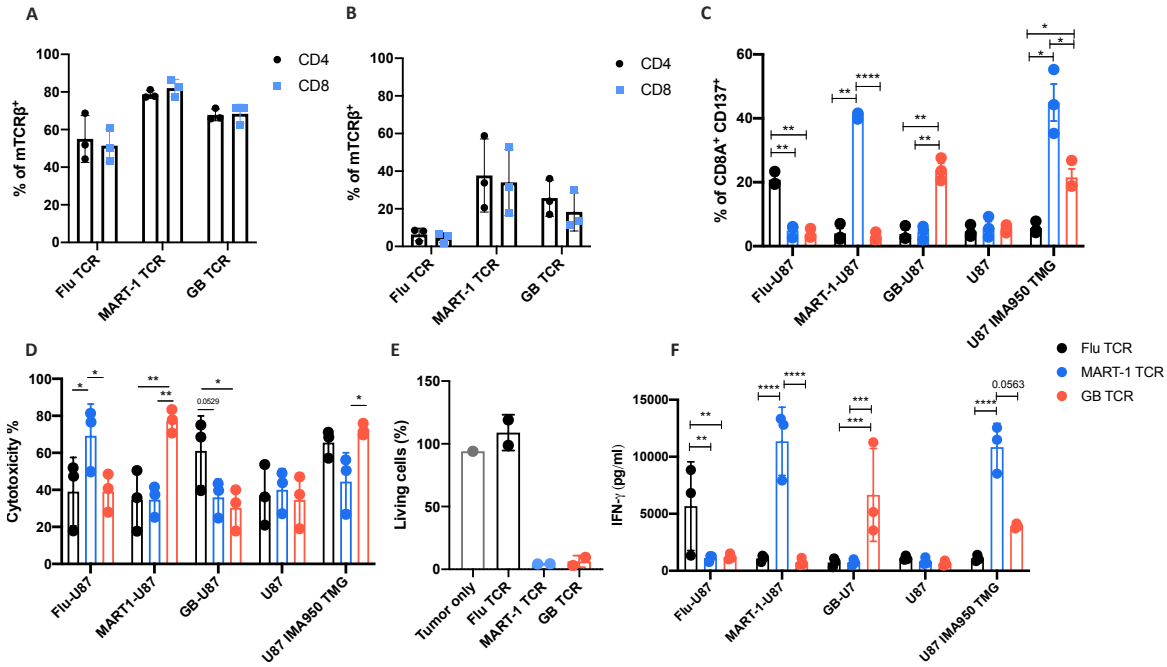

Figure 21 nS/MAR TCR T cells showed *in vitro* efficacy for GB personalized therapy. **A) B)** Bar graphs showing TCR expression of different TCRs (Flu, MART-1 and GB) before and after co-culture. **C)** Histograms showing CD8+ activation, through CD137 marker, after engagement of TCR with target cells. **D) E)** Cytotoxicity assays with E:T 2:1 of target cells and effector transgenic TCR T cells. **F)** ELISA measuring the IFN-γ release after overnight co-culture of effector and target cells (n=2 and n=3). The results are expressed as the mean ± SD (n=3). Two-ways anova test was performed followed by post hoc analysis: *p < 0.05; **p < 0.01; ***p < 0.001 ****p < 0.0001.

The GB TCR was discovered by Yu-Chan Chin, and subsequently cloned into the nS/MAR DNA vector backbone, with the sEF1α promoter driving the TCR expression. Human T cells transfected with the GB-reactive TCR were generated. Flow cytometry analysis revealed that the GB TCR could be expressed at similar levels than the anti-MART1 TCR (**Figure 21A**). To assess the functionality and specificity of this TCR T cells a co-culture experiment was performed using as target cells: the human GB U87 cell line (non-target cell line), GB U87 IMA950 TMG (target cell line expressing MelanA and the GB antigen)

and peptide loaded U87. The effector cells, the Flu (influenza) TCR (irrelevant TCR, negative control), MART-1 TCR (positive control) and GB TCR were co-cultured overnight. LDH assay and Crystal Violet assay showed specific killing of all TCRs **(Figure 21D-E),** with some background activity in the LDH assay probably due by non-specific signal or alloreactivity. Moreover, specific T cell activation was observed with CD137 marker **(Figure 21C)**. IFN-γ was also assessed and showed specific production upon engagement with target cells **(Figure 21F)**.

4.2.8.2 nS/MAR TCR T cells in vivo model

Having demonstrated the capacity of nS/MAR TCR T cells in recognizing and killing target tumor cells with off-the-shelf and patient derived TCRs in an *in vitro* setting, I next wanted to investigate the therapeutic potential of these cells *in vivo* in collaboration with Yu-Chan Chin from our laboratory. For this, a xenograft model was used: the human glioma cell line U87 IMA950 TMG stably expressing the MelanA and GB antigens (tandem-minigenes) were injected in the flank of NOD scid gamma (NSG) mice. At 9 days post tumor inoculation, when a palpable tumor was observed, two different experiments were performed. In the first experiment, therapeutic nS/MAR anti-MART-1 TCR or anti-Flu TCR-T cells were injected intravenously at day 9 and day 16 after tumor inoculation (**Figure 22A)**. Similarly, in the second experiment, T cells transfected with nS/MAR vectors or γ-retrovirally transduced to express anti-Flu TCR or anti-GB-TCR were used (**Figure 22A)**. Tumors were measured every second day, but surprisingly despite *in vitro* anti-tumor activity and previous *in vivo* work conducted by colleagues, none of the groups demonstrate therapy efficacy or reduced tumor growth for neither of the experiments (**Figure 22B-C)**.

To further investigate the lack of anti-tumor response, analysis of the tumors and other organs was performed. Flow cytometry analysis of the MART-1 model revealed infiltration of T cells in blood, spleen, liver, lung, and tumor but no TCR expression in liver and tumor was revealed (**Figure 22D)**.

However, H&E and CD3 immunohistochemistry staining, done in collaboration with Stephan Push, revealed tumor heterogenicity, high tumor density and heterogenicity in T cells infiltration (**Figure 22F-G)**. Also, for the GB model flow cytometry analysis of the tumors and blood were performed. 14 days post 2nd injection, TCR^{+} T cells were still

detectable in tumors in both virus SFG and nS/MAR groups, despite no anti-tumor activity was detected (**Figure 22E)**. Further analysis on the T cells will need to be performed in order to assess their phenotype as well as analysis of the tumors to determine whether expression of the tumor antigens is still present.

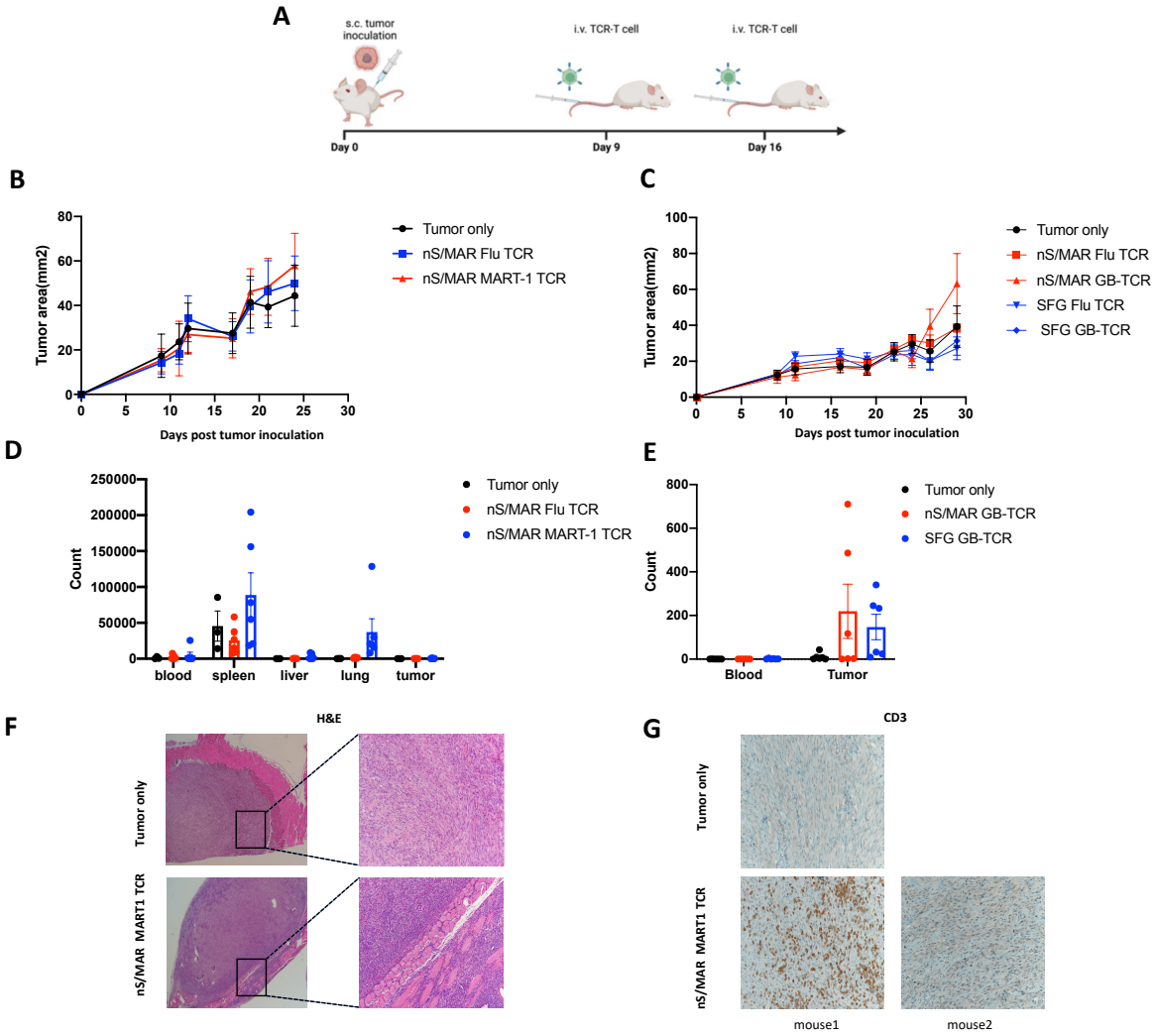

Figure 22 ***In vivo*** **activity of TCR T cells. A)** Schematic of the animal model: U87 IMA950 TMG GB cell line was subcutaneously injected into NSG mice. 9 days and 16 days after tumor inoculation effector T cells (anti-Flu, anti-MART1, anti-GB) were intravenously injected. **B) C)** Plots showing the tumor growth of the two experiments. **D)** Histogram showing T cells infiltration in blood, spleen, liver, lung and tumor of mice treated with nS/MAR and anti-MART1 and anti-Flu. **E)** Histogram showing TCR T cells persistence in blood and tumor of mice treated with nS/MAR and SFG virus anti-GB and anti-Flu. **F)** Representative H&E images of non-treated and MART-1 TCR treated groups. **G)** Representative CD3 IHC images of non-treated and MART-1 TCR treated groups.

4.2.8.3 nS/MAR transgenic patient-derived TCR T cells for brain metastasis

In a second model, reactive patient-derived TCRs from a patient with brain metastasis were discovered by my colleagues Chin Leng Tan and Katharina Lindner. These TCRs were identified through a screening and analysis of TILs after single cell RNA+VDJ sequencing (**Figure 23A**) from one patient with a brain metastasis. These TCRs were used as a proof-

of-concept to investigate the use of the S/MAR technology in a pipeline for personalised therapy.

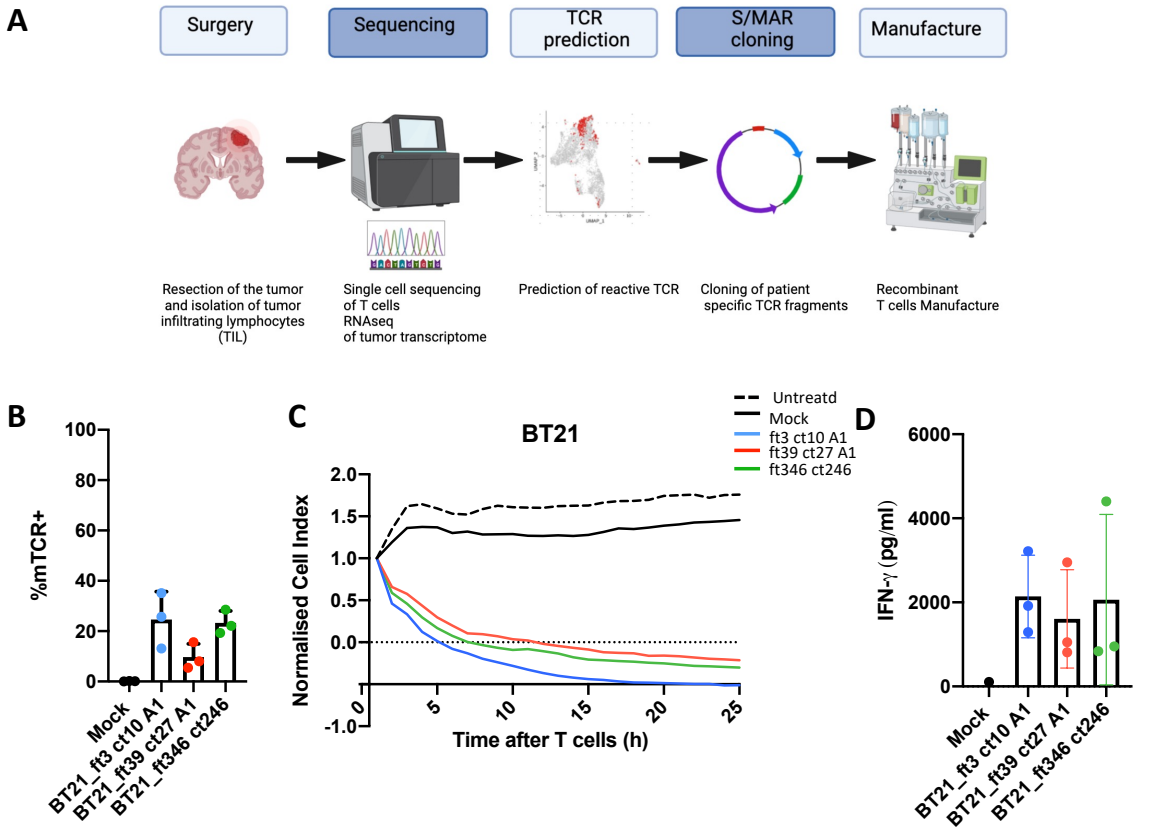

Figure 23 S/MAR transgenic patient-derived TCR T cells mediate antitumor activity.A) Cartoon showing the screening and manufacturing approach utilized for the discovery of the TCR its manufacturing. **B)** Transfection efficiency of three reactive TCRs cloned into S/MAR vectors. **C)** Real-time killing assay with target patient-derived BT21 cell line (T) and S/MAR TCR T cells (E). E:T 2:1, co-culture was performed for 24 hours, subsequently **D)** supernatant was collected and ELISA to record the release of IFN-γ cytokine performed (n=3).

BT21 a cell line, derived from this patient, was characterized for MHCI and MHCII; while MHCI was highly express MHCI expression was low even after IFN-γ stimulation (data not shown). Three reactive TCRs were selected by the TCR screening performed by Katharina Lindner. This three TCRs were then cloned into S/MAR vectors under the sEF1α promoter. CD3+ T cells from healthy donors were than transfected and TCR expression evaluated by flow cytometry (**Figure 23B**). These TCRs were then tested for anti-tumor efficacy with the BT21 patient-derived tumor cell line. BT21 cells were co-cultured at an E:T ratio 2:1 with TCR T cells in a real-time cytotoxicity assay and subsequently IFN-γ production measured (**Figure 23C-D**). TCR T cells showed killing abilities as well as capability in producing cytokines, validating the screening previously performed by my

colleague. With this I conclude that the nS/MAR platform can be used for T cell personalized therapy.

4.2.9 Clinical production of nS/MARt Transgenic TCR T cells

Finally, in order to fully demonstrate the capabilities of nS/MAR T cells in generating therapeutic T cells, my objective was to optimize a GMP-compatible manufacturing process for producing large-scale Transgenic T cells for personalized therapy. Our laboratory has previously described a rapid clinical-scale manufacturing protocol for generating 1.6 × 108 fully functional CAR-T cells, utilizing the MaxCyte ExPERT GTx platform for electroporation and the CliniMACS Prodigy system for automated cell sorting and culture dynamics [133]. However, I further refined the protocol to enhance cell yield, and assess the use of the protocol for the generation of transgenic TCR T cells, thus enabling the broad application of T cell therapies in clinical settings. The proposed protocol allows for the generation of therapeutic T cells in just 5 days, compared to the 15-day period required for lentivirus-mediated T cell production.

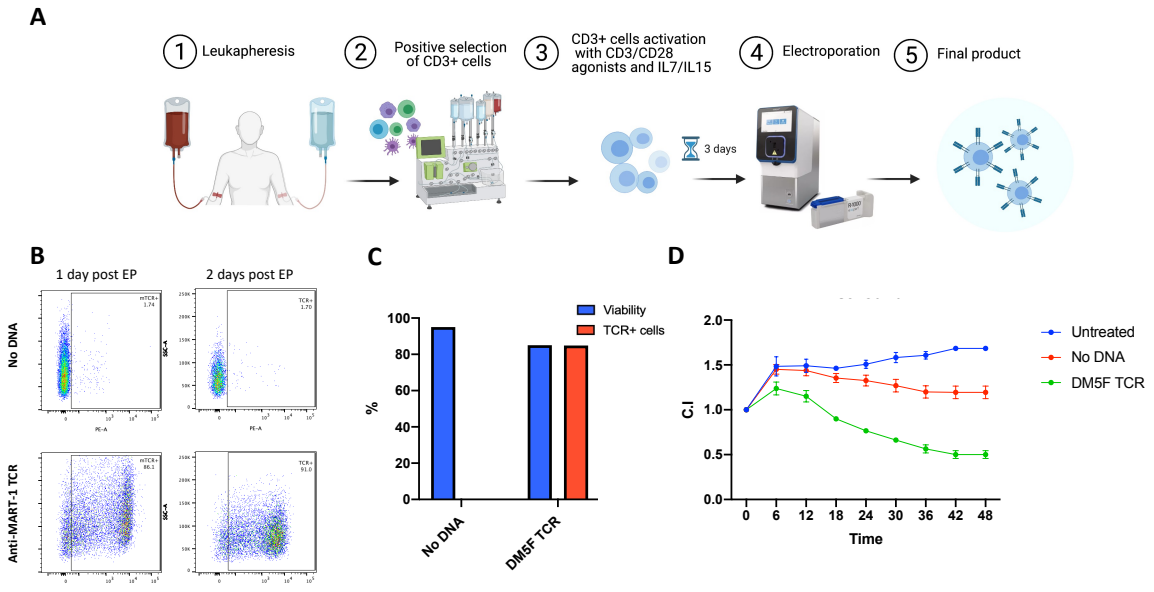

Figure 24 Large-scale TCR-T cell manufacturing using nS/MAR vectors. A) For the generation of recombinant T cells, a manufacturing protocol was developed. $CD3^+$ T cells were sorted starting from a leukapheresis product. Isolated $CD3^+$ cells were then cultured with TransAct (CD3/CD28), IL7 and IL15 for three days. Then the cells were counted and moved into the R-1000 assembly of the MaxCyte ExPERT. **B**) **C**) 24 and 48 h after the electroporation the cells were harvested and analyzed by flow cytometry for viability and TCR expression. **D**) Their capability of killing was tested in a real-time *in vitro* cytotoxicity assay with the MeWo Target cells expressing the MART-1 target epitope and the effector anti-MART-1 TCR T-cells at a 2:1 E:T ratio (n =1).

Human primary T cells were isolated from a Leukapheresis pack using the CliniMACS Prodigy device. A total of 4 × 10^8 CD3+ T cells were then activated and cultured manually

for 3 days (**Figure 24A**). After activation, T cells were transfected with the nS/MARt anti-MART-1 transgenic TCR using 4x R-1000 Process Assembly (1×10^8 CD3+ T cells each) and the MaxCyte ExPERT GTx (**Figure 24A**).The following day, and two days post-electroporation the transfected T cells were harvested and analyzed for TCR expression using flow cytometry, which revealed a transfection efficiency of 86% and 91% respectively (**Figure 24B-C**). Large-scale manufactured T cells were subsequently subjected to functional assays, including a real-time killing assay with MeWo tumor cells using the xCELLigence system (**Figure 24D**).

4.3 Armouring S/MAR DNA Vectors for ACT in solid tumor treatment: The next generation of vectors

Developing a cell product that can effectively trigger a robust and durable anti-tumor response in an immunosuppressive microenvironment, such as the one of brain tumors, remains one of the biggest challenges of therapeutic T cells [141]. Extensive investigations have been carried out to enhance the anti-tumor activity of therapeutic TCR and CAR-T cells. One approach is to generate transgenic T cells that can produce an immune-modulatory cytokine upon CAR engagement, the so-called TRUCK CAR-T cells. While TRUCK CAR-T cells have been successfully created using viral vectors, I set out to determine if nS/MAR vectors can be used also for the generation of TRUCK T cells [140].

4.3.1 Next generation of vectors: “all-in-one” or “two vector” system?

The augmentation of the T cell efficacy will require the expression of multiple genes. It has been shown that transfection efficiency is size-dependent and smaller vectors are working better than bigger ones. In the first set of validation experiments I determined the optimal strategy for the safe establishment and multigene co-expression in T cells we compared two different strategies: the “Two-vector” systems (SP-C/MAR-GFP and SP-C/MAR-dTomato (**Figure 25A-B**) and “All-in-one” vector system (SP-C/MAR GFP-P2A-dTomato) (**Figure 25C**) Jurkat 76 T cells were transfected with the two and one day post electroporation flow cytometry analysis revealed a higher transfection efficiency was achieved with the “two-vector” systems (62%) when compared to the “all-in-one” vector system (43%) (**Figure 25D**). Jurkat 76 T cells were then cultivated under normal conditions in an antibiotic-free medium and double positive cells were sorted two and four weeks after

the transfection. This was done in order to minimize the potential risk of random integration of the vector due to the selection pressure. Transgene expression was monitored once a week by flow cytometry for one month (**Figure 25D**).

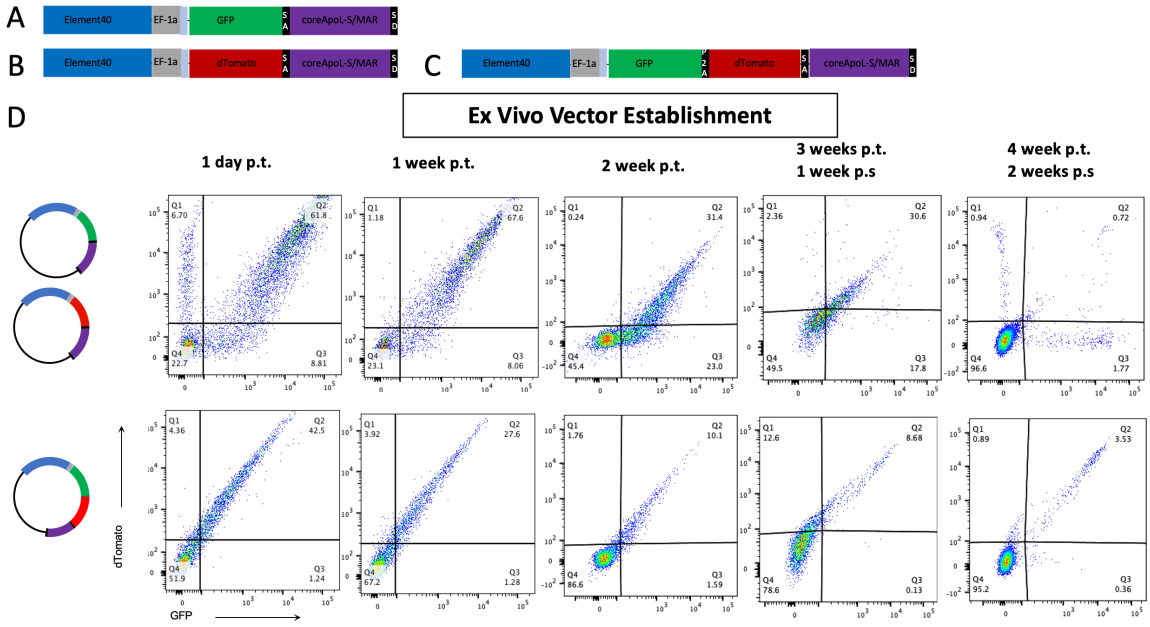

Figure 25 "All-in-one" and "two-vector" ***ex vivo*** **establishment. A) B) C)** Schematic of the S/MAR vector SP-C/MAR-GFP and SP-C/MAR- dTomato ("two-vector" system) and SP-C/MAR-GFP-P2A-dTomato ("all-in-one" system). Displayed the main features: the insulator (Element 40), the promoter sequence (sEF1α), the transgenes GFP (A), dTomato, GFP and dTomato linked by the "self-cleaving" peptide 2A and finally the coreApoL S/MAR (C/MARt) flanked by the splicing site acceptor (SA) and donor (SD). **D)** Representative flow cytometry plots. The human J76 T cell line was transfected and cultured under normal conditions, without any antibiotic selection for one month. Transgene expression was followed for one month and double-positive cells (Q2) were FACS sorted two and four weeks after the transfection.

Until the 3rd week of the establishment, the "two-vector" approach showed a higher % of double positive cells however, at the end of the establishment (4 weeks post-transfection) a large proportion of double positive cells was lost with the "two-vector", but maintained in the "all-in-one system" (**Figure 25D**).

The "all-in-one" and "2 vector "systems were then used to encode the anti-MART1 TCR under the constitutive promoter sEF1α and a reporter gene (GFP) under the (6x)NFAT responsive element. The 2 systems were then tested in a co-culture system with effector Jurkat 76 T and target cells, either the MART1^{+} MeWo or MART1^{+}-U87 tumor cells. A time course experiment, in order to find the optimal time-point for reporter activation and to determine the kinetics of NFAT, revealed that GFP was expressed in response to MART-1 antigen stimulation with a maximum signal at 24h (data not shown).

I concluded that these data suggest a separate segregation of the vectors during cell division and that the "all-in-one system" is the best approach for the generation of TRUCKs T cells.

4.3.2 Next generation of vectors: which responsive element should drive the inducible transgene expression?

Once the optimal approach for delivering two separate expression cassettes was determined, I proceeded to investigate the selection of the most suitable responsive elements for driving T cell augmentation genes. To assess this, I utilized a fluorescent triple parameter transcriptional reporter (TPR) T cell line, kindly provided by Peter Steinberger, which allowed for the simultaneous measurement of the activity of the transcription factors nuclear factor kappa-light-chain-enhancer of activated B-cells (NF-κB), nuclear factor of activated T cells (NFAT), and transcription factor activator protein-1 (AP-1). The TPR T cell line was transduced with reporter constructs NFAT-eGFP, NF-κB-CFP, and AP-1-mCherry, enabling the simultaneous measurement of NF-κB, NFAT, and AP-1 activity (**Figure 26A**). Additionally, J76 TPR cells were transfected to express the anti-MART-1 TCR and were subjected to antigen stimulation for 24 hours. Comparative analysis revealed that the NFAT responsive element induced a higher level of fluorescent protein (FP) expression and exhibited a higher mean fluorescence intensity (MFI) when effector anti-MART-1 TCR T cells were co-cultured with the target cell line MeWo MART-1l^{ow} at an E:T 2:1 (**Figure 26B-D**).

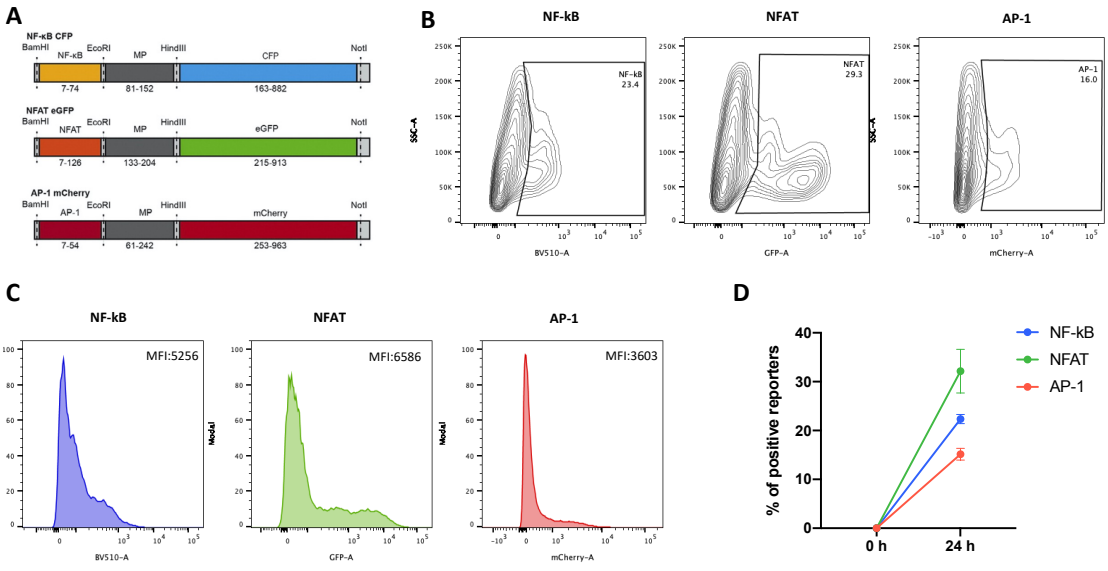

Figure 26 NFAT-mediated inducible GFP expression after transgenic TCR engagement with target antigen. A) Schematic of the J76 TPR adapted from (Jutz et al., 2015)[142]. **B) C) D)** Activity of the AP-1, NF-kB and NFAT

inducible promoter in J76 TPR T cells upon antigen-stimulation (MeWo tumor cells). **B) D**) % of positive reporters and **C)** histograms after 24 h co-culture of effector TCR anti-MART-1 T cells and MeWo target cells at E:T 2:1 (n=3).

Based on these findings, I concluded that the NFAT responsive element is the most suitable choice for our application.

4.3.3 TRUCK TCR T cells expressing hIL12: which mini promoter should drive the inducible transgene expression?

Next, I tested the potency of the "all-in-one" approach to combine TCR gene transfer with regulated cytokine expression. It has been recently shown that hIL12 can boost the cytotoxicity of CAR-T cells and reshapes the TME in a pre-clinical model of glioblastoma [66]. Based on this evidence I decided to swap the GFP with the hIL12 gene in our "all-in-one" vector backbone. Moreover, I decided to test two different mini-promoters as recent evidence suggest the importance of the minipromoter in driving inducible cytokines expression [143]. The classical IL2 minipromoter was compared to a new synthetic TATA promoter (**Figure 27A**). To assess the function of our armoured TCR construct, Jurkat 76 T were transfected with either the two "all-in-one" vector system encoding for the anti-MART1 TCR and hIL12 or the previously described sEF1α anti-MART-1 vector. All vectors resulted in comparable transfection efficiency of T cells, indicating that multiple expression cassettes don't affect the viability and the transfection efficiency of Jurkat 76 T cells (data not shown). In order to then determine their functionality, effector cells were then co-cultured with target cells (MART1^{+} Mel264 or MART1^{+}-U87) at an E:T ratio 1:1 and 48 h post co-culture supernatant was collected and hIL12 measured. Only TATA^{syn} cells were secreting IL12 after TCR stimulation (**Figure 27B**).

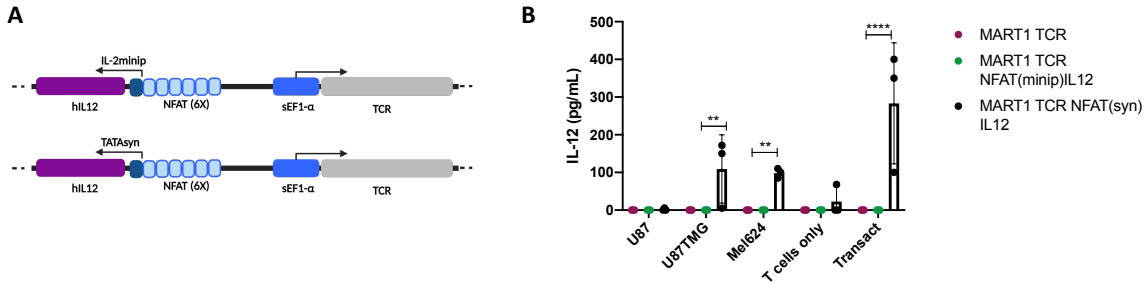

Figure 27 NFAT-TATA^{syn} drives specific hIL-12 production after TCR engagement. A) Schematic of the two TRUCKs constructs; sEF1α promoter drives constitutive expression of anti-MART-1 TCR whereas hIL-12 expression is under the NFAT responsive element and the TATA^{syn} minipromoter. **B)** ELISA showing the production of hIL12 post stimulation with tumor cells (U87 MART-1^{-}, MART-1^{+} U87 TMG and Mel264) and Transact (aCD3/CD28) (n=3). The results are expressed as the mean ± SD (n=3). Two-ways anova test was performed followed by post hoc analysis: *p < 0.05; **p < 0.01; ***p < 0.001 ****p < 0.0001.

I then conclude that NFATminiTATA^{syn} are the optimal features to generate TRUCK TCR-T cells, however future experiments need to be performed in order to translate this approach to primary CD3+ T cells. However, this data shows the potency of our system to generate vectors with different expression cassettes for T cells augmentation.

5. Discussion

Non-viral, non-integrative systems for genetic modification of cells, particularly T cells, hold tremendous promise in the field of Adoptive Cell Therapy. Despite the numerous modifications made to enhance viral vectors, they still possess several limitations, including safety concerns, risk of insertional mutagenesis, immune responses against the virus, limited cargo capacity, lengthy and costly manufacturing processes, and stringent regulatory guidelines for long-term virus monitoring [144]. On the other hand, non-viral alternatives have exhibited limited efficacy, primarily due to transient expression of therapeutic CAR or TCR and poor viability among T cells. In this thesis, I aim to address these challenges by exploring the potential of the non-viral nS/MAR DNA vector platform to generate recombinant T cells for tumor treatment, with a particular focus on the translation of this platform to clinical applications and the advancement of personalized therapy.

The S/MAR feature allows transgene expression from a vector without integrating into the host genome. MAR sequences have been shown to localize preferentially in actively transcribed regions, within promoter sequences and transcription start sites, allowing the vector to associate with the origin of replication complexes and replicate together with the cell´s genome. However, the establishment of the S/MAR vector as episomes is believed to be a random process only to some extent, and to be influenced by the nuclear compartment where the vector settles after reaching the nucleus. Following transfection, most of the DNA molecules are normally lost within few days. Only those that settle in a favourable for transcription and replication nuclear compartment can be retained as episomes and therefore, through limitless cell divisions.

As a proof of concept, I first demonstrated that nS/MAR DNA vectors have the capability to generate stable cell lines in rapidly dividing Jurkat 76 T cells. This resulted in sustained transgene expression through episomal retention, following an establishment period of approximately one month in rapidly dividing cells, although the length of this period can vary depending on the cell type. Subsequently, I explored the potential of this system in CD3+ primary cells, where transgene expression remained detectable for approximately four weeks of culture. Moreover, as already previously shown, while pEPI GFP expression declined significantly after one week, nS/MAR vectors exhibited a delayed decline. This decline can be regarded as a desirable safety feature, ensuring that only a sub-population

of modified T cells persist in the body. However, even after 27 days, still a good proportion of GFP positive cells was detectable. These findings align with previous results in the laboratory, which demonstrated the superior performance of the nano vectors compared to the original pEPI S/MAR vector. In fact, this new class of vectors reduce extra bacterial sequencing that can be responsible for the silencing of the vector as well as for increased cellular toxicity.

I also demonstrated that nS/MAR DNA vectors present numerous advantages for the generation of recombinant T cells. Specifically, I showed the universal applicability of this system in generating therapeutic T cells with a different range of CARs and TCRs for both haematological malignancies (such as the anti-CD19 CAR) and solid tumors (such as the anti-CEA CAR, the high-affinity DMF5 anti-MART-1, and four patient-derived TCRs). nS/MARt T cells exhibited potent anti-tumor efficacy without inducing molecular damage and could be compared to or even overperformed currently 'state-of-the-art' used viral and non-viral systems. While the off-the-shelf anti-CD19 CAR T cells exhibited similar efficacy to lentiviral anti-CD19 CAR T cells in a pre-clinical model for haematological malignancies, the anti-CEA CAR pre-clinical model proved superior when compared to the lentiviral CEA-CAR and comparable to the Sleeping Beauty system. A single nS/MARt CAR T cell achieved the same efficacy as four lentiviral CAR T cells. This substantial improvement in anti-tumor activity was consistently observed and validated in both *in vitro* and *in vivo* settings. In the *in vivo* study, the nS/MAR-treated group exhibited delayed tumor growth and prolonged survival compared to the lentivirus-treated group. These results emphasize the potential of the nS/MAR system in enhancing therapeutic outcomes for solid tumors.

Furthermore, CAR T cells exhibited greater infiltration capacities compared to SIN-Lenti and demonstrated long-term efficacy in an *ex-vivo* cytotoxicity assay following treatment, indicating their potential for durable anti-tumor responses. The observed long-term persistence can be attributed to the superior activity of nS/MAR CAR-T cells when compared to Lenti CAR-T cells. In fact, clinical data has consistently shown a correlation between T cell expansion, molecular characteristics, phenotype, and long-term persistence, which is critical for achieving successful outcomes in patients [145][146][147][144]. It is worth noting that traditional lentiviral protocols for generating CAR-T cells can contribute to the development of an exhausted phenotype, and recent studies have highlighted the

association between upregulated genes associated with an effector or exhausted phenotype and the absence of clinical response.

In this work, the potential toxicity associated with DNA electroporation was reduced through refinement of the vector and the substitution of the classical bacterial backbone with the NTX bacterial backbone, as well as by optimising the DNA electroporation protocol. In fact, contrary to other DNA platforms such as Sleeping Beauty, where CpG island-mediated IFN-β production has been observed and associated with molecular damage to the cells, nS/MARt vectors did not cause molecular damage or IFN-β, as shown by ELISA and RNA-seq data [133]. In fact, the transduction with SIN-lenti vectors can lead to gene expression perturbation and upregulation of genes involved in T cell activation, such as IFN-β and RANTES. In contrast, nS/MAR vectors showed minimal genomic alterations, which can be correlated with their superior activity. Moreover, nS/MAR vectors offer a superior safety profile compared to other integration-based systems, such as viral vectors and transposons, which tend to integrate into active areas of the genome, posing a risk of genotoxicity. In this context, the episomal retention and autonomous replication of nS/MAR vectors outside of the chromosomal DNA contribute to their enhanced safety.

Despite their prolonged anti-tumor potential and increased in survival it is important to note that complete eradication of tumor growth was not achieved in either pre-clinical model. This observation is consistent with the clinical outcomes for the CD19 model where, despite initially achieving significant remission rates for B-cell malignancies, the occurrence of relapse remains a major challenge in long-term therapy effectiveness [148]. Similarly, the CEA model did not exhibit a complete response, which is common in heterogeneous solid tumors. Notably, the target tumor cells in the CEA model demonstrated loss of expression of the targeted CEA antigen and overgrowth of CEA-negative subclones. This suggests that the lack of complete response does not depend on the ineffectiveness of the CAR-T cells, which still demonstrated activity *ex vivo*, but rather to a common tumor escape mechanism that can occur following tumor treatment [149]. To overcome this challenge, strategies such as targeting multiple antigens or armouring CAR T cells with inducible cytokines to recruit other immune cells (TRUCKs) can be explored.

Another important result was the demonstration of the feasibility of this approach also in generating transgenic TCR-T cells.

As a proof of concept, I could show that nS/MAR vectors are valuable systems for the generation of the high-affinity DM5F anti-MART-1 TCR, currently investigated in clinical trial (Phase I/II) in melanoma patients [137][48].

For this, the nS/MAR vector backbone was further improved by incorporating a smaller core spliced S/MAR (500 bp), resulting in a more compact vector size. Additionally, a range of strong and weaker promoters were tested to optimize the performance of the system. It is worth noting that the choice of promoter plays a crucial role in driving T cell function. Recent studies have highlighted the impact of TCR density on T cell activation, cytotoxicity, and cytokine production [139]. In this thesis, I demonstrated not only that the sEF1α promoter exhibited prolonged transgene expression in Jurkat 76 cells, but also that it showed higher transfection efficiency leading to higher levels of TCR expression, TCR molecules on the cell surface, and cytokine response in primary T cells. However, no significant difference in killing capabilities observed in bulk populations of primary TCR-T cells could be observed. Currently, subpopulations of anti-MART-1 TCR-T cells with the sEF1α promoter are being compared to those with a weaker promoter such as hTCR, to determine "super-killer" subpopulations capable of targeting multiple tumor cells. Previous studies revealed the enrichment of T cell-specific transcription factor binding sites in the sEF1α promoter, which could explain its superior transgene retention capabilities [139]. However, further bioinformatics analyses are ongoing on the promoters used in this study to determine potential binding sites for TFs and other core promoter elements that can influence the activation of the promoters.

Another important aspect I investigated with my work was the potential of the nS/MAR platform to generate patient-specific TCR T cells targeting neo-epitopes found in solid tumors. To evaluate this, the anti-MART-1 TCR with patient-reactive TCRs obtained from a previously vaccinated GMB patient and three TCRs from a secondary brain tumor patient were replaced. The versatility of the vector design allowed for easy swapping and production of vectors, demonstrating the platform's potency for personalized therapy.

In vitro assays showed cytotoxicity and cytokine production for all four nS/MAR patient-derived TCRs T cells. This highlights the broad versatility and effectiveness of the nanovector-based approach for generating customized therapeutic T cells. However, comprehensive validation of the platform requires further *in vivo* experiments.

Surprisingly, although sEF1α anti-MART-1 TCR-T cells exhibited activity in 2D and 3D, *in vitro* systems, their performance could not be recapitulated in the *in vivo* xenograft model, despite T cells tumor infiltration and engraftment. However, TCR expression was not detected in TILs for the MART-1 model. Also, the GB *in vivo* model, despite TCR-T cells showed persistence 14 days post 2nd ACT injection, no *in vivo* anti-tumor effect for both nS/MAR and SFG state-of-the-art retroviral controls was observed. Additional experiments are necessary therefore to understand possible mechanism correlated with the lack of response and determine the efficacy of TCR-T cells.

In fact, while nS/MAR CAR-T cells exhibited long-term persistence in CAR pre-clinical models, the efficacy of TCRs still needs further validation. *In vitro* killing assays simulating a consistent antigen exposure demonstrated that TCR expression and cytotoxic capacity decreased after four rounds of killing. This raises the question of whether the loss of TCR expression is due to physiological TCR turnover regulated by endocytosis or other factors [76]. Unlike TCRs, GFP expression was retained after three weeks post-transfection, suggesting the need for further analysis to investigate if T cell activation induces the internalization TCRs. This could be addressed by modifying the metabolic state or phenotype of the cells or by the administration of multiple injections. Alternatively, the concept of TRUCK (T cells redirected for antigen-unrestricted cytokine-initiated killing) CAR or TCR-T cells could also be explored. Solid tumors, like glioblastoma often possess a highly immune-suppressive tumor microenvironment, and paracrine cytokine support such as IL12 has shown enhanced anti-tumor activity and microenvironment reshaping in preclinical brain tumor models [150][151][152]. To avoid systemic toxicity, TRUCK TCR-T cells express the cytokine of interest, such as IL12, only upon TCR engagement and signaling. The production of IL12 will subsequently activate other components of the immune system, such as NK cells, therefore the transgenic TCR will provide only the first stimuli to recruit the host immune cells and provide an effective anti-immune response.

In my thesis, I described a method for generating TRUCK TCR-T cells using a single vector encoding two separate expression cassettes: the constitutive anti-MART-1 TCR under the control of the sEF1α promoter, and the inducible hIL12 under the regulation of the NFAT responsive element and a TATA^{syn} minipromoter. Unlike most studies with viral vectors, which generally employ two separate vectors to generate TRUCKs, this one-vector approach successfully produced TCR TRUCK T cells in a Jurkat 76 T cell model. The use

of a single vector offers advantages, since different vectors do not co-segregate, and it minimally affects transfection efficiency. I therefore demonstrated that the nS/MAR platform can be applied to more complex constructs, such as the generation of TCR TRUCK T cells. Furthermore, the simplicity of the vector design enables the exchange of transgenes, allowing for the application of the system in various settings, such as different TCRs or cytokines based on the tumor entity. Additionally, using a single vector reduces manufacturing costs, making it a more feasible option for translation. Nevertheless, further experiments are required to translate these findings to primary T cells.

Clinical translation

One of the major challenges in the clinical translation of therapeutic T cells is the manufacturing process. The scalability of current viral protocols poses significant limitations, as they are time-consuming, expensive, and require several weeks or months for Good Manufacturing Practice (GMP)-virus production and recombinant T cell generation. For example, the manufacturing process for Kymriah typically spans approximately 3-4 weeks and involves multiple regulatory steps [153]. Patients with advanced or aggressive cancers often face a limited treatment window of less than six months, necessitating the development of shorter manufacturing protocols. Furthermore, prolonged expansion protocols have been shown to alter the phenotype of T cells, compromising their persistence *in vivo* and impacting the clinical outcome.

Working with viral vectors under GMP conditions requires specialized expertise, resulting in limited availability of facilities capable of generating therapeutic T cells. Standardizing the manufacturing process to ensure consistent production of high-quality therapeutic T cells also remains a significant challenge. Additionally, the cost and time associated with extensive quality and safety control analyses for DNA vectors are substantial. Therefore, alternative methods for modifying and manufacturing T cells are needed [154][144].

The use of naked DNA or RNA, without the need for GMP-virus production, can overcome the cost and time restrictions. nS/MAR vectors can be produced in larger quantities under GMP conditions, reducing costs, time, and regulatory requirements. In fact, the quality and safety testing for DNA vectors required for clinical applications are simpler, more cost-effective, and time-saving, offering several advantages over currently used platforms.

Previous studies from our laboratory have demonstrated a GMP-compatible manufacturing process that generated 1.6x 10^8 CAR T cells. In this thesis, I further improved the transfection protocol to increase cell yield and reduce DNA usage, resulting in even greater cost savings using the MaxCyte ExPERT GTx platform. Based on estimates, a batch of 4 x10^8 recombinant TCR-T cells can be produced with only 250 μg of vectors. The use of nS/MAR T cells will enable large-scale production of therapeutic T cells under GMP conditions, bypassing the need for extensive quality and safety controls associated with viral vectors. In the proposed protocol, the production timeline can be significantly reduced to five days, facilitating prompt manufacturing and delivery of personalized T cell therapies for patients with solid tumors. Furthermore, compared to viruses, nS/MAR vectors allow modifications in non-dividing cells as well. Although our current protocol employs activated cells for electroporation, our system is capable of transfecting non-activated cells, further shortening the manufacturing process. However, additional research and experimentation are necessary to optimize this process and identifying the optimal conditions for successfully introduce nS/MAR DNA vectors in non-activated cells.

The use of this technology not only can address patient-specific mutations but also ensures the feasibility of providing effective treatment within the limited therapeutic window experienced by end-stage cancer patients. Moreover, compared to viruses, nS/MAR vectors allow for greater flexibility in T cells modifications, offering a promising avenue for advancing personalized immunotherapies.

6. Conclusions

In conclusion, this thesis demonstrates the efficacy of nS/MAR DNA Vectors for genetic modification of T cells in the field of ACT, holding a universal applicability for transgenic receptors, as evidenced by the demonstration of their successful applications to both CARs and TCRs.

The use of viral vectors in gene modification presents several limitations such as safety concerns, immune response, and manufacturing challenges. To overcome these obstacles, non-viral alternatives have been investigated although with limited success due to their reduced efficacy mostly caused by the transient transgene expression. In contrast, the nS/MAR vectors developed during this thesis can generate sustained reporter gene expression in both rapidly dividing Jurkat T cell line and primary human T cells, without integrating into the host genome and causing molecular damage or cell toxicity derived from DNA electroporation.

The versatility of the nS/MAR system in generating recombinant T cells with different CARs was also assessed. nS/MAR CAR-T cells exhibit potent anti-tumor efficacy, comparable or superior to viral and non-viral systems, both in haematological malignancies and solid tumors. They demonstrate long-term persistence, infiltration capacities, and durable anti-tumor responses in pre-clinical model of anti-CD19 and anti-CEA CARs. This platform was also suitable for effectively generating both off-the-shelf and patient-specific TCR-T cells targeting neo-epitopes found in solid tumors, highlighting its versatility and effectiveness. However, further *in vivo* validation is required. The platform also showed the potential of generating more complex constructs, such as TRUCKs, to armour T cells with cytokines, (e.g., IL12), to enhance therapeutic outcomes. The ability of TRUCKs constructs in re-modelling the tumor microenvironment in the context of glioblastoma and re-shape immune cells, such as NK cells, will need to be explored in future experiments. Finally, my work also addresses the challenges of the large-scale manufacturing for the clinical translation. The nS/MAR platform offers a more feasible and cost-effective approach for manufacturing therapeutic T cells, bypassing the need for expensive and time consuming GMP-virus production and controls. The simplified manufacturing process, the reduced regulatory requirements, the scalability and cost savings contribute to its potential clinical applicability making personalized T cell therapies more accessible to patients with limited treatment windows.

7. References

[1] Murphy K.M., Weaver C., Berg L.J., *Janeway's Immunobiology*, 10th ed. 2022.

[2] M. F. Flajnik and M. Kasahara, "Origin and evolution of the adaptive immune system: genetic events and selective pressures," *Nat Rev Genet*, vol. 11, no. 1, pp. 47–59, Jan. 2010, doi: 10.1038/nrg2703.

[3] S. McComb, A. Thiriot, B. Akache, L. Krishnan, and F. Stark, "Introduction to the Immune System," in *Immunoproteomics*, K. M. Fulton and S. M. Twine, Eds., in Methods in Molecular Biology, vol. 2024. New York, NY: Springer New York, 2019, pp. 1–24. doi: 10.1007/978-1-4939-9597-4_1.

[4] M. M. Davis and P. J. Bjorkman, "T-cell antigen receptor genes and T-cell recognition," *Nature*, vol. 334, no. 6181, pp. 395–402, Aug. 1988, doi: 10.1038/334395a0.

[5] C. B. Thompson, "New insights into V(D)J recombination and its role in the evolution of the immune system," *Immunity*, vol. 3, no. 5, pp. 531–539, Nov. 1995, doi: 10.1016/1074-7613(95)90124-8.

[6] Y. Yin, X. X. Wang, and R. A. Mariuzza, "Crystal structure of a complete ternary complex of T-cell receptor, peptide–MHC, and CD4," *Proc. Natl. Acad. Sci. U.S.A.*, vol. 109, no. 14, pp. 5405–5410, Apr. 2012, doi: 10.1073/pnas.1118801109.

[7] J. E. Smith-Garvin, G. A. Koretzky, and M. S. Jordan, "T Cell Activation," *Annu. Rev. Immunol.*, vol. 27, no. 1, pp. 591–619, Apr. 2009, doi: 10.1146/annurev.immunol.021908.132706.

[8] G. Gaud, R. Lesourne, and P. E. Love, "Regulatory mechanisms in T cell receptor signalling," *Nat Rev Immunol*, vol. 18, no. 8, pp. 485–497, Aug. 2018, doi: 10.1038/s41577-018-0020-8.

[9] M. N. Artyomov, M. Lis, S. Devadas, M. M. Davis, and A. K. Chakraborty, "CD4 and CD8 binding to MHC molecules primarily acts to enhance Lck delivery," *Proc. Natl. Acad. Sci. U.S.A.*, vol. 107, no. 39, pp. 16916–16921, Sep. 2010, doi: 10.1073/pnas.1010568107.

[10] L. Chen and D. B. Flies, "Molecular mechanisms of T cell co-stimulation and co-inhibition," *Nat Rev Immunol*, vol. 13, no. 4, pp. 227–242, Apr. 2013, doi: 10.1038/nri3405.

[11] T. H. Watts, "TNF/TNFR FAMILY MEMBERS IN COSTIMULATION OF T CELL RESPONSES," *Annu. Rev. Immunol.*, vol. 23, no. 1, pp. 23–68, Apr. 2005, doi: 10.1146/annurev.immunol.23.021704.115839.

[12] E. Corse and J. P. Allison, "Cutting Edge: CTLA-4 on Effector T Cells Inhibits In *Trans*," *The Journal of Immunology*, vol. 189, no. 3, pp. 1123–1127, Aug. 2012, doi: 10.4049/jimmunol.1200695.

[13] M. Sznol and L. Chen, “Antagonist Antibodies to PD-1 and B7-H1 (PD-L1) in the Treatment of Advanced Human Cancer,” *Clinical Cancer Research*, vol. 19, no. 5, pp. 1021–1034, Mar. 2013, doi: 10.1158/1078-0432.CCR-12-2063.

[14] J. L. Riley, “PD-1 signaling in primary T cells,” *Immunological Reviews*, vol. 229, no. 1, pp. 114–125, May 2009, doi: 10.1111/j.1600-065X.2009.00767.x.

[15] E. Baixeras *et al.*, “Characterization of the lymphocyte activation gene 3-encoded protein. A new ligand for human leukocyte antigen class II antigens.,” *Journal of Experimental Medicine*, vol. 176, no. 2, pp. 327–337, Aug. 1992, doi: 10.1084/jem.176.2.327.

[16] S. Hannier, M. Tournier, G. Bismuth, and F. Triebel, “CD3/TCR Complex-Associated Lymphocyte Activation Gene-3 Molecules Inhibit CD3/TCR Signaling,” *The Journal of Immunology*, vol. 161, no. 8, pp. 4058–4065, Oct. 1998, doi: 10.4049/jimmunol.161.8.4058.

[17] R. B. Jones *et al.*, “Tim-3 expression defines a novel population of dysfunctional T cells with highly elevated frequencies in progressive HIV-1 infection,” *Journal of Experimental Medicine*, vol. 205, no. 12, pp. 2763–2779, Nov. 2008, doi: 10.1084/jem.20081398.

[18] J. V. Gorman and J. D. Colgan, “Regulation of T cell responses by the receptor molecule Tim-3,” *Immunol Res*, vol. 59, no. 1–3, pp. 56–65, Aug. 2014, doi: 10.1007/s12026-014-8524-1.

[19] C. Zhu *et al.*, “The Tim-3 ligand galectin-9 negatively regulates T helper type 1 immunity,” *Nat Immunol*, vol. 6, no. 12, pp. 1245–1252, Dec. 2005, doi: 10.1038/ni1271.

[20] G. P. Dunn, L. J. Old, and R. D. Schreiber, “The Immunobiology of Cancer Immunosurveillance and Immunoediting,” *Immunity*, vol. 21, no. 2, pp. 137–148, Aug. 2004, doi: 10.1016/j.immuni.2004.07.017.

[21] C. M. Koebel *et al.*, “Adaptive immunity maintains occult cancer in an equilibrium state,” *Nature*, vol. 450, no. 7171, pp. 903–907, Dec. 2007, doi: 10.1038/nature06309.

[22] I. Algarra, T. Cabrera, and F. Garrido, “The HLA crossroad in tumor immunology,” *Human Immunology*, vol. 61, no. 1, pp. 65–73, Jan. 2000, doi: 10.1016/S0198-8859(99)00156-1.

[23] S. Fulda, “Tumor resistance to apoptosis,” *Int. J. Cancer*, vol. 124, no. 3, pp. 511–515, Feb. 2009, doi: 10.1002/ijc.24064.

[24] H. T. Khong and N. P. Restifo, “Natural selection of tumor variants in the generation of ‘tumor escape’ phenotypes,” *Nat Immunol*, vol. 3, no. 11, pp. 999–1005, Nov. 2002, doi: 10.1038/ni1102-999.

[25] D. I. Gabrilovich and S. Nagaraj, “Myeloid-derived suppressor cells as regulators of the immune system,” *Nat Rev Immunol*, vol. 9, no. 3, pp. 162–174, Mar. 2009, doi: 10.1038/nri2506.

[26] J. A. Joyce and D. T. Fearon, “T cell exclusion, immune privilege, and the tumor microenvironment,” *Science*, vol. 348, no. 6230, pp. 74–80, Apr. 2015, doi: 10.1126/science.aaa6204.

[27] Y. Xing and K. A. Hogquist, “T-Cell Tolerance: Central and Peripheral,” *Cold Spring Harbor Perspectives in Biology*, vol. 4, no. 6, pp. a006957–a006957, Jun. 2012, doi: 10.1101/cshperspect.a006957.

[28] T. F. Gajewski *et al.*, “Immune resistance orchestrated by the tumor microenvironment,” *Immunol Rev*, vol. 213, no. 1, pp. 131–145, Oct. 2006, doi: 10.1111/j.1600-065X.2006.00442.x.

[29] F. M. Burnet, “The Concept of Immunological Surveillance,” in *Progress in Tumor Research*, R. S. Schwartz, Ed., S. Karger AG, 1970, pp. 1–27. doi: 10.1159/000386035.

[30] L. Thomas, “On immunosurveillance in human cancer,” *Yale J Biol Med*, vol. 55, no. 3–4, pp. 329–333, 1982.

[31] A. D. Waldman, J. M. Fritz, and M. J. Lenardo, “A guide to cancer immunotherapy: from T cell basic science to clinical practice,” *Nat Rev Immunol*, vol. 20, no. 11, pp. 651–668, Nov. 2020, doi: 10.1038/s41577-020-0306-5.

[32] T. Bartkowiak and M. A. Curran, “4-1BB Agonists: Multi-Potent Potentiators of Tumor Immunity,” *Front. Oncol.*, vol. 5, Jun. 2015, doi: 10.3389/fonc.2015.00117.

[33] K. K.-L. Fang, J. B. Lee, and L. Zhang, “Adoptive Cell Therapy for T-Cell Malignancies,” *Cancers*, vol. 15, no. 1, p. 94, Dec. 2022, doi: 10.3390/cancers15010094.

[34] S. A. Rosenberg *et al.*, “A Progress Report on the Treatment of 157 Patients with Advanced Cancer Using Lymphokine-Activated Killer Cells and Interleukin-2 or High-Dose Interleukin-2 Alone,” *N Engl J Med*, vol. 316, no. 15, pp. 889–897, Apr. 1987, doi: 10.1056/NEJM198704093161501.

[35] S. A. Rosenberg *et al.*, “Use of Tumor-Infiltrating Lymphocytes and Interleukin-2 in the Immunotherapy of Patients with Metastatic Melanoma,” *N Engl J Med*, vol. 319, no. 25, pp. 1676–1680, Dec. 1988, doi: 10.1056/NEJM198812223192527.

[36] S. Stevanović *et al.*, “Complete Regression of Metastatic Cervical Cancer After Treatment With Human Papillomavirus–Targeted Tumor-Infiltrating T Cells,” *JCO*, vol. 33, no. 14, pp. 1543–1550, May 2015, doi: 10.1200/JCO.2014.58.9093.

[37] R. Andersen *et al.*, “T-cell Responses in the Microenvironment of Primary Renal Cell Carcinoma—Implications for Adoptive Cell Therapy,” *Cancer Immunology Research*, vol. 6, no. 2, pp. 222–235, Feb. 2018, doi: 10.1158/2326-6066.CIR-17-0467.

[38] H. J. Lee *et al.*, “Expansion of tumor-infiltrating lymphocytes and their potential for application as adoptive cell transfer therapy in human breast cancer,” *Oncotarget*, vol. 8, no. 69, pp. 113345–113359, Dec. 2017, doi: 10.18632/oncotarget.23007.

[39] R. Ben-Avi *et al.*, “Establishment of adoptive cell therapy with tumor infiltrating lymphocytes for non-small cell lung cancer patients,” *Cancer Immunol Immunother*, vol. 67, no. 8, pp. 1221–1230, Aug. 2018, doi: 10.1007/s00262-018-2174-4.

[40] M. W. Rohaan, S. Wilgenhof, and J. B. A. G. Haanen, “Adoptive cellular therapies: the current landscape,” *Virchows Arch*, vol. 474, no. 4, pp. 449–461, Apr. 2019, doi: 10.1007/s00428-018-2484-0.

[41] M. Lauss *et al.*, “Author Correction: Mutational and putative neoantigen load predict clinical benefit of adoptive T cell therapy in melanoma,” *Nat Commun*, vol. 11, no. 1, p. 1714, Apr. 2020, doi: 10.1038/s41467-020-15531-2.

[42] G. U. Mehta *et al.*, “Outcomes of Adoptive Cell Transfer With Tumor-infiltrating Lymphocytes for Metastatic Melanoma Patients With and Without Brain Metastases,” *Journal of Immunotherapy*, vol. 41, no. 5, pp. 241–247, Jun. 2018, doi: 10.1097/CJI.0000000000000223.

[43] R. O. Dillman *et al.*, “Intracavitary Placement of Autologous Lymphokine-Activated Killer (LAK) Cells after Resection of Recurrent Glioblastoma:,” *Journal of Immunotherapy*, vol. 27, no. 5, pp. 398–404, Sep. 2004, doi: 10.1097/00002371-200409000-00009.

[44] R. O. Dillman *et al.*, “Intralesional Lymphokine-activated Killer Cells as Adjuvant Therapy for Primary Glioblastoma,” *Journal of Immunotherapy*, vol. 32, no. 9, pp. 914–919, Nov. 2009, doi: 10.1097/CJI.0b013e3181b2910f.

[45] I. C. Poschke *et al.*, “The Outcome of *Ex Vivo* TIL Expansion Is Highly Influenced by Spatial Heterogeneity of the Tumor T-Cell Repertoire and Differences in Intrinsic *In Vitro* Growth Capacity between T-Cell Clones,” *Clinical Cancer Research*, vol. 26, no. 16, pp. 4289–4301, Aug. 2020, doi: 10.1158/1078-0432.CCR-19-3845.

[46] Q. Zhao *et al.*, “Engineered TCR-T Cell Immunotherapy in Anticancer Precision Medicine: Pros and Cons,” *Front. Immunol.*, vol. 12, p. 658753, Mar. 2021, doi: 10.3389/fimmu.2021.658753.

[47] Y. Liu *et al.*, “TCR-T Immunotherapy: The Challenges and Solutions,” *Front. Oncol.*, vol. 11, p. 794183, Jan. 2022, doi: 10.3389/fonc.2021.794183.

[48] R. A. Morgan *et al.*, “Cancer Regression in Patients After Transfer of Genetically Engineered Lymphocytes,” *Science*, vol. 314, no. 5796, pp. 126–129, Oct. 2006, doi: 10.1126/science.1129003.

[49] L. A. Johnson *et al.*, “Gene therapy with human and mouse T-cell receptors mediates cancer regression and targets normal tissues expressing cognate antigen,” *Blood*, vol. 114, no. 3, pp. 535–546, Jul. 2009, doi: 10.1182/blood-2009-03-211714.

[50] P. F. Robbins *et al.*, “A Pilot Trial Using Lymphocytes Genetically Engineered with an NY-ESO-1–Reactive T-cell Receptor: Long-term Follow-up and Correlates with Response,” *Clinical Cancer Research*, vol. 21, no. 5, pp. 1019–1027, Mar. 2015, doi: 10.1158/1078-0432.CCR-14-2708.

[51] T. S. Nowicki *et al.*, “A Pilot Trial of the Combination of Transgenic NY-ESO-1–reactive Adoptive Cellular Therapy with Dendritic Cell Vaccination with or without Ipilimumab,” *Clinical Cancer Research*, vol. 25, no. 7, pp. 2096–2108, Apr. 2019, doi: 10.1158/1078-0432.CCR-18-3496.

[52] G. R. Blumenschein *et al.*, “Phase I clinical trial evaluating the safety and efficacy of ADP-A2M10 SPEAR T cells in patients with MAGE-A10 $^{+}$ advanced non-small cell lung cancer,” *J Immunother Cancer*, vol. 10, no. 1, p. e003581, Jan. 2022, doi: 10.1136/jitc-2021-003581.

[53] S. Kageyama *et al.*, “Adoptive Transfer of MAGE-A4 T-cell Receptor Gene-Transduced Lymphocytes in Patients with Recurrent Esophageal Cancer,” *Clinical Cancer Research*, vol. 21, no. 10, pp. 2268–2277, May 2015, doi: 10.1158/1078-0432.CCR-14-1559.

[54] E. Baulu, C. Gardet, N. Chuvin, and S. Depil, “TCR-engineered T cell therapy in solid tumors: State of the art and perspectives,” *Sci. Adv.*, vol. 9, no. 7, p. eadf3700, Feb. 2023, doi: 10.1126/sciadv.adf3700.

[55] A. M. Gallegos and M. J. Bevan, “Central tolerance: good but imperfect,” *Immunol Rev*, vol. 209, no. 1, pp. 290–296, Feb. 2006, doi: 10.1111/j.0105-2896.2006.00348.x.

[56] A. G. Chapuis *et al.*, “T-Cell Therapy Using Interleukin-21–Primed Cytotoxic T-Cell Lymphocytes Combined With Cytotoxic T-Cell Lymphocyte Antigen-4 Blockade Results in Long-Term Cell Persistence and Durable Tumor Regression,” *JCO*, vol. 34, no. 31, pp. 3787–3795, Nov. 2016, doi: 10.1200/JCO.2015.65.5142.

[57] G. Gross, G. Gorochov, T. Waks, and Z. Eshhar, “Generation of effector T cells expressing chimeric T cell receptor with antibody type-specificity,” *Transplant Proc*, vol. 21, no. 1 Pt 1, pp. 127–130, Feb. 1989.

[58] Z. Eshhar, T. Waks, G. Gross, and D. G. Schindler, “Specific activation and targeting of cytotoxic lymphocytes through chimeric single chains consisting of antibody-binding domains and the gamma or zeta subunits of the immunoglobulin and T-cell receptors.,” *Proc. Natl. Acad. Sci. U.S.A.*, vol. 90, no. 2, pp. 720–724, Jan. 1993, doi: 10.1073/pnas.90.2.720.

[59] H. M. Finney, A. N. Akbar, and A. D. G. Lawson, “Activation of Resting Human Primary T Cells with Chimeric Receptors: Costimulation from CD28, Inducible Costimulator, CD134, and CD137 in Series with Signals from the TCRζ Chain,” *The Journal of Immunology*, vol. 172, no. 1, pp. 104–113, Jan. 2004, doi: 10.4049/jimmunol.172.1.104.

[60] H. M. Finney, A. D. Lawson, C. R. Bebbington, and A. N. Weir, “Chimeric receptors providing both primary and costimulatory signaling in T cells from a single gene product,” *J Immunol*, vol. 161, no. 6, pp. 2791–2797, Sep. 1998.

[61] J. Maher, R. J. Brentjens, G. Gunset, I. Rivière, and M. Sadelain, “Human T-lymphocyte cytotoxicity and proliferation directed by a single chimeric TCRζ /CD28

receptor," *Nat Biotechnol*, vol. 20, no. 1, pp. 70–75, Jan. 2002, doi: 10.1038/nbt0102-70.

[62] C. Imai *et al.*, "Chimeric receptors with 4-1BB signaling capacity provoke potent cytotoxicity against acute lymphoblastic leukemia," *Leukemia*, vol. 18, no. 4, pp. 676–684, Apr. 2004, doi: 10.1038/sj.leu.2403302.

[63] M. A. Pule *et al.*, "Virus-specific T cells engineered to coexpress tumor-specific receptors: persistence and antitumor activity in individuals with neuroblastoma," *Nat Med*, vol. 14, no. 11, pp. 1264–1270, Nov. 2008, doi: 10.1038/nm.1882.

[64] C. Carpenito *et al.*, "Control of large, established tumor xenografts with genetically retargeted human T cells containing CD28 and CD137 domains," *Proc. Natl. Acad. Sci. U.S.A.*, vol. 106, no. 9, pp. 3360–3365, Mar. 2009, doi: 10.1073/pnas.0813101106.

[65] X.-S. Zhong, M. Matsushita, J. Plotkin, I. Riviere, and M. Sadelain, "Chimeric Antigen Receptors Combining 4-1BB and CD28 Signaling Domains Augment PI3kinase/AKT/Bcl-XL Activation and CD8+ T Cell–mediated Tumor Eradication," *Molecular Therapy*, vol. 18, no. 2, pp. 413–420, Feb. 2010, doi: 10.1038/mt.2009.210.

[66] M. Chmielewski, C. Kopecky, A. A. Hombach, and H. Abken, "IL-12 Release by Engineered T Cells Expressing Chimeric Antigen Receptors Can Effectively Muster an Antigen-Independent Macrophage Response on Tumor Cells That Have Shut Down Tumor Antigen Expression," *Cancer Research*, vol. 71, no. 17, pp. 5697–5706, Sep. 2011, doi: 10.1158/0008-5472.CAN-11-0103.

[67] M. Chmielewski and H. Abken, "CAR T Cells Releasing IL-18 Convert to T-Bethigh FoxO1low Effectors that Exhibit Augmented Activity against Advanced Solid Tumors," *Cell Reports*, vol. 21, no. 11, pp. 3205–3219, Dec. 2017, doi: 10.1016/j.celrep.2017.11.063.

[68] Y. Kagoya *et al.*, "A novel chimeric antigen receptor containing a JAK–STAT signaling domain mediates superior antitumor effects," *Nat Med*, vol. 24, no. 3, pp. 352–359, Mar. 2018, doi: 10.1038/nm.4478.

[69] Ö. Umut, A. Gottschlich, S. Endres, and S. Kobold, "CAR T cell therapy in solid tumors: a short review," *memo*, vol. 14, no. 2, pp. 143–149, Jun. 2021, doi: 10.1007/s12254-021-00703-7.

[70] D. L. Porter, B. L. Levine, M. Kalos, A. Bagg, and C. H. June, "Chimeric Antigen Receptor–Modified T Cells in Chronic Lymphoid Leukemia," *N Engl J Med*, vol. 365, no. 8, pp. 725–733, Aug. 2011, doi: 10.1056/NEJMoa1103849.

[71] A. J. Kansagra *et al.*, "Clinical utilization of Chimeric Antigen Receptor T-cells (CAR-T) in B-cell acute lymphoblastic leukemia (ALL)–an expert opinion from the European Society for Blood and Marrow Transplantation (EBMT) and the American Society for Blood and Marrow Transplantation (ASBMT)," *Bone Marrow Transplant*, vol. 54, no. 11, pp. 1868–1880, Nov. 2019, doi: 10.1038/s41409-019-0451-2.

[72] M. Irving, E. Lanitis, D. Migliorini, Z. Ivics, and S. Guedan, “Choosing the Right Tool for Genetic Engineering: Clinical Lessons from Chimeric Antigen Receptor-T Cells,” *Human Gene Therapy*, vol. 32, no. 19–20, pp. 1044–1058, Oct. 2021, doi: 10.1089/hum.2021.173.

[73] W. A. Lim and C. H. June, “The Principles of Engineering Immune Cells to Treat Cancer,” *Cell*, vol. 168, no. 4, pp. 724–740, Feb. 2017, doi: 10.1016/j.cell.2017.01.016.

[74] J. A. Burger and J. G. Gribben, “The microenvironment in chronic lymphocytic leukemia (CLL) and other B cell malignancies: Insight into disease biology and new targeted therapies,” *Seminars in Cancer Biology*, vol. 24, pp. 71–81, Feb. 2014, doi: 10.1016/j.semcancer.2013.08.011.

[75] H. J. Jackson, S. Rafiq, and R. J. Brentjens, “Driving CAR T-cells forward,” *Nat Rev Clin Oncol*, vol. 13, no. 6, pp. 370–383, Jun. 2016, doi: 10.1038/nrclinonc.2016.36.

[76] K. Teppert, X. Wang, K. Anders, C. Evaristo, D. Lock, and A. Künkele, “Joining Forces for Cancer Treatment: From ‘TCR versus CAR’ to ‘TCR and CAR,’” *IJMS*, vol. 23, no. 23, p. 14563, Nov. 2022, doi: 10.3390/ijms232314563.

[77] S. S. Chandran and C. A. Klebanoff, “T cell receptor-based cancer immunotherapy: Emerging efficacy and pathways of resistance,” *Immunol Rev*, vol. 290, no. 1, pp. 127–147, Jul. 2019, doi: 10.1111/imr.12772.

[78] A. I. Salter *et al.*, “Comparative analysis of TCR and CAR signaling informs CAR designs with superior antigen sensitivity and in vivo function,” *Sci. Signal.*, vol. 14, no. 697, p. eabe2606, Aug. 2021, doi: 10.1126/scisignal.abe2606.

[79] N. Frey and D. Porter, “Cytokine Release Syndrome with Chimeric Antigen Receptor T Cell Therapy,” *Biology of Blood and Marrow Transplantation*, vol. 25, no. 4, pp. e123–e127, Apr. 2019, doi: 10.1016/j.bbmt.2018.12.756.

[80] C. Bonini, M. K. Brenner, H. E. Heslop, and R. A. Morgan, “Genetic Modification of T Cells,” *Biology of Blood and Marrow Transplantation*, vol. 17, no. 1, pp. S15–S20, Jan. 2011, doi: 10.1016/j.bbmt.2010.09.019.

[81] A. Telesnitsky, “Retroviruses: Molecular Biology, Genomics and Pathogenesis,” *Future Virology*, vol. 5, no. 5, pp. 539–543, Sep. 2010, doi: 10.2217/fvl.10.43.

[82] T. Maetzig, M. Galla, C. Baum, and A. Schambach, “Gammaretroviral vectors: biology, technology and application,” *Viruses*, vol. 3, no. 6, pp. 677–713, Jun. 2011, doi: 10.3390/v3060677.

[83] T. Maetzig, M. Galla, C. Baum, and A. Schambach, “Gammaretroviral vectors: biology, technology and application,” *Viruses*, vol. 3, no. 6, pp. 677–713, Jun. 2011, doi: 10.3390/v3060677.

[84] V. Poletti and F. Mavilio, “Designing Lentiviral Vectors for Gene Therapy of Genetic Diseases,” *Viruses*, vol. 13, no. 8, p. 1526, Aug. 2021, doi: 10.3390/v13081526.

[85] E. Papanikolaou *et al.*, “Cell Cycle Status of CD34+ Hemopoietic Stem Cells Determines Lentiviral Integration in Actively Transcribed and Development-related Genes,” *Molecular Therapy*, vol. 23, no. 4, pp. 683–696, Apr. 2015, doi: 10.1038/mt.2014.246.

[86] C. Baum *et al.*, “Chance or necessity? Insertional Mutagenesis in Gene Therapy and Its Consequences,” *Molecular Therapy*, vol. 9, no. 1, pp. 5–13, Jan. 2004, doi: 10.1016/j.ymthe.2003.10.013.

[87] D. Cesana *et al.*, “Uncovering and Dissecting the Genotoxicity of Self-inactivating Lentiviral Vectors In Vivo,” *Molecular Therapy*, vol. 22, no. 4, pp. 774–785, Apr. 2014, doi: 10.1038/mt.2014.3.

[88] J. Scholler *et al.*, “Decade-Long Safety and Function of Retroviral-Modified Chimeric Antigen Receptor T Cells,” *Sci. Transl. Med.*, vol. 4, no. 132, May 2012, doi: 10.1126/scitranslmed.3003761.

[89] K. T. Marcucci *et al.*, “Retroviral and Lentiviral Safety Analysis of Gene-Modified T Cell Products and Infused HIV and Oncology Patients,” *Molecular Therapy*, vol. 26, no. 1, pp. 269–279, Jan. 2018, doi: 10.1016/j.ymthe.2017.10.012.

[90] S. Newrzela *et al.*, “Resistance of mature T cells to oncogene transformation,” *Blood*, vol. 112, no. 6, pp. 2278–2286, Sep. 2008, doi: 10.1182/blood-2007-12-128751.

[91] J. A. Fraietta *et al.*, “Disruption of TET2 promotes the therapeutic efficacy of CD19-targeted T cells,” *Nature*, vol. 558, no. 7709, pp. 307–312, Jun. 2018, doi: 10.1038/s41586-018-0178-z.

[92] K. Hennig *et al.*, “HEK293-Based Production Platform for γ-Retroviral (Self-Inactivating) Vectors: Application for Safe and Efficient Transfer of *COL7A1* cDNA,” *Human Gene Therapy Clinical Development*, vol. 25, no. 4, pp. 218–228, Dec. 2014, doi: 10.1089/humc.2014.083.

[93] A. Barahona, “Barbara McClintock and the transposition concept,” *Arch Int Hist Sci (Paris)*, vol. 46, no. 137, pp. 309–329, Dec. 1997.

[94] P. Kebriaei, Z. Izsvák, S. A. Narayanavari, H. Singh, and Z. Ivics, “Gene Therapy with the Sleeping Beauty Transposon System,” *Trends in Genetics*, vol. 33, no. 11, pp. 852–870, Nov. 2017, doi: 10.1016/j.tig.2017.08.008.

[95] C. F. Magnani *et al.*, “Transposon-Based CAR T Cells in Acute Leukemias: Where Are We Going?,” *Cells*, vol. 9, no. 6, p. 1337, May 2020, doi: 10.3390/cells9061337.

[96] A. Gogol-Döring *et al.*, “Genome-wide Profiling Reveals Remarkable Parallels Between Insertion Site Selection Properties of the MLV Retrovirus and the piggyBac Transposon in Primary Human CD4+ T Cells,” *Molecular Therapy*, vol. 24, no. 3, pp. 592–606, Mar. 2016, doi: 10.1038/mt.2016.11.

[97] Z. Ivics, P. B. Hackett, R. H. Plasterk, and Z. Izsvák, “Molecular Reconstruction of Sleeping Beauty, a Tc1-like Transposon from Fish, and Its Transposition in

Human Cells," *Cell*, vol. 91, no. 4, pp. 501–510, Nov. 1997, doi: 10.1016/S0092-8674(00)80436-5.

[98] Z. Jin *et al.*, "The hyperactive Sleeping Beauty transposase SB100X improves the genetic modification of T cells to express a chimeric antigen receptor," *Gene Ther*, vol. 18, no. 9, pp. 849–856, Sep. 2011, doi: 10.1038/gt.2011.40.

[99] K. P. Micklethwaite *et al.*, "Investigation of product-derived lymphoma following infusion of *piggyBac* -modified CD19 chimeric antigen receptor T cells," *Blood*, vol. 138, no. 16, pp. 1391–1405, Oct. 2021, doi: 10.1182/blood.2021010858.

[100] D. C. Bishop *et al.*, "Development of CAR T-cell lymphoma in 2 of 10 patients effectively treated with *piggyBac* -modified CD19 CAR T cells," *Blood*, vol. 138, no. 16, pp. 1504–1509, Oct. 2021, doi: 10.1182/blood.2021010813.

[101] M. Jinek, K. Chylinski, I. Fonfara, M. Hauer, J. A. Doudna, and E. Charpentier, "A Programmable Dual-RNA–Guided DNA Endonuclease in Adaptive Bacterial Immunity," *Science*, vol. 337, no. 6096, pp. 816–821, Aug. 2012, doi: 10.1126/science.1225829.

[102] J. A. Doudna and E. Charpentier, "The new frontier of genome engineering with CRISPR-Cas9," *Science*, vol. 346, no. 6213, p. 1258096, Nov. 2014, doi: 10.1126/science.1258096.

[103] Y. Fu *et al.*, "High-frequency off-target mutagenesis induced by CRISPR-Cas nucleases in human cells," *Nat Biotechnol*, vol. 31, no. 9, pp. 822–826, Sep. 2013, doi: 10.1038/nbt.2623.

[104] J. Shin and J.-W. Oh, "Development of CRISPR/Cas9 system for targeted DNA modifications and recent improvements in modification efficiency and specificity," *BMB Rep.*, vol. 53, no. 7, pp. 341–348, Jul. 2020, doi: 10.5483/BMBRep.2020.53.7.070.

[105] J. Eyquem *et al.*, "Targeting a CAR to the TRAC locus with CRISPR/Cas9 enhances tumour rejection," *Nature*, vol. 543, no. 7643, pp. 113–117, Mar. 2017, doi: 10.1038/nature21405.

[106] Y. Lu *et al.*, "Safety and feasibility of CRISPR-edited T cells in patients with refractory non-small-cell lung cancer," *Nat Med*, vol. 26, no. 5, pp. 732–740, May 2020, doi: 10.1038/s41591-020-0840-5.

[107] Z. Wang *et al.*, "Phase I study of CAR-T cells with PD-1 and TCR disruption in mesothelin-positive solid tumors," *Cell Mol Immunol*, vol. 18, no. 9, pp. 2188–2198, Sep. 2021, doi: 10.1038/s41423-021-00749-x.

[108] J. Ren, X. Liu, C. Fang, S. Jiang, C. H. June, and Y. Zhao, "Multiplex Genome Editing to Generate Universal CAR T Cells Resistant to PD1 Inhibition," *Clinical Cancer Research*, vol. 23, no. 9, pp. 2255–2266, May 2017, doi: 10.1158/1078-0432.CCR-16-1300.

[109] Z. Cui *et al.*, “The comparison of ZFNs, TALENs, and SpCas9 by GUIDE-seq in HPV-targeted gene therapy,” *Molecular Therapy - Nucleic Acids*, vol. 26, pp. 1466–1478, Dec. 2021, doi: 10.1016/j.omtn.2021.08.008.

[110] J. Miller, A. D. McLachlan, and A. Klug, “Repetitive zinc-binding domains in the protein transcription factor IIIA from Xenopus oocytes.,” *The EMBO Journal*, vol. 4, no. 6, pp. 1609–1614, Jun. 1985, doi: 10.1002/j.1460-2075.1985.tb03825.x.

[111] J. Boch *et al.*, “Breaking the Code of DNA Binding Specificity of TAL-Type III Effectors,” *Science*, vol. 326, no. 5959, pp. 1509–1512, Dec. 2009, doi: 10.1126/science.1178811.

[112] A. Bhardwaj and V. Nain, “TALENs—an indispensable tool in the era of CRISPR: a mini review,” *J Genet Eng Biotechnol*, vol. 19, no. 1, p. 125, Dec. 2021, doi: 10.1186/s43141-021-00225-z.

[113] R. Benjamin *et al.*, “UCART19, a first-in-class allogeneic anti-CD19 chimeric antigen receptor T-cell therapy for adults with relapsed or refractory B-cell acute lymphoblastic leukaemia (CALM): a phase 1, dose-escalation trial,” *The Lancet Haematology*, vol. 9, no. 11, pp. e833–e843, Nov. 2022, doi: 10.1016/S2352-3026(22)00245-9.

[114] P. M. Rabinovich *et al.*, “Chimeric receptor mRNA transfection as a tool to generate antineoplastic lymphocytes,” *Hum Gene Ther*, vol. 20, no. 1, pp. 51–61, Jan. 2009, doi: 10.1089/hum.2008.068.

[115] K. Schutsky *et al.*, “Rigorous optimization and validation of potent RNA CAR T cell therapy for the treatment of common epithelial cancers expressing folate receptor,” *Oncotarget*, vol. 6, no. 30, pp. 28911–28928, Oct. 2015, doi: 10.18632/oncotarget.5029.

[116] G. L. Beatty *et al.*, “Mesothelin-Specific Chimeric Antigen Receptor mRNA-Engineered T Cells Induce Antitumor Activity in Solid Malignancies,” *Cancer Immunology Research*, vol. 2, no. 2, pp. 112–120, Feb. 2014, doi: 10.1158/2326-6066.CIR-13-0170.

[117] W. S. Koh, J. R. Porter, and E. Batchelor, “Tuning of mRNA stability through altering 3′-UTR sequences generates distinct output expression in a synthetic circuit driven by p53 oscillations,” *Sci Rep*, vol. 9, no. 1, p. 5976, Apr. 2019, doi: 10.1038/s41598-019-42509-y.

[118] K. Leppek *et al.*, “Combinatorial optimization of mRNA structure, stability, and translation for RNA-based therapeutics,” *Nat Commun*, vol. 13, no. 1, p. 1536, Mar. 2022, doi: 10.1038/s41467-022-28776-w.

[119] M. K. Panjwani *et al.*, “Feasibility and Safety of RNA-transfected CD20-specific Chimeric Antigen Receptor T Cells in Dogs with Spontaneous B Cell Lymphoma,” *Molecular Therapy*, vol. 24, no. 9, pp. 1602–1614, Sep. 2016, doi: 10.1038/mt.2016.146.

[120] Cummins KD, “Treating relapsed/refractory (RR) AML with biodegradable anti-CD123 CAR modified T cells.,” *Blood*, p. 130:1359, 2017.

[121] J. Svoboda *et al.*, “Nonviral RNA chimeric antigen receptor–modified T cells in patients with Hodgkin lymphoma,” *Blood*, vol. 132, no. 10, pp. 1022–1026, Sep. 2018, doi: 10.1182/blood-2018-03-837609.

[122] J. Mirkovitch, M.-E. Mirault, and U. K. Laemmli, “Organization of the higher-order chromatin loop: specific DNA attachment sites on nuclear scaffold,” *Cell*, vol. 39, no. 1, pp. 223–232, Nov. 1984, doi: 10.1016/0092-8674(84)90208-3.

[123] P. N. Cockerill and W. T. Garrard, “Chromosomal loop anchorage sites appear to be evolutionarily conserved,” *FEBS Letters*, vol. 204, no. 1, pp. 5–7, Aug. 1986, doi: 10.1016/0014-5793(86)81377-1.

[124] C. Piechaczek, C. Fetzer, A. Baiker, J. Bode, and H. J. Lipps, “A vector based on the SV40 origin of replication and chromosomal S/MARs replicates episomally in CHO cells,” *Nucleic Acids Research*, vol. 27, no. 2, pp. 426–428, Jan. 1999, doi: 10.1093/nar/27.2.426.

[125] A. Baiker *et al.*, “Mitotic stability of an episomal vector containing a human scaffold/matrix-attached region is provided by association with nuclear matrix,” *Nat Cell Biol*, vol. 2, no. 3, pp. 182–184, Mar. 2000, doi: 10.1038/35004061.

[126] C. H. Hans J Lipps, “pEPI for Gene Therapy Non viral episomes and their Application in Somatic Gene Therapy,” *J Cell Sci Ther*, vol. 04, no. 02, 2013, doi: 10.4172/2157-7013.S6-001.

[127] M. Kalos and R. E. K. Fournier, “Position-Independent Transgene Expression Mediated by Boundary Elements from the Apolipoprotein B Chromatin Domain,” *Molecular and Cellular Biology*, vol. 15, no. 1, pp. 198–207, Jan. 1995, doi: 10.1128/MCB.15.1.198.

[128] I. P. Chernov, S. B. Akopov, and L. G. Nikolaev, “Structure and Functions of Nuclear Matrix Associated Regions (S/MARs),” *Russian Journal of Bioorganic Chemistry*, vol. 30, no. 1, pp. 1–11, Jan. 2004, doi: 10.1023/B:RUBI.0000015767.28683.69.

[129] R. Haase *et al.*, “pEPito: a significantly improved non-viral episomal expression vector for mammalian cells,” *BMC Biotechnol*, vol. 10, no. 1, p. 20, Dec. 2010, doi: 10.1186/1472-6750-10-20.

[130] B. W. Bigger, O. Tolmachov, J.-M. Collombet, M. Fragkos, I. Palaszewski, and C. Coutelle, “An araC-controlled Bacterialcre Expression System to Produce DNA Minicircle Vectors for Nuclear and Mitochondrial Gene Therapy,” *Journal of Biological Chemistry*, vol. 276, no. 25, pp. 23018–23027, Jun. 2001, doi: 10.1074/jbc.M010873200.

[131] L. Vaysse, L. G. Gregory, R. P. Harbottle, E. Perouzel, O. Tolmachov, and C. Coutelle, “Nuclear-targeted minicircle to enhance gene transfer with non-viral

vectorsin vitro andin vivo," *J. Gene Med.*, vol. 8, no. 6, pp. 754–763, Jun. 2006, doi: 10.1002/jgm.883.

[132] Matthias Bozza, "The development of a novel S/MAR DNA vector platform for the stable, persistent and safe Genetic Engineering of Dividing Cells," Heidelberg University, 2017.

[133] M. Bozza *et al.*, "A nonviral, nonintegrating DNA nanovector platform for the safe, rapid, and persistent manufacture of recombinant T cells," *Sci. Adv.*, vol. 7, no. 16, p. eabf1333, Apr. 2021, doi: 10.1126/sciadv.abf1333.

[134] M. Bozza *et al.*, "Novel Non-integrating DNA Nano-S/MAR Vectors Restore Gene Function in Isogenic Patient-Derived Pancreatic Tumor Models," *Molecular Therapy - Methods & Clinical Development*, vol. 17, pp. 957–968, Jun. 2020, doi: 10.1016/j.omtm.2020.04.017.

[135] J. A. Williams and P. A. Paez, "Improving cell and gene therapy safety and performance using next-generation Nanoplasmid vectors," *Molecular Therapy - Nucleic Acids*, vol. 32, pp. 494–503, Jun. 2023, doi: 10.1016/j.omtn.2023.04.003.

[136] A. Roig-Merino *et al.*, "An episomal DNA vector platform for the persistent genetic modification of pluripotent stem cells and their differentiated progeny," *Stem Cell Reports*, vol. 17, no. 1, pp. 143–158, Jan. 2022, doi: 10.1016/j.stemcr.2021.11.011.

[137] ROSENBERG A., "Phase II Study of Metastatic Melanoma With Lymphodepleting Conditioning and Infusion of Anti-MART-1 F5 TCR-Gene-Engineered Lymphocytes.," *Accessed 05.09.2022, 2022. https://clinicaltrials.gov/ct2/show/results/NCT00509288*.

[138] A. H. Rad S. M., A. Poudel, G. M. Y. Tan, and A. D. McLellan, "Promoter choice: Who should drive the CAR in T cells?," *PLoS ONE*, vol. 15, no. 7, p. e0232915, Jul. 2020, doi: 10.1371/journal.pone.0232915.

[139] J.-Y. Ho *et al.*, "Promoter usage regulating the surface density of CAR molecules may modulate the kinetics of CAR-T cells in vivo," *Molecular Therapy - Methods & Clinical Development*, vol. 21, pp. 237–246, Jun. 2021, doi: 10.1016/j.omtm.2021.03.007.

[140] N. Hilf *et al.*, "Actively personalized vaccination trial for newly diagnosed glioblastoma," *Nature*, vol. 565, no. 7738, pp. 240–245, Jan. 2019, doi: 10.1038/s41586-018-0810-y.

[141] A. S. Luksik, E. Yazigi, P. Shah, and C. M. Jackson, "CAR T Cell Therapy in Glioblastoma: Overcoming Challenges Related to Antigen Expression," *Cancers*, vol. 15, no. 5, p. 1414, Feb. 2023, doi: 10.3390/cancers15051414.

[142] S. Jutz *et al.*, "Assessment of costimulation and coinhibition in a triple parameter T cell reporter line: Simultaneous measurement of NF-κB, NFAT and AP-1," *Journal of Immunological Methods*, vol. 430, pp. 10–20, Mar. 2016, doi: 10.1016/j.jim.2016.01.007.

[143] S. E. Mann *et al.*, “Multiplex T Cell Stimulation Assay Utilizing a T Cell Activation Reporter-Based Detection System,” *Front. Immunol.*, vol. 11, p. 633, Apr. 2020, doi: 10.3389/fimmu.2020.00633.

[144] C. Sheridan, “Why gene therapies must go virus-free,” *Nat Biotechnol*, vol. 41, no. 6, pp. 737–739, Jun. 2023, doi: 10.1038/s41587-023-01824-6.

[145] A. L. Garfall *et al.*, “T-cell phenotypes associated with effective CAR T-cell therapy in postinduction vs relapsed multiple myeloma,” *Blood Advances*, vol. 3, no. 19, pp. 2812–2815, Oct. 2019, doi: 10.1182/bloodadvances.2019000600.

[146] N. Watanabe, F. Mo, and M. K. McKenna, “Impact of Manufacturing Procedures on CAR T Cell Functionality,” *Front. Immunol.*, vol. 13, p. 876339, Apr. 2022, doi: 10.3389/fimmu.2022.876339.

[147] B. L. Levine, J. Miskin, K. Wonnacott, and C. Keir, “Global Manufacturing of CAR T Cell Therapy,” *Molecular Therapy - Methods & Clinical Development*, vol. 4, pp. 92–101, Mar. 2017, doi: 10.1016/j.omtm.2016.12.006.

[148] M. Martino, C. Alati, F. A. Canale, G. Musuraca, G. Martinelli, and C. Cerchione, “A Review of Clinical Outcomes of CAR T-Cell Therapies for B-Acute Lymphoblastic Leukemia,” *IJMS*, vol. 22, no. 4, p. 2150, Feb. 2021, doi: 10.3390/ijms22042150.

[149] H. J. Jackson and R. J. Brentjens, “Overcoming Antigen Escape with CAR T-cell Therapy,” *Cancer Discovery*, vol. 5, no. 12, pp. 1238–1240, Dec. 2015, doi: 10.1158/2159-8290.CD-15-1275.

[150] G. Agliardi *et al.*, “Intratumoral IL-12 delivery empowers CAR-T cell immunotherapy in a pre-clinical model of glioblastoma,” *Nat Commun*, vol. 12, no. 1, p. 444, Jan. 2021, doi: 10.1038/s41467-020-20599-x.

[151] S. S. Wang, P. Bandopadhayay, and M. R. Jenkins, “Towards Immunotherapy for Pediatric Brain Tumors,” *Trends in Immunology*, vol. 40, no. 8, pp. 748–761, Aug. 2019, doi: 10.1016/j.it.2019.05.009.

[152] A. R. Liuzzi, G. Agliardi, B. Becher, and M. Pule, “A Single Dose of Local IL-12 Promotes Anti-Tumor Effect of Anti-EGFRvIII-CAR-T Cells in a Syngeneic Murine Model of Glioblastoma,” *Annals of Oncology*, vol. 30, p. xi40, Dec. 2019, doi: 10.1093/annonc/mdz451.015.

[153] S. Rafiq, C. S. Hackett, and R. J. Brentjens, “Engineering strategies to overcome the current roadblocks in CAR T cell therapy,” *Nat Rev Clin Oncol*, vol. 17, no. 3, pp. 147–167, Mar. 2020, doi: 10.1038/s41571-019-0297-y.

[154] A. Moretti, M. Ponzo, C. A. Nicolette, I. Y. Tcherepanova, A. Biondi, and C. F. Magnani, “The Past, Present, and Future of Non-Viral CAR T Cells,” *Front. Immunol.*, vol. 13, p. 867013, Jun. 2022, doi: 10.3389/fimmu.2022.867013.

8. Acknowledgments

I would like to express my deepest gratitude and appreciation to all those who have provided invaluable support and made significant contributions to the completion of this thesis.

First, I would like to express my gratitude to my supervisors, Prof Dr Michael Platten and Dr Richard Harbottle, for giving me the opportunity to join their groups and for your support throughout my PhD journey. Your guidance, expert knowledge, and constant encouragement have been invaluable. I am truly grateful for the freedom you have given me to pursue my interests and for the trust you have placed in me. Your mentorship has been invaluable in my growth as a researcher and as a person.

I then would like to thank Dr Ed Green and Dr Lukas Bunse for your feedback and constructive insights which have played a fundamental role in this work. I also would like to thank Dr Matthias Bozza for the guidance and supervison since the very first day I joined the lab. I extend also my thanks to Prof Dr Hinrich Abken for accepting to be in my TAC committee and for providing invaluable feedback during our meetings. Your insights and contributions have greatly enriched this project. A special thanks goes also to Dr Stefan Push for joining the UNITE meetings and for his assistance with the histology of this project. Your support and contribution have been greatly appreciated. I also would like to thank Prof Dr Ralf Bartenschlager and Prof Dr Martin Müller to have accepted to be part of my defense committee. I would also like to thank our collaborator Dr Patrick Schmidt for his invaluable help with the CAR project. Your expertise and contributions have been fundamental to the success of this project. I am truly fortunate to have had the opportunity to work with such knowledgeable and supportive individuals. Their contributions and guidance have been invaluable to the successful completion of this work.

Special thank you also to all my colleagues who helped me with the experiments. Yu-Chan for the *in vivo* work as well as Dennis, Amelie and Philipp for your assistance throughout the process. A heartfelt thanks goes to Katharina to your continuous help, kindness and support over the years. I would like to extend my thanks also to the current and former members of F160, including Anna, Annabel, Francisca, Laura, Luisa, João, Julia, Patrick, and Toros. It has been a pleasure to work alongside you all. Thanks to Ali and Manu for the lab times, the fun times and our friendship.

I would also like to thank all the lab neighbours and friends. A special thanks goes to my partner in crime, Gayatri. I am grateful to have met you on this journey. Thank you for engaging in scientific discussions, being my accountability partner, and always being the best cheerleader I could ask for. Our crazy moments together and those yet to come have made this experience unforgettable. Thank you for growing with me not only as a scientist but also as a person. Big big thank you also to (San) Francesco Baccianti da Sesto Fiorentino. A special thanks goes to you for all the negative fractions, the illimited help inside and outside the lab, for sharing weekends and the long nights in the lab together, for the 'abbuffate', for the fun time and for the 'figuracce', but specially, thank you for your friendship. The PhD journey would not have been the same without your presence and support. Thanks also to Michael for the enjoyable moments we shared during your time in ATV. Thanks for the warm welcome in the HD life and introducing me to the Italian family.

"Beh?" I also cannot forget to thank my adoptive Italian family here. Ale, Ila, Leo, Sendru, Silvia e Vale. Thank you for i 'pranzi domenicali', the crazy and fun times, the 'partite a burraco', the concerts, the spontaneity, the trips and for made me feel at home. You have enriched my life in HD and it wouldn't have been so fun without your presence.

Thanks also to another important adopted family here, the Steinzeitweg fam. Gayatri and Alexo, quarantine brought us something truly special. Words cannot express the love I have for both of you. A special thank also to Suchi. Thank you for our philosophical discussion, your wisdom, the shared gym time, and for being the most attentive listener and an essential friend here. Even during challenging times, I am grateful that our paths crossed, allowing us to grow together. I extend my thanks to all the other people I have met here and who became part of this life in HD.

Thanks also to all my dear friends back home, Fili, Silvi, Ire, Pier, Buz, Gio, Mary, Lore e Fra. I am grateful for the reunions we've had in these years, even if life brought us in different parts of the world. I am deeply grateful for the everlasting friendship we share. Even from afar, your presence remains fundamental in my life.

Thanks to my mom and Marti for the endless love, for always being my pillars of strength and always allowing me the freedom and curiosity to explore the world. I am deeply grateful for all your support and the values you gave me. You are a constant inspiration for me, and you have shaped me into the person I am today. I could have not asked for a better

mom and sister. Thank you for always believing in me, this thesis would have not being possible without you. Finally, thanks to all the rest of my family, I am forever grateful for your presence in my life.